BIOPOLYMER BASED MICRONEEDLE PATCH FOR POLIO VACCINATION AND DIAGNOSTIC APPLICATIONS

A Dissertation
Presented to
The Academic Faculty

by

Chandana Kolluru

In Partial Fulfillment
of the Requirements for the Degree
Doctor of Philosophy in Materials Science and Engineering in the
School of Materials Science and Engineering

Georgia Institute of Technology
August 2018

Biopolymer based microneedle patch for Polio vaccination and diagnostic applications

Approved by:

Dr. Mark Prausnitz, Advisor
School of Chemical and Biomolecular Engineering
Georgia Institute of Technology

Dr. Sundaresan Jayaraman
School of Materials Science and Engineering
Georgia Institute of Technology

Dr. Valeria Milam
School of Materials Science and Engineering
Georgia Institute of Technology

Dr. Mostafa El-Sayed
School of Chemistry and Biochemistry
Georgia Institute of Technology

Dr. Vladimir Tsukruk
School of Materials Science and Engineering
Georgia Institute of Technology

Date Approved: [July 2nd, 2018]

To my children, my true inspiration

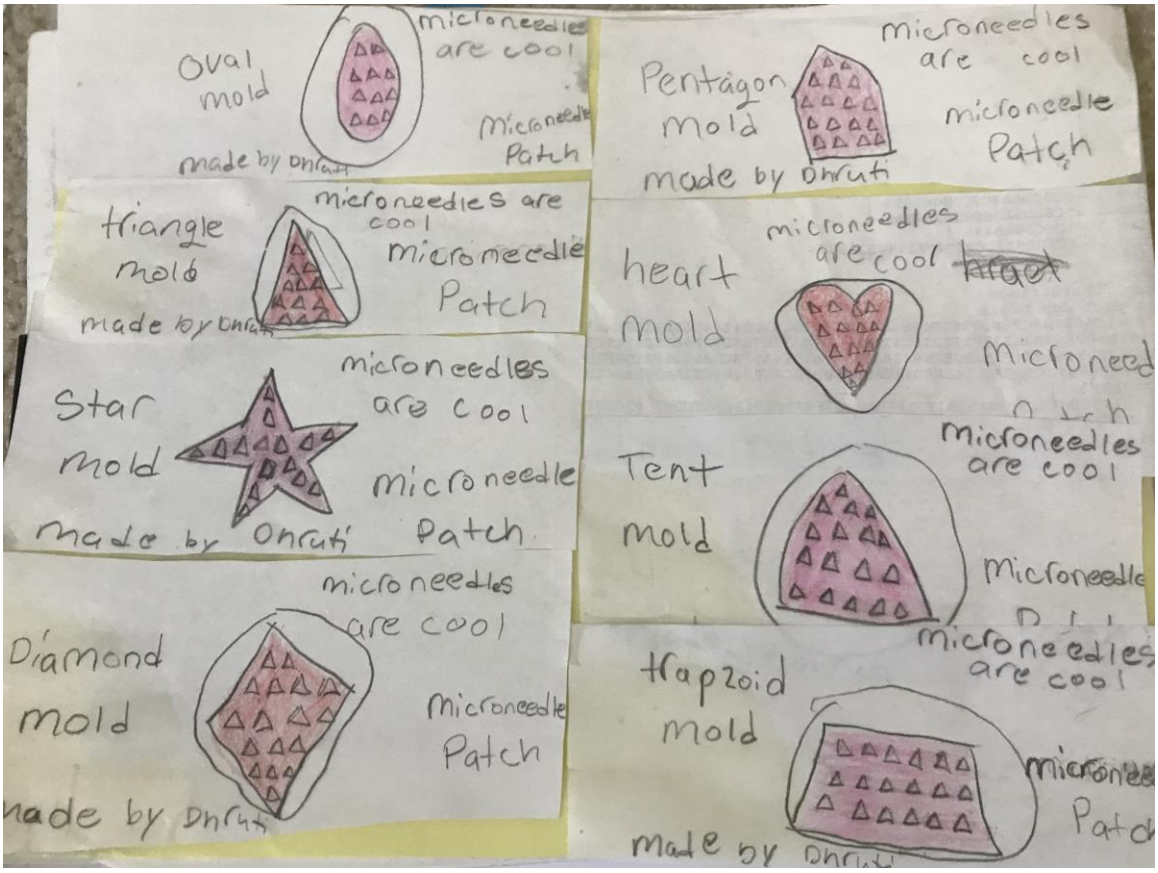

Drawings made by Dhruti in 2015 when she visited Gatech for the 1st time

ACKNOWLEDGEMENTS

"Everything you want is just outside your comfort zone" – Robert Allen

And this degree is what I always wanted. Many people (*knowingly or unknowingly*) helped me get outside my comfort zone, and I would like to thank each and every one.

The desire was kindled when I heard Dr. Mark Prausnitz give a talk on Microneedles at CRS conference in 2011 (*yes, angels singing in C-major in the background is a real thing!)*. He inspired me then, and has continued to inspire me in many ways! I wholeheartedly thank him for his guidance throughout my PhD journey. I have learnt from him essential scientific, technical knowhow, good communication skills and the importance of discipline in research. I look up to him as a strong mentor who leads by example. His passion for research is contagious. Working with him closely over the years, I have learnt to stay grounded and humble while being successful. I couldn't have asked for a better advisor. I would also like to acknowledge my committee members Dr. Valeria Milam, Dr. Vladimir Tsukruk, Dr. Sundaresan Jayaraman, and Dr. Mostafa El-Sayed for their insightful comments and continued support.

A lot of this work would have been impossible without the support of my drug delivery lab mates. I would especially like to thank Donna Bondy, our administrative coordinator. She is the lifeline of our lab. She has helped and advised me from ordering chemicals, getting travel reimbursement to the best places in US to go for a hike (*Her exercise regimen for strong biceps is a still a secret)*

There were phases in my research when it felt like I was getting nowhere (*Microneedles are painless upon administration as cited in references 3-5, but not when being*

researched). It was my privilege to have some very smart colleagues *(Georgia Tech surely has some helluva engineers and scientists!)* to bounce off ideas and creatively solve problems. I would like to thank all my colleagues including but not limited to – Dr. Yasmine Gomaa, Dr. Andrew Tadros, Dr. Pradnya Samant, Dr. Jessica Joyce, Dr. Matthew Mistilis, Dr. Jaya Arya, Dr. Bryce Chiang, Brandon Gerberich, Sebastien Henry, Dr. Stefany Holguin, Dr. Haripriya Kalluri, Dr. Jae Hwan Jung, Simple Kumar, Juan Mena-Lapaix, Dr. Jeong Woo Lee, Dr. Song Li, Dr. Wei Li, Dr. Devin McAllister, Dr. Wilmarie Medina-Ramos, Dr. Mohammad Mofidfar, Joshua Palacios, Monica Perez, Winston Pewin, Richard Shafer, Dr. Andrey Romanyuk, Youngeun Kim, Amir Hejri, Dr. Jeremy Chae, Dr. Dengning Xia, Kaddu, and Richard Terry. The lab has a very friendly, casual and collaborative environment which made the research enjoyable.

I enjoyed working with Yasmine and Jeong Woo on the polio microneedles project. Yasmine has especially been a great friend and a shoulder to lean on whenever I needed it. I also enjoyed my discussions with Pradnya, Juan and Youneun about ISF collection. My special thanks to my undergrad assistant, Mikayla Williams and all of the people from PRL facitlity- Dr. Laura O'Farell, Dr. Richard Noel, Ogeda Blue, Andrea for helping me with all the animal studies *(they saved me from the wrath of the rats!)*. I also thank Dr. Ruilong Ma, Qisheng Jiang, for their collaboration.

I thank Prasanna Kolluru for being a wonderful support and thank Sammy Bell, Maria Dunkle, and Yasuo Matsuzawa for their encouragement.

I would also like to thank my parents, brother, in-laws and my friends (*a.k.a. UNO group)* for encouraging me. Their support is definitely statistically significant (*ANOVA, p<*

0.00001). Finally, I would like to thank my husband, Lakshmana Anupindi and my wonderful kids, Dhruv and Dhruti Anupindi for their encouragement. I couldn't have done this without them.

My Ph.D. journey (*~73,873 miles of commute to Gatech*) had been more of a roller coaster ride. It was interspersed with some crazy animal studies (*79 rats which lost their lives for my research)* and some wonderful moments like making it to the finals of "Dance your PhD" (*I consider depicting 'microneedles' in Kuchipudi style one of my greater achievements)*. One sentence to sum it all up- *A satisfying journey*!

TABLE OF CONTENTS

ACKNOWLEDMENTS **iv**

LIST OF TABLES **x**

LIST OF FIGURES **xi**

LIST OF SYMBOLS AND ABBREVIATIONS **xxvi**

CHAPTER 1. Introduction **1**

CHAPTER 2. Literature review **4**
2.1 Poliomyelitis **4**
2.1.1 Vaccine Delivery 4
2.1.2 Current polio vaccine delivery routes 4
2.1.3 Microneedle patches for vaccine delivery 6
2.1.4 Current polio vaccine stabilization strategies 9
2.1.5 Motivation for research on MN patch for IPV administration 10
2.2 Disease diagnosis and monitoring **11**
2.2.1 Sources for biomarkers 12
2.2.2 Interstitial fluid (ISF) 13
2.2.3 Methods for ISF collection 16
2.2.4 Microneedles for sampling ISF 19
2.2.5 Motivation for research on ISF collection using microneedles 22

CHAPTER 3. Specific aims and hypotheses **24**

CHAPTER 4. Development of a thermostable microneedle patch for polio vaccination **25**
4.1 Introduction **25**
4.2 Materials and methods **26**
4.2.1 Concentration of inactivated polio vaccine 26
4.2.2 Vaccine stability screening 27
4.2.3 Microneedle patch fabrication 27
4.2.4 Microneedle composition 28
4.2.5 Lyophilization 29
4.2.6 Microneedle patch characterization 29
4.2.7 ELISA assay measurements 30
4.2.8 Thermogravimetric analysis 30
4.2.9 Differential scanning calorimetry 31
4.2.10 X-ray diffraction 31

4.2.11 Fourier-transform infrared spectroscopy 32
4.2.12 Statistics and Design of Experiments 32
4.3 Results and discussion 32
4.3.1 Excipient screening for IPV stabilization 32
4.3.2 Buffer and pH screening 35
4.3.3 Optimization of polio MN patches 36
4.3.4 Effect of drying conditions 39
4.3.5 Polio MN patch characterization 42
4.3.6 Long- term stability of polio MN patches 43
4.3.7 Correlation of residual moisture content in patch to IPV stability 44
4.3.8 Characterization of changes in MN matrix material properties during patch storage 46
4.4 Discussion 50
4.5 Conclusions 53
4.6 Acknowledgements 53

CHAPTER 5. Recruitment and collection of dermal interstitial fluid using a microneedle patch 55
5.1 Introduction 55
5.2 Materials and methods 56
5.2.1 Microneedle patch fabrication 56
5.2.2 MN surface pretreatment 57
5.2.3 Paper reservoir 58
5.2.4 Modified Cobb and Klemm methods for determining water absorptiveness of paper 59
5.2.5 Contact angle measurements 59
5.2.6 Quantification of ISF volume collected 60
5.2.7 ISF collection from pig skin ex vivo 60
5.2.8 ISF collection from rat skin in-vivo 61
5.2.9 Statistical analysis 64
5.3 Results 64
5.3.1 Microneedle patch design 64
5.3.2 Effect of multiple skin insertions, number of MNs per patch and MN thickness on ISF collected 66
5.3.3 Effect of MN surface properties on ISF collected 68
5.3.4 Effect of skin pre-treatment on ISF collected 69
5.4 Discussion 72
5.4.1 Design of MN patch for simplified collection of ISF 72
5.4.2 Factors affecting ISF collection 73
5.4.3 Effects of MN patch puncture on skin 74
5.4.4 Limitations of this study 75
5.5 Conclusions 76
5.6 Acknowledgements 77

CHAPTER 6. Monitoring drug pharmacokinetics and immunologic biomarkers in dermal interstitial fluid using a microneedle patch 78
6.1 Introduction 78

6.2 Materials and methods 80
6.2.1 Materials 80
6.2.2 Microneedle patch fabrication 81
6.2.3 ISF collection procedure 81
6.2.4 Vancomycin pharmacokinetic study 82
6.2.5 Extraction of vancomycin from ISF/serum samples 83
6.2.6 HPLC-MS/MS analysis 83
6.2.7 Polio immunization 84
6.2.8 Statistical analysis 86
6.3 Results 87
6.3.1 ISF collection by microneedle patch 87
6.3.2 Vancomycin pharmacokinetics 88
6.3.3 Immune responses to inactivated polio vaccination 91
6.4 Discussion 94
6.4.1 MN patch for simplified ISF sampling 94
6.4.2 Drug monitoring in ISF 94
6.4.3 Immunodiagnostic markers in ISF 96
6.5 Conclusion 96
6.6 Acknowledgments 97

CHAPTER 7. Conclusions 98
7.1 Dissolving MN patch for polio vaccination 98
7.2 Paper based MN patch for ISF sampling and detection of biomarkers 98

CHAPTER 8. Future directions 100
8.1 MN patch with faster dissolution kinetics, shorter wear time with biocompatible excipients 102
8.2 Microneedle patch for ISF collection 103
8.3 Microneedles for detection of biomarkers in ISF 103

CHAPTER 9. Appendix A. supporting information for chapter 4 106
A.1.2 Buffer and pH Screening 108
A.2 Optimization of IPV MN patches 109
A.2.1 Optimization of 1st cast formulation 109
A.2.2 Optimization of second cast 110
A.3. Effect of drying conditions 111
A.4 Long term stability of polio MN patches 112
A.5 Correlation of residual moisture content in patch to IPV stability 112
A.6 Correlation of IPV stability to storage temperature 113
A.7 XRD patterns for raw materials used for MN matrix patch preparation 114

REFERENCES 115

LIST OF TABLES

Table 6-1: Comparison of AUC, C_{max} and T_{max} values of vancomycin pharmacokinetics between ISF and serum 90

Table A-1: Design of Experiments table showing excipient combinations tested for IPV stabilization[1] 106

LIST OF FIGURES

Figure 2-1: Example of a dissolving MN patch. A: Dissolving MN patch at high magnification. B: Pig skin after insertion and dissolution of a dye-containing MN patch. C: Side by side comparison of a dissolving MN patch to a US nickel coin. D: Dissolving MN patch before and after insertion. Image reproduced from Sullivan et al.[3]. 8

Figure 2-2: Pie chart showing the percentages of intracellular and extracellular fluids[74,75]..... 14

Figure 4-1: Effect of stabilizing excipients on IPV type 3 activity before drying, after air drying, after subsequent lyophilization and after storage. Vaccine was formulated with combinations of different excipients (each present at a concentration of 5% w/v) in 0.1 M histidine buffer at pH 6.5 (see Table S1 in SI for key to excipient formulations). In each set of bars, the first bar shows activity of liquid IPV formulated with excipients before drying. The second bar shows IPV activity after air drying at 5°C with desiccant overnight after casting onto PDMS chips. The third bar shows IPV activity after lyophilization. The fourth bar shows IPV activity after storage lyophilized vaccine at 25 °C with desiccant for 1 week. The unformulated vaccine control data is shown as D6 bars on the far left. All IPV activity (determined by ELISA) is shown as percentage of the starting stock solutions of concentrated vaccine. Asterisk (*) indicates excipient formulation that maintained >80%

activity after drying and storage. Data represent mean ± SEM (standard error of the mean) of n= 3 replicates. Companion data on IPV types 1 and 2 are show in Figure A-1 in Appendix A. 34

Figure 4-2: Effect of formulation buffer and pH on IPV type 3 activity after drying on PDMS chips followed by lyophilization and storage. IPV was formulated with 5% w/v maltodextrin and 5% w/v D-sorbitol in 0.1 M buffer with pH adjusted using 1 N HCl or 1 N NaOH. Storage was carried out at 40 °C for 3 or 7 days with desiccant. KHP: Potassium hydrogen pthalate, M199: Medium 199. In each set of bars, IPV activity is shown in the first bar after air drying at 5°C overnight and lyophilization, in the second bar after storage in a desiccator at 40 °C for 3 days and in the last bar after storage at 40 °C in a desiccator for 1 week. Stability of unformulated IPV (i.e., without maltodextrin or D-sortibol) in M199 media is shown in the bars on the far right. Asterisk (*) represents buffer which had the most adverse effect on IPV stability (general linear model, $p < 0.03$). All IPV activity is shown as percentage of IPV activity vaccine casting solution. Data represent mean ± SEM of n= 3 replicates. Companion data on IPV types 1 and 2 are show in Figure A-2 in Appendix A. 36

Figure 4-3: Effect of 1st cast excipient ratio (maltodextrin:D-sorbitol) on IPV type 3 activity after fabricating MN patches, air drying, lyophilization and storage with desiccant at 40 °C for 2 days. Trivalent IPV was formulated with stabilizing excipients at a total concentration of 10% w/v in the vaccine casting solution. The maltodextrin: D-sorbitol mass ratios were 80:20 (MS80),

50:50 (MS50) and 20:80 (MS20). The 2nd cast polymer matrix solution consisted of excipients at a total concentration of 45% w/v fish gelatin and D-sorbitol (at a mass ratio of 78:22) in 0.15 mM histidine buffer at pH 6.3. All IPV activity is expressed as a percentage of IPV activity in the vaccine casting solution. In each set of bars, the first bar shows IPV activity in MN patch after air drying at 5°C in a desiccator for 2 days; the second bar shows IPV activity after additional lyophilization; and the last bar shows IPV activity after storage at 40 °C for 1 week with desiccant. There was no significant difference between the different ratios of maltodextrin-to-D-sorbitol (2-way ANOVA, $p > 0.8$). Data represent mean ± SEM of n= 3 replicates. Companion data on IPV types 1 and 2 are show in Figure A-3 in Appendix A. 37

Figure 4-4: Effect of 2nd cast excipient ratio (fish gelatin-to-D-sorbitol) on IPV type 3 activity after fabricating MN patches, air drying, lyophilization and storing with desiccant at 40 °C for 7 days. Trivalent IPV was formulated with stabilizing excipients at a total concentration of 10% w/v in the vaccine casting solution. The maltodextrin: D-sorbitol mass ratios were Trivalent IPV was formulated with stabilizing excipients at a total concentration of 10% w/v in the vaccine casting solution. The maltodextrin: D-sorbitol ratio was 20:80 in 0.35 mM histidine buffer. The 2nd casting solution containined 45% w/v with varying mass ratios of fish gelatin-to-D-sorbitol in 0.15 mM histidine buffer. The mass ratios used were GS88 (fish gelatin:D-sorbitol = 88:11), GS78 (fish gelatin:D-sorbitol = 78:22) and GS55 (fish gelatin:D-sorbitol =

55:45). All IPV activity is expressed as a percentage of IPV activity in the vaccine casting solution. In each set of bars, the first bar shows IPV activity in MN patch after air drying followed by lyophilization and the second bar shows the IPV activity after storage at 40 °C for 1 week with desiccant. Asterisk (*) depicts a significant difference between IPV activity compared to other two ratios (ANOVA, $p < 0.05$). Data represent mean ± SEM of n= 3 replicates. Companion data on IPV types 1 and 2 are show in Figure A-4 in Appendix A. 39

Figure 4-5: A) Effect of air drying, subsequent lyophilization and storage conditions on residual moisture content of MN patches. MN patches were fabricated and air dried at 5 °C, 25 °C or 40 °C with desiccant for 2 days. Half of the patches were stored at 40 °C for 1 week with desiccant. The other half of the patches were subjected to lyophilization followed by storage at 40 °C for 1 week with desiccant. In each set of bars, the first bar shows residual moisture content of MN patch after initial drying, the second bar shows the residual moisture content after subsequent lyophilization, the third bar shows residual moisture content for MN patches stored at 40 °C for 1 week with desiccant (no lyophilization) and the last bar shows residual moisture content for MN patches stored at 40 °C for 1 week with desiccant after lyophilization. Hash (#) depicts no statistical difference between the two samples (1-way ANOVA, $p > 0.05$). B) Effect of air drying, subsequent lyophilization and storage conditions on IPV type 3 activity. All IPV activity is expressed as a percentage of IPV activity in the liquid casting solution. In each set of bars,

the first bar shows IPV type 3 activity in MN patches after air drying, the second bar shows the activity after lyophilization, the third bar shows activity for MN patches stored at 40 °C for 1 week with desiccant (no lyophilization) and the last bar shows the activity for MN patches stored at 40 °C for 1 week with desiccant after lyophilization. Hash (#) depicts no statistical difference between the two samples (1-way ANOVA, $p > 0.05$). Asterisk (*) indicates a significant difference in IPV activity (1-way ANOVA, $p < 0.05$). Data represent mean ± SEM of n= 3 replicates. Companion data on IPV types 1 and 2 are show in Figure A-5 in Appendix A. 41

Figure 4-6: MN patch containing a 10 x 10 array of microneedles was manually inserted into shaved porcine cadaver skin and imaged (A) before insertion and (B) 15 min after..... 43

Figure 4-7: IPV activity in MN patches stored at 5, 25 or 40 °C with desiccant for up to 1 year. MN patches were analyzed using ELISA for (A) IPV type 1, (B) IPV type 2 and (C) IPV type 3 activity at various time points. IPV activity is expressed as a percentage of IPV activity of MN patches immediately after fabrication. Data represent mean ± SEM of n= 3 replicates. 44

Figure 4-8: A) Effect of storage conditions on residual moisture content of polio MN patches stored at 5, 25 or 40 °C with desiccant or at 40 °C and 50% relative humidity (RH). B) Correlation of IPV type 3 stability in MN patches to residual moisture content of the patches stored at 5, 25 or 40 °C with desiccant or at 40 °C and 50% relative humidity (RH). Regression analysis showed an R^2 value of 0.009, indicating poor correlation. Data represent

mean ± SEM of n= 3 replicates. Companion data on IPV types 1 and 2 are show in Figure A-7 in Appendix A. 45

Figure 4-9: Effect of storage time and temperature on T_g of MN matrix material measured by DSC. T_g was measured at specific times for up to 30 days at 5 °C, 25 °C or 40 °C with desiccant. Data represent mean ± SEM of n= 3 replicates. 47

Figure 4-10: FTIR spectrum of MN matrix samples measured 30 days after storage at 5 °C, 25 °C or 40 °C with desiccant. Data represents averages of n= 3 replicates. 49

Figure 4-11: X-ray diffraction patterns corresponding to MN matrix samples stored at 5 °C, 25 °C or 40 °C for up to 30 days. Data represent averages of n= 3 replicates. 50

Figure 5-1: Experimental plan for study to determine the effect of skin pre-treatment on the amount of ISF collected from rat skin in vivo. Group 1 only received MN treatment to collect ISF, in which a MN patch containing 9 MNs with a 2 mm x 7 mm piece of filter paper glued on the patch backing was applied 10 times to the skin on the lateral side of the rat using a force of 20 – 40 N. Group 2 skin was pretreated with a MN patch backing with MNs cut off to provide a blunt pretreatment, followed by MN treatment to collect ISF after a 5 min delay. Group 3 followed the same protocol as Group 2, except sharp-tipped MNs were used during the pretreatment. Each treatment was performed on 3 sites per rat. 62

Figure 5-2: Representative images of MN patch for ISF collection. A) A patch comprising a row of nine microneedles (arrow) with a strip of white filter paper adhered

to the patch backing. B) Magnified image of a single microneedle. C) Image of ISF collection after 5 insertions of a MN patch in the skin of a hairless rat in vivo. The MNs are on the lower edge of the patch and cannot be seen because they are inserted into the skin. Clear ISF is collected in the paper reservoir as observed by wetness of the paper (arrow). 65

Figure 5-3: Water absorptiveness of different types of paper determined by modified Cobb method and modified Klemm method. (A) For the Cobb method, 10 cm^2 paper strips were weighed before and after soaking in DI water for 30, 60, 90 and 120 s. The Cobb value is the amount of water absorbed by the paper normalized to the initial paper mass to account for thickness differences between the paper strips. (B) For the Klemm method, 10 cm^2 paper strips were suspended vertically with their lower end immersed in 10 ml of DI water for 30, 60, 90 and 120 s. The Klemm value is the capillary rise of water determined by measuring the vertical distance travelled by water. The Klemm value was normalized to the initial paper mass to account for thickness differences between the paper strips. Data represents mean ± SEM (standard error of the mean) of n= 3 replicates. 66

Figure 5-4: Effect of microneedle (MN) patch design on the amount of ISF collected. Patches were prepared with MN measuring either 50 µm or 100 µm in thickness and comprising either 5 or 9 MNs per patch. ISF was collected by applying a MN patch 1, 3, 5 or 20 times to stretched pig ear skin ex-vivo artificially hydrated with fluorescein row. Data represents mean ± SEM (standard error of the mean) of n= 3 replicates. 67

Figure 5-5: Effect of microneedle (MN) surface properties on ISF collection from skin. MN patches made of stainless steel (type 304) were (i) treated with air plasma for 5 min to increase hydrophilicity (ii) untreated or (iii) coated with 1 µm thick Parylene C to impart hydrophobicity. The y axis shows sessile drop contact angle of water of the MN surfaces and the secondary y-axis shows the number of insertions required to collect 2 µl of ISF from hairless rats in vivo. Asterisk (*) and cross (†) identify values significantly different from the corresponding value with no coating/treatment for mean contact angle and # skin insertions, respectively (2-way ANOVA $p < 0.01$). Data represent mean ± SEM (standard error of the mean) of n= 6 replicates. 69

Figure 5-6: Effect of skin pre-treatment on amount of ISF collected and skin hydration. ISF was collected from the skin of shaved Wistar rats in vivo using 10 skin insertions with MN patches (Group 1), using a pre-treatment of 10 skin applications with a blunt MN patch backing (i.e., not expected to puncture skin) followed 5 min later by 10 skin insertions with MN patches (Group 2) or using a pre-treatment of 10 skin applications with a conventional, sharp-tipped MN patch backing (i.e., expected to puncture skin) followed 5 min later by 10 skin insertions with MN patches (Group 3), as described in Figure 1. A) Effect of skin pre-treatment of amount of ISF collected from shaved Wistar rat skin in vivo. B) Effect of skin pre-treatment on skin hydration in hairless rats in vivo. Immediately after the experiment in Part A, the weight of skin samples biopsied from the skin treatment area was measured before and after lyophilization (expected to fully dehydrate the skin) to determine

hydration level. The percent increase in hydration due to skin pretreatment was determined by hydration levels of treated samples normalized to untreated control samples. Data represent mean ± SEM (standard error of the mean) of n= 15. Asterisk (*) depicts a significant increase in amount of ISF collected or percent increase in skin hydration compared to Group 1 (2 way ANOVA, $p < 0.01$). 71

Figure 5-7: Representative images of H & E-stained sections of skin from shaved Wistar rats after ISF collection shown in Figure 6.The study plan for Groups 1, 2 and 3 is shown in Figure 1. Sections from skin treated with MN patches (Treated) is compared to skin from the same animals at untreated sites (Control). All skin samples showed mild signs of immune response, as evidenced by infiltration of immune cells (arrows), possibly due to hair removal due to shaving and application of depilatory cream. However, no meaningful differences in immune cell infiltration was observed between controls and treated samples or between the three test groups. 72

Figure 6-1: Collection of ISF using a microneedle (MN) patch. A) Representative photographic image of a MN patch showing a row of nine MNs measuring 650 μm in length extending from a patch backing with rectangular strips of filter paper adhered to both sides. B) Representative photographic image of ISF collection from hairless rat skin in vivo. Upon application of the MN patch to the skin, clear interstitial fluid (ISF) flowed out of the skin through micropores created by the MNs and was collected in the paper reservoirs. The paper reservoir shown in this image is mostly wetted by ISF, with only the

upper left corner still dry, as indicated by different visual appearance. C) Representative photographic image of a MN patch after ISF collection by repeated application to skin. The amount of ISF collected on each strip of paper was ~2 µl, for a total of ~4 µl per MN patch..... 88

Figure 6-2: Pharmacokinetics of vancomycin in rat ISF and serum. A) Pharmacokinetic profile of vancomycin concentration in ISF and serum samples collected from rats administered a 1 mg/kg bolus intravenous injection of vancomycin. Data points show mean ± standard deviation (SD) (n = 6 rats). B) Correlation between vancomycin concentration in paired serum and ISF samples (r= 0.61, p<0.005, Pearson's correlation coefficient test). Dashed lines represent ± 30 % of the slope of the linear regression line (shown as solid black line), which are included as a visual guide. Data are the same as shown in (A)..... 90

Figure 6-3: Anti-polio IgG responses to inactivated polio vaccination in rats. a) Anti-polio IgG titers determined by ELISA in ISF and serum samples collected before and 1, 3 and 4 weeks after vaccination with trivalent IPV by intramuscular injection. Each data point represents a single animal while the bars represents the median values of each group (n = 6 rats). Asterisk (*) represents a significant difference (Student's t-test, p < 0.03). b) Correlation between anti-polio IgG titers in paired serum and ISF samples (r = 0.90, p<0.005, Pearson's correlation coefficient test). Dotted lines represent ± 30% of the slope of the linear regression line (shown as solid black line), which are included as a visual guide. Data are the same as shown in (a) 92

Figure 6-4: Neutralizing antibody responses to inactivated polio vaccination. Neutralizing antibody titers to a) IPV type 1, b) IPV type 2 and c) IPV type 3 in ISF and serum samples collected before and 1 and 2 weeks after administration of a booster dose of trivalent IPV by intramuscular injection in rats (the first dose was administered 12 weeks earlier). The limit of detection for the assay was 2.5 $\log_2$. Each data point represents a single animal while the bars represents the median values of each group (n = 6 rats). Asterisk (*) represents a significant difference (Student's t-test, $p < 0.01$). Correlation between neutralizing antibody titers in paired serum and ISF samples for d) IPV type 1, ($r= 0.89$, $p<0.005$, Pearson's correlation coefficient test), e) IPV type 2 ($r= 0.87$, $p<0.005$) and f) IPV type 3 ($r= 0.91$, $p<0.005$). Dotted lines represent ± 30% of the slope of the linear regression line (shown as solid black line), which are included as a visual guide. Data are the same as shown in (a) 93

Figure A-1: Effect of stabilizing excipients on (A) IPV type 1 and (B) IPV type 2 activity before drying, after air drying, after subsequent lyophilization and after storage. Vaccine was formulated with combinations of different excipients (each present at a concentration of 5% w/v) in 150 mM histidine buffer at pH 6.5 (see Table S1 for key to excipient formulations). In each set of bars, the first bar shows activity of liquid IPV formulated with excipients before drying. The second bar shows IPV activity after air drying at 5°C with desiccant overnight after casting onto PDMS chips. The third bar shows IPV activity after lyophilization. The fourth bar shows IPV activity after storage at 25 °C with desiccant for 1 week. The unformulated vaccine control data is

shown as D6 bars on the far left. All IPV activity (determined by ELISA) is shown as percentage of concentrated stock vaccine solution. Asterisk (*) indicates combination excipient formulation which maintained >80% activity drying and storage. Data represent mean ± SEM (standard error of the mean) of n= 3 replicates. 107

Figure A-2: Effect of formulation buffer and pH on (A) IPV type 1 and (B) IPV type 2 activity after air drying on PDMS chips, after subsequent lyophilization and after storage. IPV was formulated with 5% w/v maltodextrin and 5% w/v D-sorbitol in 0.1 M buffer with pH adjusted using 1 N HCl or 1 N NaOH. Storage was carried out at 40 ˚C for 3 or 7 days with desiccant. KHP: Potassium hydrogen pthalate, M199: Medium 199. In each set of bars, IPV activity (determined by ELISA) is shown in the first bar after air drying at 5°C overnight and lyophilization, in the second bar after storage in a desiccator at 40 ˚C for 3 days and in the last bar after storage at 40 ˚C in a desiccator for 1 week. Stability of unformulated IPV (i.e., without maltodextrin or D-sorbitol) in M199 media is shown in the bars on the far right. Hash (#) represents buffer which did not significantly affect IPV activity compared to activity in the vaccine casting solution (general linear model, $p > 0.80$). Asterisk (*) represents buffer which had the most adverse effect on IPV stability compared to activity in the vaccine casting solution (general linear model, $p < 0.03$). All IPV activity is shown as percentage of activity in the vaccine casting solution. Data represent mean ± SEM (standard error of the mean) of n= 3 replicates. 108

Figure A-3: Effect of 1st cast excipient ratio (maltodextrin to D-sorbitol) on (A) IPV type 1 and (B) IPV type 2 activity after fabricating MN patches, air drying, subsequent lyophilization and storage with desiccant at 40 °C for 2 days. Trivalent IPV was formulated with stabilizing excipients at a total concentration of 10 w/v% in the vaccine casting solution. The mass ratios used were MS80 (maltodextrin: D-sorbitol 80:20), MS50 (maltodextrin: D-sorbitol 50:50) and MS20 (maltodextrin: D-sorbitol 20:80). The 2nd cast polymer matrix solution consisted of 45 wt% fish gelatin to D-sorbitol (78:22) in 0.15 mM histidine buffer. All IPV activity (determined by ELISA) is shown as percentage of vaccine activity in the casting solution. In each set of bars, the first bar shows IPV activity in MN patch after air drying at 5°C in a desiccator for 2 days, the second bar shows IPV activity after additional lyophilization and the last bar shows the IPV activity after storage at 40 °C for 1 week with desiccant. There was no significant difference between the different ratios of maltodextrin to D-sorbitol (Student's t-test, $p > 0.05$). Data represent mean ± SEM (standard error of the mean) of n= 3 replicates..... 109

Figure A-4: Effect of 2nd cast excipient ratio (fish gelatin to D-sorbitol) on (A) IPV type 1 and (B) IPV type 2 activity after fabricating MN patches, air drying, further lyophilization and storing with desiccant at 40 °C for 7 days. Trivalent IPV was formulated with 10 w/v% casting solution of maltodextrin: D-sorbitol (20:80) and a 45 wt% 2nd cast solution consisting of varying mass ratios of fish gelatin to D-sorbitol. GS88 (fish gelatin: D-sorbitol 88:11), GS78 (fish gelatin: D-sorbitol 78:22) and GS55 (fish gelatin: D-sorbitol 55:45) in 0.15

mM histidine buffer. All IPV activity (determined by ELISA) is expressed as a percentage of IPV activity in the vaccine casting solution. In each set of bars, the first bar shows IPV activity in MN patch after air drying followed by lyophilization and the second bar shows the IPV activity after storage at 40 °C for 1 week with desiccant. Asterisk (*) indicates a significant difference between the IPV activity compared to other samples (Student's t test, $p < 0.05$). Data represent mean ± SEM (standard error of the mean) of n= 3 replicates. 110

Figure A-5: Effect of air drying, subsequent lyophilization and storage conditions on (A) IPV type 1 and (B) IPV type 2 activity of MN patches air dried at 5 °C, 25 °C or 40°C with desiccant. Trivalent IPV was formulated with 10 w/v% casting solution of maltodextrin: D-sorbitol (20:80) and a 45 wt% 2nd cast solution consisting of fish gelatin to D-sorbitol (78:22). All IPV activity (determined by ELISA) is expressed as a percentage of IPV activity in the vaccine casting solution. In each set of bars, the first bar shows IPV type 2 activity in MN patch after air drying, the second bar shows the activity after subsequent lyophilization, the third bar shows activity for MN patches storage at 40 °C for 1 week with desiccant (no lyophilization) and the last bar shows the activity for MN patches storage at 40 °C for 1 week with desiccant after lyophilization. Data represent mean ± SEM (standard error of the mean) of n= 3 replicates. 111

Figure A-6: Effect of storage temperature on IPV types 1, 2 and 3 activities of commercially available vaccine, IPOL® Sanofi Pasteur SA, Rockville, MD)

stored with desiccant for up to 1 months at 40 ˚C. Data represent mean ± SEM (standard error of the mean) of n= 3 replicates. 112

Figure A-7: Correlation of (A) IPV type 1 and (B) IPV type 2 activity in MN patches to RMC of the patches measured after storage at 5, 25 or 40 °C with desiccant or after storage at 40 °C and 50% relative humidity (RH). Regression analysis showed an R^2 value of 0.032 and 0.049 for IPV type 1 and IPV type 2, respectively. Data represent mean ± SEM (standard error of the mean) of n= 3 replicates. 112

Figure A-8: Correlation of (A) IPV type 1 and (B) IPV type 2 (C) IPV type 3 activity in MN patches to storage temperature of 5, 25 or 40 °C with desiccant. Regression analysis showed an R^2 value of 0.38, 0.39 and 0.67 for IPV type 1, IPV type 2, and IPV type 3 respectively. Data represent mean ± SEM (standard error of the mean) of n= 3 replicates. 113

Figure A-9: Representative X-ray diffraction (XRD) patterns corresponding to fish gelatin, maltodextrin and D-sorbitol used in preparation of MN matrix samples. 114

LIST OF SYMBOLS AND ABBREVIATIONS

ANOVA	Analysis of variance
AUC	Area under the curve
CDC	Centers for Disease Control and Prevention
cVDPV	Circulating vaccine-derived poliovirus
DMEM	Dulbecco's Modified Eagle Media
DSC	Differential scanning calorimetry
ELISA	Enzyme-linked immunosorbent assay
FBS	Fetal bovine serum
FTIR	Fourier-transform infrared spectrometry
GCC	Global Commission for the Certification of the Eradication of Poliomyelitis
GPEI	Global Polio Eradication Initiative
IgG	Immunoglobulin G
IM	Intramuscular
IPV	Inactivated polio vaccine
ISF	Interstitial fluid
KHP	Potassium hydrogen pthalate
MN	Microneedle
MSG	L-glutamic monosodium salt monohydrate
OPV	Oral polio vaccine
PDMS	Polydimethylsiloxane
PLGA	Polylactic-co-glycolic acid

PVP	Polyvinylpyrrolidone
RH	Relative Humidity
RMC	Residual moisture content
SC	Stratum corneum
SD	Standard deviation
SEM	Standard error of mean
Tg	Glass transition temperature
TGA	Thermogravimetric analysis
VAPP	Vaccine-associated paralytic polio
WHO	World Health Organization
XRD	X-ray diffraction

SUMMARY

The first half of this thesis is focused on the development of a dissolving microneedle (MN) patch for polio vaccination. Poliomyelitis (polio) is a highly infectious disease with no cure. Thus, the most effective strategy to eradicate polio is by vaccination. We developed a dissolving microneedle patch for administration of inactivated polio vaccine (IPV) with improved thermal stability when compared with commercial liquid IPV. A combination of maltodextrin, D-sorbitol and fish gelatin in histidine buffer was found to best preserve IPV activity during MN patch fabrication and storage. After 1 month at 40 °C, IPV activity was < 10 % for all three serotypes in a commercial liquid vaccine formulation but was > 40 % for all three serotypes in MN patches. In addition, activity remained >40% after 2 months and > 20% after 1 year of storage at 40 °C for all three IPV serotypes based on D-antigen content measured by ELISA. Residual moisture content in MN patches measured by thermogravimetric analysis, glass transition temperature measured by differential scanning calorimetry, structural changes measured by X-ray diffraction and molecular interactions measured by Fourier-transform infrared spectroscopy showed changes in MN matrix properties but did not correlate with IPV activity changes during storage. We conclude that appropriately formulated MN patches can exhibit thermostability that could enable distribution of IPV with less reliance on cold-chain storage.

The second half of the thesis is dedicated to the development of a simple MN patch for the collection of interstitial fluid (ISF) for diagnostic applications. ISF that surrounds cells in tissues of the body is a novel source of biomarkers similar to blood but relatively unexplored due to limitations in sampling techniques. To overcome difficulties in harvesting ISF, we developed a minimally invasive, rapid, simple-to-use and cost-effective method to collect ISF from the skin involving a MN patch. By pressing 650 µm long MNs at an angle just below the skin surface, blood-free ISF flowed through micropores to the skin surface and was absorbed into a thin strip of paper on the MN patch backing for subsequent analysis. An optimized method in rat skin in vivo was well tolerated and able

to collect > 2 µl of ISF within 1 min. Brief skin pre-treatment with MNs followed by a 5 min delay dramatically increased subsequent ISF collection by a mechanism believed to involve increased skin hydration. We demonstrated the suitability of our MN patch for therapeutic drug monitoring in ISF by showing similar vancomycin concentration-time profiles and pharmacokinetic parameters in the ISF and blood in rat in-vivo. We also, for the first time, detected polio specific neutralizing antibodies, and anti-polio IgG in ISF similar to blood in rats immunized with the polio vaccine. ISF collection using a MN patch has the potential to simplify access to biomarkers in ISF for research and future immunodiagnostic and monitoring applications.

CHAPTER 1. INTRODUCTION

This research presented in this thesis comprises of two projects. The goal of the first project was to develop a thermostable dissolving microneedle patch for Polio vaccination. The goal of the second project was to develop a paper based microneedle patch for collection of dermal interstitial fluid (ISF) to capture and detect a biomarker of interest.

1.1 Microneedle patch for polio vaccination

Polio is a highly infectious disease which can best be prevented by immunization [1]. The two most common routes of vaccination are IPV (Inactivated Polio Vaccine) which is administered as an intramuscular injection and OPV (Oral Polio Vaccine) which is administered orally. IPV is the safer method of vaccination but has several drawbacks, such as the need for a trained medical personnel, a reliance on the cold-chain for transportation and storage, and a possibility of needle-stick injuries[2]. Dissolving microneedles (MN) are micron-scale structures that can be designed to painlessly pierce the skin and deliver vaccines or drugs [3-5]. The advantages being the possibilities of self- administration, cold chain removal and lack of biohazardous sharps waste. The development of thermostable dissolvable MN patch for IPV could prove to be very useful for better vaccination coverage in developing countries.

The crux of this project was focused on fabrication and characterization of a dissolvable MN patch for polio vaccination which is thermally stable, mechanically robust, and

biocompatible. The development work was specifically geared towards the following areas:

a. Formulation optimization: finding the right combination and concentration of biopolymer (ex. silk fibroin and gelatin) along with other sugars or alcohols (ex. trehalose, sorbitol), buffer to stabilize dried IPV.

b. Processing parameter optimization: Drying temperature and time during microneedle fabrication.

The mechanical properties and long term thermal stability of the optimized MN patches were tested. Mechanistic studies were performed to correlate MN matrix properties to IPV activity using techniques such as Thermogravimetric analysis (TGA), Differential scanning calorimetry (DSC) and X -ray diffraction.

1.2 Paper based microneedle patch for collection of ISF

Rapid and reliable detection of a diverse set of biomolecules, such as metabolites, proteins and peptides are critical for disease management and regular health monitoring. Current diagnostic devices detect these biomarkers in body fluids such as blood, urine, saliva and sweat. Some of the issues with current diagnostic devices include the need for trained health care professional for blood collection by painful venipuncture, and need for large sample size. ISF is an unexplored body fluid which does not clot and has been shown to contain many biomarkers of interest for systemic and dermatological analysis [6-8]. However, ISF is not widely used for diagnostic applications due to limitations of existing sampling technologies such as limited sample volumes, patient discomfort and

need for sophisticated equipment. Hence, there is a need for an easy to use, reliable method for collection of microliters of ISF within minutes.

This project was geared towards development of an easy to use paper based MN patch for collection of microliters of ISF within minutes. Factors affecting ISF collection were tested and the optimized MN patch was tested in rats in-vivo to collect ISF for detection of biomarkers of interest. Simplified access to biomarkers in ISF using a MN patch may be beneficial for research and future medical diagnostic and monitoring applications.

CHAPTER 2. LITERATURE REVIEW

2.1 Poliomyelitis

Poliomyelitis, often known as polio is a highly contagious disease caused by any one of the three serotypes, wild polio virus type 1(WPV1), type 2(WPV2) or type 3(WPV3). Most of the infected people (~90%) are asymptomatic[9]. However, only in a small percentage of cases the virus enters the nervous system[10]. This can lead to paralysis of limbs and in some rare fatal cases, paralysis of respiratory system as well.

Poliovirus is a member of the enterovirus subgroup, family Picornaviridae[11]. This means that polio virus is a transient inhabitant of the gastrointestinal tract and a small virus with an RNA genome enclosed in a protein shell called a capsid. It is known to infect via the fecal-oral route [12]. The Global Polio Eradication Initiative (GPEI) was established by the World Health Organization (WHO) in 1989 to spearhead the efforts to eradicate polio[13]. Thanks to GPEI's continuous efforts, the number of polio cases have dropped from 350,000 in 1988 to only 22 reported cases in 2017[14]. WPV2 has been eradicated and has not been detected since 1999. The Global Commission for the Certification of the Eradication of Poliomyelitis (GCC) certified WPV2 as eradicated in September 2015. WPV3 was last detected in November 2012 in Nigeria. WPV1 is the only serotype that is currently endemic to three countries (Afghanistan, Nigeria, and Pakistan). However, the WHO predicts that failure to eradicate this disease can cause as many as 200,000 new cases every year in 10 years[15].

2.1.1 Vaccine Delivery

2.1.2 Current polio vaccine delivery routes

There are two types of vaccines that protect against polio: IPV and OPV. IPV which is also known as “Salk vaccine” is an intramuscular injection of inactivated (killed) polio vaccine of all three serotypes[16]. OPV which is also known as “Sabin vaccine” consists of a mixture of live attenuated (weakened) polio viruses[17]. OPV is the vaccine of choice in developing countries because it is significantly cheaper, easy to administer, only requiring an oral delivery of 2 drops of vaccine[18]. The attenuated virus can then, infect the lymph tissues of the gut. This mimics the natural route of infection and generates a potent immune response. However, a major concern with OPV is the possibility of causing vaccine-associated paralytic polio (VAPP)[19]. Another low risk is the possibility of a viral recombination of attenuated strain reverting to the wild type. This is known as circulating vaccine-derived poliovirus (cVDPV). The risk of reintroducing polio in US led to the phase out of OPV from the childhood immunization schedule[20]. OPV was replaced by IPV in US and UK in 2000 and 2004 respectively[21].

The biggest drawbacks with IPV are the need for intramuscular (IM) injection [22] and the high cost of the vaccine[16]. The current IPV formulation requires multiple doses for a potent immune response[23]. Two doses of IPV provide 90% immunity to all three polio serotypes and 3 doses provides at least 99% immunity.

IPV requires that healthcare personnel administer the vaccine, and even with the training healthcare personnel receive, needle-stick injuries are common. These can lead to the exposure to unknown pathogens and the transmission of blood-borne infectious diseases[24]. Medical waste and safe disposal of sharps can pose problems especially for large scale campaigns [25]. Also, trained healthcare professionals many not be available especially in rural areas of developing countries.

Patients can be hesitant to receive any treatment via an injection due to the pain of injection and needle-phobia. This decreases patient compliance [26]. Disposal of used needles presents a hazard too. Also, IPV is currently formulated as a liquid (in medium 199)[27] and is stable for over a year at 4°C, but loses potency in only weeks at 25 °C or 37 °C [28].

Hence, it is of great interest to develop an easy to administer, thermostable IPV formulation.

2.1.3 Microneedle patches for vaccine delivery

A novel method for vaccine delivery is by using MN patches. As a micron-scale device, a MN patch has the ability to penetrate the barrier layers of the skin in a minimally invasive manner[29].

Skin is the largest and most accessible organ of our body. This makes it attractive for drug or vaccine delivery. Skin essentially consists of three layers: the epidermis, the dermis and the subcutaneous layer. The epidermis consists of the outermost layer, stratum corneum (SC) and the viable epidermis. SC is a 20 μm thick[30] layer made up of brick and mortar type flat dead corneocytes tightly joined by intercellular lipids. The viable epidermis (50-100 μm thick) is avascular and consists of ten layers of randomly oriented living cells like keratinocytes and basal cells. The epidermis is rich in Langerhan cells which can help invoke an immune response[31].

The epidermis and dermis are separated by the basement membrane. The dermis is the thickest layer of the skin and has thickness ranging from 1-2 mm. The dermis has a water content of about 70%. It is vascular, has hair follicles, sebaceous glands, sweat glands and

lymphatic system. The dermis contains dendritic cells which are thought to induce cell-mediated immune responses[32]. They have also been shown to enhance antibody production by B cells. The dermis also plays a role in inflammatory response and also provides nutrition to the epidermis.

The subcutaneous tissue consists of the interstitial tissue and the adipose tissue[33]. It has water content similar to the dermis and its functions include preserving body heat and acting as shock absorber.

Vaccines are typically made up of either whole virus particles or selected antigen subunits. They are macromolecules and do not passively diffuse across the SC easily. Traditional vaccine delivery by injection bypasses the skin's immune system and delivers the antigen into the muscle or sub-cutaneous tissue. The premise behind using microneedle technology is that vaccine delivery can be significantly improved if the SC layer is breached [34]. The MN patch is designed to be long enough to penetrate the SC, but short and thin enough to avoid the blood vessels and nerves in the dermis layer. Hence, MNs have the unique advantage to be large enough to deliver almost any vaccine, but still be small enough to avoid pain, fear and the need for expert training to administer. MN patches have also been demonstrated to be patient-friendly and user compatible[35]. There is a potential for greater immunogenicity too because the vaccine is delivered in the epidermis region.

There are various types of microneedles such as the solid microneedles, coated microneedles, hollow microneedles, dissolving microneedles and swellable microneedles.

Zhu et al. demonstrated that metal microneedles coated with inactivated influenza vaccine could immunize mice by simple skin insertion[36]. The group receiving MN patch had

superior protection against a challenge with live influenza virus compared with mice receiving the same dose via an IM injection. Other vaccines such as hepatitis C [37] and Bacillus anthracis[38] have also been delivered using coated steel microneedles.

Further development of microneedle technology resulted in dissolving polymeric MN patches. Dissolving polymer MN patches are composed of a vaccine and other excipients such as stabilizers, adjuvants loaded in a water soluble, biocompatible polymer matrix. A variety of polymers such as polylactic-co-glycolic acid (PLGA), polyvinylpyrrolidone (PVP) and maltose [3,39,40] have been used for MN patch fabrication. The needles have been shown to be mechanically robust to penetrate the SC and dissolved by the ISF thereby delivering the vaccine. An example of dissolving polymer microneedle is shown in Figure 2-1.

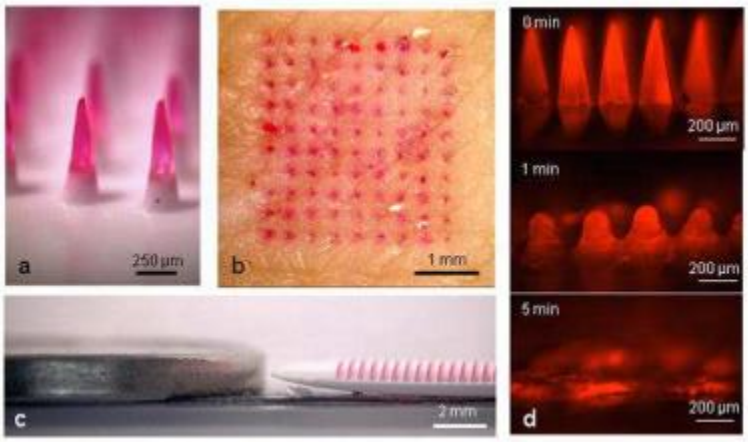

Figure 2-1: Example of a dissolving MN patch. A: Dissolving MN patch at high magnification. B: Pig skin after insertion and dissolution of a dye-containing MN patch. C: Side by side comparison of a dissolving MN patch to a US nickel coin. D:

Dissolving MN patch before and after insertion. Image reproduced from Sullivan et al.[3].

Dissolving MN patches can be self-administered painlessly[41] with no sharps as waste. Dissolving MN patches have been used for various vaccinations such as measles[42] and influenza[43]. In the influenza vaccine study, Sullivan et al. encapsulated the vaccine in a PVP MN patch and deposited in the skin of mice. This resulted in a potent immune response that protected the mice against a lethal challenge.

2.1.4 Current polio vaccine stabilization strategies

Commercially available full human dose of IPV vaccine contains a trivalent dose of 40 D-antigen units (DU) of type 1, 8 DU of type 2 and 32 DU of type 3 polio virus[44]. It is formulated in aqueous medium (Medium 199) along with other chemicals. 2-phenoxyethanol, a glycol ether is used as preservative. Formaldehyde is added to inactivate the virus while antibiotics such as neomycin, streptomycin, polymyxin B are added to prevent bacterial contamination [43]. $MgCl_2$ is currently used in the pharmaceutical industry to stabilize Sabin vaccine or OPV[45].

Other researchers have tried to stabilize polio virus (IPV/OPV) and increase thermal stability by addition of various stabilizing agents. Robinson et al. showed that lipolysachcharides (LPS) and peptidoglycan increased the thermal stability of Sabin serotype 1 by binding to the capsid protein[46]. Dorval et al. showed that fatty acids, in particular, lyotropic salts significantly stabilize poliovirus[47]. They also showed that amino acids such as L-lysine and L-arginine are effective in preventing heat inactivation of poliovirus[48]. Other groups showed addition of pirodavir[49], or replacement of water with deuterated water[50] were beneficial. However, all of these studies were performed

in liquid formulations and on Sabin vaccine and may not be useful for MN patches, which are dried and use Salk vaccine.

MN patch fabrication involves drying of the formulation for the formation of solid MNs. As the vaccine is removed from an aqueous environment, it undergoes changes that decrease its specific antigenicity[51]. Hence, sugars such as trehalose, or sucrose may have to be added to help maintain the environment necessary for the native structure of the biomolecule[52].

Other researchers showed that virus particles can be encapsulated in silk or other proteins to prevent conformational changes and improve thermal stability[53] [54].

Lyophilization is one of the oldest and commonly used technique for preparation of solid protein pharmaceuticals. However, this process can generate different types of stresses, such as solute concentration, formation of ice crystals, pH changes etc. Kraan et al. performed extensive excipient screening and developed a formulation containing sorbitol, $MgCl_2$ and L-glutamic monosodium salt monohydrate (MSG) for stabilization of lyophilized IPV[55]. They also performed in-vivo studies and showed comparable immunogenicity to liquid IM injection when administered in a booster regime[56].

2.1.5 Motivation for research on MN patch for IPV administration

Since 1988, the world has come very close to eradicating polio. Despite numerous efforts to simplify delivery of the polio vaccines, hurdles still exist. The requirement for trained medical personnel limits the reach of large-scale campaigns especially in the polio endemic countries. Necessity for cold chain to maintain vaccine stability can be burdensome too. A

safe, thermostable, dissolving MN patch for IPV administration would represent a significant advance, removing many of the hurdles remaining in the eradication of this disease.

2.2 Disease diagnosis and monitoring

The analysis of body fluids is vital for the diagnosis and monitoring of a disease. An alteration in concentration or composition of a particular biomarker in a body fluids is used as an indicator of a physiological or pathological condition [57].

Traditionally, diagnostic procedures are performed mainly by health care professionals during a doctor's visit or in a hospital setting. Recent trend in diagnostics is the emergence of point of care diagnostics. Point of care diagnostics enables rapid diagnosis for efficient management of variety of conditions and diseases in a clinic, an ambulance or even at home. The point of care testing is an emerging trend in diagnostics and is driving innovation in global health [58].

Many diagnostic devices detect changes in certain biomarkers. The measured response could be a physiological, biochemical, functional or a molecular interaction.

Many biomarkers have been validated for monitoring and treatment of various disease. Detection of such markers at an early stage can lead to a prompt diagnosis, and reduction in rising healthcare costs[59]. Infectious diseases such as malaria, and dengue can be easily diagnosed with a simple blood test for a timely treatment. Routine monitoring of blood sugar levels is performed by diabetics. Blood pressure and cholesterol levels are periodically checked by people with cardiovascular diseases.

2.2.1 Sources for biomarkers

Biomarkers have been detected in various body fluids. Most commonly used body fluids for biomarker detection are blood[60], urine[61], saliva[62], tears[63], and sweat[64]. However, the gold standard for most diagnostic tests is blood because it is well studied and is systemic. Blood may be collected via venipuncture, or finger stick. Venipuncture is the extraction of blood from the vein by using a needle and a syringe. Finger stick, also known as capillary puncture, involves blood collection by puncturing the fingers, ear lobes, or the big toe side of the heel (in infants) with the use of a lancet.

Finger sticks are routinely done by patients to collect capillary blood. Finger sticks are commonly done at home for blood glucose monitoring, pro-thrombin measurements. However, blood volume collected by finger sticks are variable and may be erroneous due to contaminants from skin surface[65].

Venipuncture allows for multiple blood collections and collection of larger blood volumes. The samples can be stored in vacutainer containers for future testing too. It provides more reliable results because the specimens are collected directly from the systemic circulation. However, the main disadvantage of venipuncture is the need for a skilled phlebotomist to perform the blood draw. Another disadvantage is the difficulty to perform it in infants, obese people or burn victims.

Other body fluids such as tears, sweat, urine and saliva are easy to access. Most commonly used urine based test is for detection of ovulation, or pregnancy [66]. However, concentration of biomarkers in urine can be affected by circadian variations [67] and water intake [68].

Saliva can be used for detection of drug concentrations and diseases pertaining to the gastrointestinal track [69]. Saliva has also been used for diagnosis of glucocorticoid related diseases[70]. Antibodies present in saliva could be used for diagnosis of many infections such as hepatitis A and B [71]. However, the accuracy of these assays are affected by presence of food substances in the mouth.

There has been a significant interest in sweat analysis due to its potential for detecting sodium content which can provide valuable information about an individual's physical and mental wellbeing[72]. However, currently available methods for sweat analysis are not optimized for in home usage.

Tear fluid also has the potential to be used for diagnosis. Proteomic pattern of tear fluid has been shown to be useful for breast cancer detection[73]. However, it is challenging to collect tear fluid samples frequently.

2.2.2 Interstitial fluid (ISF)

The human body fluids can be conceptually divided into two main fluid compartments: intracellular and extracellular compartments. The intracellular compartment comprises of fluid enclosed in the cells by their plasma membranes. Cytosol or cytoplasm is the principal component of intercellular compartment. The extracellular fluid compartments mainly consists of blood (also called plasma), and ISF. A small portion of the extracellular fluid comprises of cerebrospinal fluid (fluid in brain and spinal cord), synovial fluid (fluid in joints), pleural fluid (fluid in the pleural cavities), pericardial fluid (fluid in cardiac sac),

peritoneal fluid (fluid in the peritoneal cavity) and the eye's aqueous and vitreous humor

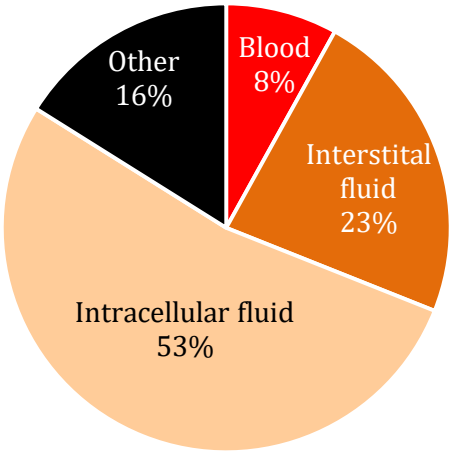

.

Figure 2-2: Pie chart showing the percentages of intracellular and extracellular fluids[74,75]

Also known as tissue fluid, ISF is the fluid found between the cell spaces. It leaks out of the blood capillaries due to transcapillary exchange during blood flow from arterioles and venules. The main function of ISF is to provide oxygen and essential nutrients to the cells. The ISF is constantly reabsorbed into the systemic circulation or drains into the lymph vessels. ISF forms around 20-25% of body weight [74].

There are several mechanisms involved in transcapillary exchange of fluid. The most important are bulk flow and diffusion. The net driving force is determined by the hydrostatic pressure, oncotic pressure and the permeability of the capillary wall separating the blood and the interstitium[76].

There are two opposing hydrostatic pressures: capillary hydrostatic pressure (P_c) and tissue interstitial hydrostatic pressure (P_i). The net hydrostatic pressure gradient (P_C - P_i) across the capillary is positive, because P_c is normally higher than P_i. Hence, the net hydrostatic pressure gradient drives the fluid out of the capillaries.

The two opposing oncotic pressures are: capillary oncotic pressure ($\prod_c$) and tissue oncotic pressure($\prod_i$). The capillary oncotic pressure is dependent on plasma proteins which are impermeable through the capillary. The net oncotic pressure gradient ($\prod_c$ - $\prod_i$) would reabsorb the fluid back into the capillary. The net oncotic pressure is also dependent on the permeability of the capillary walls. Hence, the net driving force (NDF) for fluid movement is dependent on individual pressure gradients.

Equation 1

$$\mathbf{NDF = (P_C - P_i) - \sigma(\prod_c - \prod_i)} \quad \mathbf{(1)}$$

where σ is the reflectance coefficient, a measure of the permeability of the capillaries to proteins causing oncotic pressure. NDF > 0 results in filtration of fluid from the capillaries to the interstitium while NDF < 0 results in reabsorption.

The capillary walls allow most hydrophilic small molecules to freely equilibrate between the plasma and ISF. Hence, the concentration of sodium, chloride and glucose should be similar between ISF and plasma. ISF contains important amino acids, fatty acids, hormones, salts, coenzymes etc.[77] from cells and cell debris.

Many previous studies have shown the potential to use ISF for diagnosis of biomarkers of interest. ISF contains many unique biomarkers and certain biomarkers are elevated in ISF

compared to plasma[78]. Since it contains cellular and systemic biomarkers, ISF can be a valuable body fluid that can be used to detect systemic and local environmental changes.

Unlike blood, ISF does not clot. This provides ISF the unique advantage for continuous monitoring such as analysis of biomarkers for exhaustion prediction[79]. This is the reason for the recently developed commercial glucose monitoring devices by companies such as Dexcom[80] and Medtronic[81].

2.2.3 Methods for ISF collection

Various methods have been developed to collect ISF from skin. Some of the methods are suction blister, microdialysis/microperfusion, reverse iontophoresis, use of ultrasound and microneedles.

2.2.3.1 Suction blister method

Suction blister method, initially developed in 1968[82], is the most widely used method for ISF collection. As the name implies, this method involves artificially inducing blisters by usage of negative pressure for up to 2 hours at an elevated temperature of up to 40°C. The procedure involves slow detachment of the epidermis from the underlying dermis which induces the blister to be filled with ISF. The ISF can then be collected with a conventional needle and syringe. This technique has been used to assess wound healing[83], and effectiveness of psoriasis[84] and vitiligo treatment[85]. However, the disadvantages of this method include the need for specialized equipment and expertise, long procedure times (up to 2 hours), and increased risk of infections. The wound could take 7-10 days to heal. Some subjects develop hyperpigmentation at the wound site which

could last for several months. This is still the only technique available to sample large volumes of ISF.

2.2.3.2 Suction effusion

This method involves using an adhesive tape to remove the SC followed by application of a suction device. Kayashima et al. collected 35ul/hr of ISF for 3 hours by applying 400mm Hg of negative pressure after tape stripping 7.1cm^2 of skin area of rabbit[86]. However, concerns regarding the invasive nature of tape stripping have limited the utility of this method.

2.2.3.3 Wick sampling

This method was first performed by Aukland et al. in 1973[87]. It involves implanting nylon wick into the subcutaneous tissue of rats to collect ISF. The wicks imbibe the ISF which is later extracted by centrifugation. Some of the disadvantages of this method are small sample volumes and its invasive nature. However, wick sampling has been used by several investigators both in animals[88] and humans[89].

2.2.3.4 In-vivo ultrafiltration

This method involves insertion of a small probe with semipermeable membrane into the tissue. Application of negative pressure induces the convective flow of ISF. The semipermeable membrane has a molecular cutoff of 20kDa to 50kDa, thereby excluding protein and cell fragments. Ultrafiltration probes have only been used in animal studies due to the invasive nature of the procedure and potential risk of infection. However, this method does allow sampling of microliter quantities of ultrafiltrate from skin, or even bone interstitium[90].

2.2.3.5 Microdialysis and microperfusion

Microdialysis was first used by Ungerstedt and Pycock in 1974 for measurement of neurotransmitter concentrations in rat brain[91]. This technique can be used for continuous sampling of unbound analyte concentrations in extracellular fluid from any tissue.

The microdialysis system involves a dialysate pump, a microdialysis probe and a collection system for the microdialysate. The probe with a semipermeable hollow dialysis membrane is implanted into the skin. The perfusate is flown through the probe at a predetermined flow rate by means of a volumetric micropump. The solutes present in ISF slowly diffuse into the perfusate due to concentration gradient. The perfusate containing components of ISF is finally collected. Microdialysis is a useful method for measuring concentrations of low molecular weight analytes. This method has been used for measurement of glucose[92] and other biomarkers[93,94][i]. However it is not suitable for measuring protein concentrations due to the molecular weight cut off of the semipermeable membrane. Also, frequent calibration is required to ensure sensitivity and precision in concentration measurements.

Open flow microperfusion method involves implantation of a stainless steel mesh into the skin. The perfusate flows through the mesh and collects components from ISF via diffusion. Since, no dialysis or filtration occurs, the perfusate collects proteins too. This method has been used for monitoring drug concentrations in the skin[95]. The disadvantage of this method is the small amount of ISF collected over time, which results in poor time resolution, and the invasive nature of the procedure.

2.2.3.6 Reverse Iontophoresis

This technique was first used by Benjamin et al. to extract subcorneal potassium and sodium[96]. In this method, a small electric current (usually 0.2-0.8mA) is applied across the skin. Since skin is negatively charged, it allows for preferential electromigration of small cationic substances towards the cathode. The movement of these ions induces a convective flow of ISF that contains uncharged water-soluble substances such as glucose and urea by electrosmosis towards the skin surface. The non-invasive nature of this method has resulted in development of point of care diagnostic devices.
Glucowatch is one such device that measures concentration of glucose in skin by reverse iontophoresis[97]. However, some of the limitations of this method include the need for frequent calibration to maintain accuracy[98] and the possibility for skin irritation due to continuous use and prolonged application of electric current across skin.

2.2.3.7 Low frequency ultrasound

This method can be used to sample dermal ISF non-invasively. This method uses low frequency ultrasound (20 kHz and 7W/cm^2 intensity for < 1 min) to disrupt the SC and enhance the permeability of ISF onto the skin surface[99].

2.2.4 Microneedles for sampling ISF

There has been a rapid progress in microfabrication techniques. MNs have not only been used to deliver vaccines, drugs but have also been investigated as a diagnostic tool to extract analytes from the skin for sensing[100]. MNs can enable minimally invasive sampling of dermal ISF. They are portable, hence can be easily adapted to point of care devices. Unlike the transdermal patches, MNs penetrate the SC and directly access the ISF.

There could be two approaches for using MNs in diagnostics. MNs could be used to form micropores on the skin surface to provide pathway for the flow of ISF onto the surface. The ISF can then be collected and analyzed for the biomarker of interest.

Another approach could be to have a MN device with a built in sensor for collection and detection of a specific biomarker. Research has been focused on both of these approaches.

Kobayashi et al. developed a hollow MN system inspired by blood extraction action of a mosquito. The MN system was made with a phase transition gel as actuator[101]. The gel characteristics were modified for continuous glucose monitoring[102].

Mukerjee et al. developed a hollow silicon MN patch using deep reactive ion etching[103]. Upon insertion in the skin, the hollow MNs drew ISF via capillary forces and collected into a reservoir. The device was tested in humans for qualitative glucose detection onto a colorimetric paper after 15-20 min extraction [104]. In one approach, up to a few microliters of ISF were extracted under suction from skin pretreated with MNs; measured glucose concentrations in the extracted ISF showed excellent correlation with corresponding blood glucose levels in rats and human subjects [105].

Miller et al. developed MNs with integrated carbon fibers in the bore for detection of small analytes such as ascorbic acid [106].They also performed in-vivo human studies and successfully detected hydrogen peroxide and lactate concentrations [107]. They further developed a multiplexed MN sensor by enzyme functionalizing the carbon paste and demonstrated the utility of this MN sensor to simultaneously detect pH, lactate and glucose [108]. Miller et al. also developed a hollow MN device with built in solid state ion selective electrodes for sensitive detection of potassium ion concentrations [109].

Wang et al. used solid glass MNs to form micropores in the skin. A negative pressure (200-500 mmHg) was then applied for 2-10 min. ISF (1-10 µl) was then collected from skin surface of mice and humans. Glucose concentrations in ISF and blood were found to be well correlated and a lag time of change in glucose concentration in ISF was found to be ~10 min [110].

Zimmerman et al. developed a MN patch with built in glucose sensor. The MNs were 250 µm long and used capillary action to collect ISF. In-vitro testing showed linear response to glucose concentration, however, the device response was variable in vivo due to variation in flowrates [111].

Other researchers developed a similar device based on hollow MN device with built in glucose oxidase based sensor [112]. There is a growing interest in the area of continuous glucose monitoring with new innovations such as a self-powered biofuel cell based glucose sensor[72] and a single MN patch system for glucose sensing and insulin delivery [113].

Corrie et al. developed a MN array coated with a capture protein for in-situ detection of influenza specific antibodies in mouse plasma and ISF [114]. Similarly Muller et al. coated microneedles with dengue virus NS1 and IgG specific proteins and demonstrated that the NS1 levels in ISF and blood correlated well [115].

Sato et al. developed a microneedle system for measurement of interstitial glucose. They used solid MNs to make micro pores on the skin, and then placed a hydrogel patch with an osmolyte on the pretreated site for ISF extraction. The study compared blood glucose levels on diabetic and non-diabetic patients. The blood and ISF glucose levels were well correlated and the lag time was found to be ~10 min [116]. Donnelly et al. developed

swellable microneedles made of copolymer of methyl vinyl ether and maleic acid. The MNs remained in dry state initially but were swollen by ISF upon insertion into skin [117]. Caffarel-Salavdor et al. inserted these MN patches in human subjects and correlated caffeine and glucose concentrations in ISF and blood. The caffeine and glucose concentrations were 2-3 orders of magnitude lower in the ISF and the lag time was as high as 3 hours. This implies that the ISF extraction rate was very low [118]. Romanyuk et al. developed crosslinked hydrogel microneedles composed of poly (methyl vinyl ether-alt-maleic acid) and poly (ethylene glycol). They demonstrated that upon skin insertion, the MN patches swelled with ISF which was later collected by centrifugation [119]. Chang et al. showed that their swellable microneedles could collect up to 3ul of ISF in 30 min. They demonstrated good correlation between glucose and cholesterol levels in ISF and blood [120]. More recently, Samant et al. used MN patch to form micropores on skin and collected 1-10 µl of ISF by applying vacuum. They demonstrated that the rate-limiting step for ISF sampling is often transport through the skin to the site of MN puncture, and forces that generate convective flow in the skin can significantly facilitate ISF collection[121].

2.2.5 Motivation for research on ISF collection using microneedles

Most of research previously conducted for ISF collection involved usage of MN devices which collect submicroliters of fluids, and the ISF collection process is time consuming. ISF remains an unexplored body fluid because of a general need for simple methods to sample this fluid reliably and quickly.

The goal of this study is to develop a simple, easy to use MN device for collection of microliters of ISF within minutes. The development of a reliable and simple MN system could enable exploratory research on biomarkers in ISF.

Development of such a MN device could have a large impact on clinical medical diagnostics. Having a portable MN device for quick and easy detection and monitoring of chronic disease such as diabetes, cardiovascular disease could be beneficial. Such devices could also be used by elite athletes or people with high stress jobs for detection of biomarkers such as lactate, creatinine, and uric acid. A MN device made with inexpensive and easily available materials and that requires minimal training to use, could be well suited for use as diagnostic or monitoring systems, including in developing countries.

Other potential uses include detection of drugs and other biomarkers of interest in ISF. For example, Vancomycin is an antibiotic which has a very narrow therapeutic index and warrants a therapeutic drug monitoring (TDM) to ensure efficacy and minimize toxicity during patient care [122]. Kiang et al. used ultrafiltration probe to sample ISF and demonstrated similar vancomycin concentration-time profiles in ISF and blood, in rabbits [123]. Other researchers have shown promising results with similar AUC between serum and ISF samples for drugs such as scopolamine, theophylline, methotrexate, carbamazepine and phenobarbital in ISF [124-126]. However, the methods employed for ISF collection are invasive and may not be translated into humans. Hence, there is a need for a minimally invasive device for collection of microliters of ISF for future diagnostic applications.

CHAPTER 3. SPECIFIC AIMS AND HYPOTHESES

Aim 1a: Formulate thermostable MN patch for polio vaccination

Hypothesis: *Fabrication of MN patch by optimization of formulation i.e. excipients and biopolymers and processing conditions, i.e. drying time stabilizes polio vaccine during extended storage at elevated temperature.*

Expected outcomes: Characterization of how formulation and process parameters affect IPV stability and design of optimized MN patch which is thermostable.

Aim 1b: Characterize relationships between changes in MN patch material properties and IPV stability

Hypothesis: *Characterization of the optimized MN patch will help understand excipient-IPV interactions.*

Expected outcomes: Identification of possible correlations between MN patch properties and IPV by DSC, TGA, and other techniques.

Aim 2: Develop an easy to use paper based MN patch for ISF collection

Hypothesis: *Optimization of MN patch parameters will result in an MN patch for easy ISF sampling.*

Expected outcomes: Identification of possible MN parameters which influence the ISF collection and design of an optimized MN patch which can easily collect 2- 4 µl of ISF within a minute.

Aim 3: Demonstrate the utility of the optimized MN patch for detection of biomarkers of interest in ISF

Hypothesis: *The optimized MN patch will be able to collect sufficient quantities of ISF for quantitative detection of biomarkers of interest in ISF.*

Expected outcomes: Extraction and quantification of biomarkers of interest in ISF and correlation to blood concentrations.

CHAPTER 4. DEVELOPMENT OF A THERMOSTABLE MICRONEEDLE PATCH FOR POLIO VACCINATION

4.1 Introduction

Poliomyelitis is a highly infectious disease which mainly affects children. The disease can be caused by any of the three serotypes of IPV (type 1, type 2 or type 3) and can be prevented by immunization[127] Thanks to the Global Polio Eradication Initiative (GPEI), the number of polio cases has dropped from 350,000 in 1988 to only 22 reported cases in 2017[ii]. IPV type 1 is the only serotype that is currently endemic to three countries (Afghanistan, Nigeria, and Pakistan) and wild-type IPV type 2 has been eradicated[128]. However, WHO predicts that failure to eradicate this disease can reverse these advances and cause as many as 200,000 new cases every year in 10 years[15].

The progress made so far is predominantly due to mass vaccination using the oral polio vaccine (OPV) which is a live-attenuated virus given my mouth[129]. OPV offers advantages such as low cost, ease of administration only requiring oral delivery of two drops of vaccine, no sharps and generation of mucosal immunity. However, a major concern with OPV is the possibility of genetic reversion to a virulent form that can cause vaccine-associated paralytic polio (VAPP)[19] and can be transmitted to others. A safer alternative is inactivated polio vaccine (IPV), which does not carry the risk of paralysis or transmission, but is administered as an intramuscular (IM) injection[130].

To eliminate the risks of VAPP, OPV was replaced by IPV in United States and United Kingdom in 2000 and 2004, respectively[21], and plans to discontinue use of OPV worldwide by 2019 are underway[131]. However, the biggest drawbacks of

switching to IPV are the need for trained medical professionals administer IM injections, generation of sharps waste, need for cold chain storage, high cost of the vaccine, and need for multiple doses for a protective immune response[16,23,28].

In this study, we propose the use of a dissolving microneedle (MN) patch for IPV vaccination. When a MN patch is applied to the skin, micron-scale, solid needles made of safe, water-soluble excipients that encapsulate vaccine penetrate the outer barrier layer of the skin, where they dissolve and release their vaccine payload[29]. MN patches can be self-administered painlessly[41,132,133] generating no sharps as waste and have been used previously for various vaccinations[134] ,including IPV[135] and a recent clinical trial on influenza [43]. Encapsulation of vaccines in appropriately formulated MN patches has been shown to increase vaccine thermostability [136]. It was therefore our objective to formulate a MN patch for IPV vaccination that can provide thermostability that reduces reliance on cold-chain storage, eliminate the need for administration by trained health care professionals and avoid the safety risks and disposal costs of sharps waste. This approach could facilitate mass vaccination campaigns, especially in developing countries, which are needed to achieve polio eradication [137].

4.2 Materials and methods

4.2.1 Concentration of inactivated polio vaccine

Monovalent, bulk IPV (Mahoney strain of type 1, Middle East Forces (MEF) of type 2 and Saukett of type 3) was kindly provided by Bilthoven Biologicals (Bilthoven, Netherlands). The initial antigen concentrations were 1675, 963 and 950 D-antigen units (DU)/ml for

IPV types 1, 2 and 3, respectively. The bulk IPV was concentrated using Amicon Ultra centrifuge spin filters with 100 kDa MW cutoff (EMD Millipore, Billerica, MA) either ~10-fold by volume to a final antigen concentration of 1.7×10^4, 9.6×10^3 and 9.5×10^3 DU/ml for IPV types 1, 2 and 3, respectively, or ~47- fold by volume to a final antigen concentration of 7.9×10^4, 4.8×10^4 and 4.5×10^4 DU/ml for IPV types 1, 2 and 3, respectively. All D-antigen values were determined by ELISA, as described below.

4.2.2 Vaccine stability screening

To increase throughput of formulation screening, candidate vaccine-excipient formulations were dried on polydimethylsiloxane (PDMS) chips, which are representative of the surface of a MN patch mold. PDMS chips were prepared by curing a thin film of Sylgard 184 (Dow Corning, Midland, MI) and preparing 6 mm diameter circular discs using a hammer punch. IPV was concentrated 10-fold by volume and mixed with selected excipients. A 10 µl drop of formulated vaccine solution was placed on each chip and allowed to dry at 5 °C in a desiccator filled with desiccant (Drierite, W A Hammond Drierite, Xenia, OH) overnight. After reconstituting the dried IPV in 999 µl media M199, the D-antigen content of the IPV was determined by ELISA, as described below. All excipients were purchased from Sigma Aldrich (St. Louis, MO).

4.2.3 Microneedle patch fabrication

PDMS molds consisting of a 10 x 10 array of cavities that form the MNs were fabricated as described previously[138]. The antigen casting solution was prepared by mixing 47-fold

concentrated vaccine with a solution consisting of a 10% w/v maltodextrin and D-sorbitol in 0.35 mM histidine buffer at pH 6.3. Fifty microliters of the antigen solution was cast onto a MN mold, which was then centrifuged for 1 h at 5 °C to fill the mold cavities with solution and partially dry the solution in the mold, following a procedure previously described[139].

The polymer matrix solution used to form the MN patch backing consisted of 35% w/v fish gelatin and 10% w/v D-sorbitol in 0.15 mM histidine buffer. The solution was mixed for 1 h at 35 °C until completely dissolved. Two hundred microliters of polymer matrix solution was cast onto a mold pre-filled with partially dried antigen solution. The mold was then placed under vacuum for 2 h at room temperature (20 – 25 °C) and stored in a desiccator at room temperature for 2 days before demolding. Demolded patches were packaged with desiccant in aluminum pouches to maintain 0% RH (relative humidity) and stored at a given temperature (i.e. 5, 25 or 40 °C) in stability chambers. For experiments involving storage at ~50% RH, patches were stored in a desiccator containing a saturated solution of magnesium nitrate in distilled water[140].

4.2.4 Microneedle composition

The composition of MNs (i.e., just the MNs without the patch backing) was determined by preparing placebo patches (i.e., with no IPV, but otherwise fabricated in the same way) and carefully cutting off the MNs. The MNs were reconstituted in water and the protein content was determined using micro BCA protein assay kit (Thermo Fisher Scientific, Waltham, MA), which was interpreted to be roughly equal to the gelatin content, since the only

protein in a placebo patch should be gelatin from the polymer matrix solution used during the second cast which could migrate into the MN during the fabrication process. In this way, the composition of the MNs was estimated to be fish gelatin, D-sorbitol and maltodextrin in a mass ratio of 55: 38: 7. This formulation was used when studying IPV stability on chips that simulate MN composition. The chips were stored at a given temperature (i.e. 5, 25 or 40 ℃) for specified times in stability chambers.

4.2.5 Lyophilization

To study the effect of lyophilization on IPV stability, demolded MN patches and dried IPV-excipient chips were subjected to lyophilization (VirTis AdVantage 2.0 BenchTop lyophilizer, SP Industries, Warminster, PA). The lyophilization process involved a primary drying at -45 ℃ (10 mTorr) for 3 h followed by a secondary drying at 25 ℃ (10 mTorr) for 24 h. The samples were removed from the lyophilizer and stored in a desiccator until tested.

4.2.6 Microneedle patch characterization

MN patches were imaged using brightfield microscopy (Hirox KH-8700, Tokyo, Japan). To assess MN insertion into skin, patches were pressed by thumb onto stretched porcine cadaver skin. The MNs were left in the skin for 15 min, and then removed. The skin was stained for 5 min, with gentian violet (2% solution, Humco, Texarkana, TX), which was

then wiped off to show preferentially stained sites of MN penetration into skin[4]. The removed MN patches were imaged to determine extent of MN dissolution.

4.2.7 ELISA assay measurements

The D-antigen content of IPV from chips and MN patches was determined by antigen-capture sandwich ELISA, as previously described[42]. Polio-specific monoclonal antibodies were used for both capture and detection. The capture antibody solutions were prepared by adding type 1 (HYB295-15-02), type 2 (HYB294-06-02) or type 3 (HYB300-05-02) (Thermo Fisher Scientific) specific antibodies to 0.05 M carbonate-bicarbonate buffer, pH 9.6. Type 1 and type 3 antibodies were diluted at 1:1000 and type 2 was diluted in 1:500.

4.2.8 Thermogravimetric analysis

Thermogravimetric analysis (TGA, Q50, TA Instruments, New Castle, DE) was used to determine the residual moisture content of the MN patches. Samples obtained from MN patch (each weighing 15–20 mg) were heated at 10 °C/min from room temperature to 110 °C and then maintained isothermally for 10 min. The residual moisture content (%) was determined by the stable weight loss (%) at 110 °C using TA Instruments Universal Analysis 2000 software.

4.2.9 Differential scanning calorimetry

Differential scanning calorimetry (DSC, Q200, TA Instruments) was used to measure the glass transition temperature of the samples. Samples obtained from MN chips (each weighing 10–15 mg) were placed in hermetically sealed aluminum pans (TA Instruments, cooled from room temperature to 0 °C at a rate of 10 °C/min and subsequently heated to 200 °C at a heating rate of 10 °C/min. The sample chamber was purged with dry nitrogen at 50 ml/min. Empty pans were used as a reference control. The onset temperature of the discontinuities in the heat flow versus temperature curve was taken as the glass transition point, which was determined using TA Instruments Universal Analysis 2000 software.

4.2.10 X-ray diffraction

X-ray diffraction (XRD, X'pert Pro Multi-Purpose Diffractometer, PANalytical, West-borough, MA) analysis was used to study structural changes of MN chips stored at specified temperatures over time. The measurements were made in the θ - 2θ *mode* on the MN chip samples using a bracket sample holder with a Cu Kα radiation source (Cu Kα = 1.54059 Å) at room temperature. Data were collected between 2θ values of 5° and 50° using a step size of 0.013° and an acquisition time of 30 s per step. Samples were measured at 45 kV and 40 mA. X-ray diffraction patterns were analyzed using Jade 8 software (MDI Materials Data, Livermore, CA) and shown after background correction. Diffraction peaks were fitted to a Gaussian profile.

4.2.11 Fourier-transform infrared spectroscopy

Fourier-transform infrared spectrometry (FTIR, Nicolet iS 50 FT-IR, Thermo Fisher Scientific, Waltham, MA) was used to study structural changes of MN chips stored at specified temperatures over time. The FTIR spectra of the samples were recorded at room temperature from 4000 to 600 cm^{-1} and shown after background correction.

4.2.12 Statistics and Design of Experiments

The Design of Experiments model for excipient screening was developed using MiniTab software version 18 (MiniTab, State College, PA). Statistics were calculated using either MiniTab or Excel (Microsoft, Redmond, WA). All listed averages represent the arithmetic mean of the samples. Comparison between three or more samples was performed by one-way ANOVA or the data were fit to a general linear model. Comparisons between individual samples were done using an unpaired t-test. Probability (p) values of <0.05 were considered to be significant.

4.3 Results and discussion

4.3.1 Excipient screening for IPV stabilization

To identify formulations that stabilize IPV during MN patch fabrication, we studied excipients including maltodextrin, which was previously shown to stabilize IPV[42], and D-sorbitol, sucrose and trehalose, which are widely used to stabilize proteins during drying or lyophilization[55,141]. Using a Design of Experiments model [see Table A-1 in

Appendix A], we studied the effect of individual excipients as well as combinations of up to four excipients, because multiple stabilizers have often been shown to provide better stability than individual excipients[142].

Trivalent concentrated IPV was formulated with combinations of different excipients in histidine buffer and dried on PDMS chips at 5 °C overnight. The samples were then lyophilized and stored at 25 °C with desiccant for 1 week. Each sample was reconstituted and assayed for D-antigen binding activity by ELISA.

In general, varying formulation of IPV type 3 (Figure 4-1) and types 1 and 2 (Figure A-1) had little effect of vaccine stability (two-way ANOVA, $p > 0.05$), as determined by D-antigen content measured by ELISA, probably because we selected excipients already shown or expected to stability IPV. After air drying, IPV typically lost very little activity (two-way ANOVA, $p > 0.05$), but then lost significant activity after subsequent lyophilization (two-way ANOVA, $p < 0.004$). Sometimes there were additional losses in IPV activity after storage at 25 °C, 0% RH for 1 week, but in most cases post-lyophilization and post-storage activity values were similar (two-way ANOVA, $p > 0.05$). In general, IPV type 2 was most stable, followed by IPV type 1 and IPV type 3 (three-way ANOVA, $p > 0.05$). This is consistent with literature, which reports that IPV type 2 exhibits the best thermostability[143].

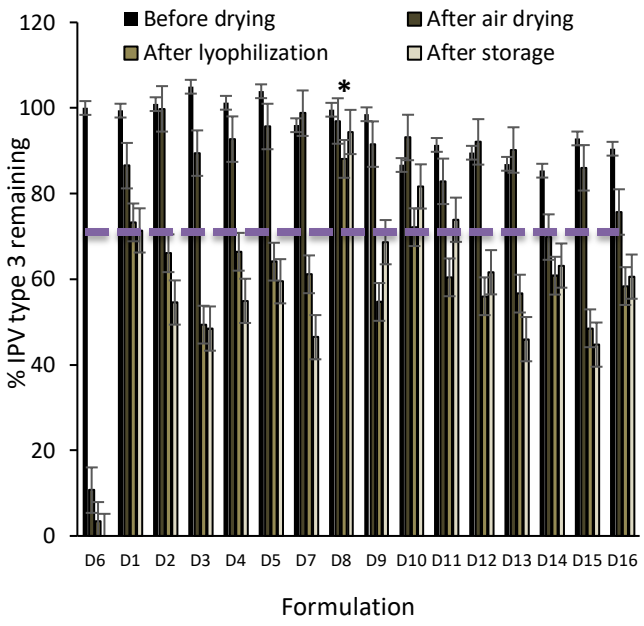

Figure 4-1: Effect of stabilizing excipients on IPV type 3 activity before drying, after air drying, after subsequent lyophilization and after storage. Vaccine was formulated with combinations of different excipients (each present at a concentration of 5% w/v) in 0.1 M histidine buffer at pH 6.5 (see Table S1 in SI for key to excipient formulations). In each set of bars, the first bar shows activity of liquid IPV formulated with excipients before drying. The second bar shows IPV activity after air drying at 5°C with desiccant overnight after casting onto PDMS chips. The third bar shows IPV activity after lyophilization. The fourth bar shows IPV activity after storage lyophilized vaccine at 25 °C with desiccant for 1 week. The unformulated vaccine control data is shown as D6 bars on the far left. All IPV activity (determined by ELISA) is shown as percentage of the starting stock solutions of concentrated vaccine. Asterisk (*) indicates excipient formulation that maintained >80% activity after drying and storage. Data represent mean ± SEM (standard error of the mean) of n= 3 replicates. Companion data on IPV types 1 and 2 are show in Figure A-1 in Appendix A.

It is notable that all three serotypes of unformulated IPV lost ~75 – 90% activity after air drying and lost ~90 - 100% activity after lyophilization (and storage). In contrast, none of the formulated vaccine samples lost more than 60% activity after drying, lyophilization and storage of IPV types 1, 2 or 3. The optimal formulation was the combination of

maltodextrin and D-sorbitol (50:50 mass ratio), which maintained at least 80% activity after drying, lyophilization and storage.

4.3.2 Buffer and pH screening

To assess the effect of buffer and pH, IPV activity was determined after air drying, lyophilization and storage at 40 °C for 3 days and 7 days using three different buffers and three pH values. Overall, buffer had a greater effect on activity loss (general linear model, $p < 0.05$) than pH (general linear model, $p < 0.12$), over the range of conditions studied (Figure 4-2 and Figure A-2 in Appendix A). Histidine buffer maintained activity of type 3 IPV (general linear model, $p > 0.80$) while potassium hydrogen pthalate (KHP) buffer had the most adverse effect (general linear model, $p < 0.03$) (Figure 4-2); similar findings were observed in IPV types 1 and 2 (Figure A-2 in Appendix A), although the differences in effects of pH and buffer were less dramatic compared to IPV type 3. Histidine buffer at pH 6 was selected as the best buffer to stabilize all three serotypes. Subsequent MN patch optimization experiments led to 0.35 mM histidine buffer for the first cast formulation and 0.15 mM histidine buffer for the second cast formulation. These buffer concentrations in combination with the other excipients (that can also influenza pH) were selected to yield a final pH of 6.3.

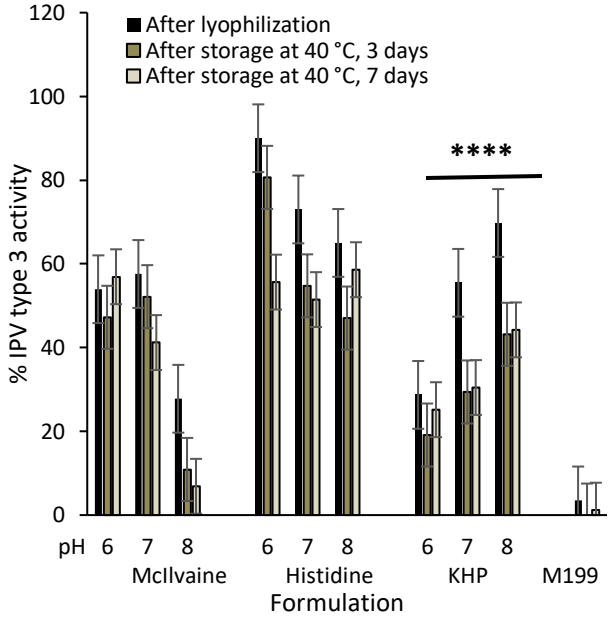

Figure 4-2: Effect of formulation buffer and pH on IPV type 3 activity after drying on PDMS chips followed by lyophilization and storage. IPV was formulated with 5% w/v maltodextrin and 5% w/v D-sorbitol in 0.1 M buffer with pH adjusted using 1 N HCl or 1 N NaOH. Storage was carried out at 40 ˚C for 3 or 7 days with desiccant. KHP: Potassium hydrogen pthalate, M199: Medium 199. In each set of bars, IPV activity is shown in the first bar after air drying at 5°C overnight and lyophilization, in the second bar after storage in a desiccator at 40 ˚C for 3 days and in the last bar after storage at 40 ˚C in a desiccator for 1 week. Stability of unformulated IPV (i.e., without maltodextrin or D-sortibol) in M199 media is shown in the bars on the far right. Asterisk (*) represents buffer which had the most adverse effect on IPV stability (general linear model, $p < 0.03$). All IPV activity is shown as percentage of IPV activity vaccine casting solution. Data represent mean ± SEM of n= 3 replicates. Companion data on IPV types 1 and 2 are show in Figure A-2 in Appendix A.

4.3.3 Optimization of polio MN patches

Initial formulation studies above were performed by casting onto flat PDMS chips to facilitate higher throughput. We next assessed formulation optimization in the context of MN patches fabrication by a two-cast process.

4.3.3.1 Optimization of 1st cast formulation

The first solution cast onto the MN mold contained IPV formulated with maltodextrin and D-sorbitol in different ratios (IPV type 3 in Figure 4-4; IPV types 1 and type 2 in Figure A-3 in Appendix A). There was no significant effect of maltodextrin:D-sorbitol ratio on activity of IPV types 1, 2 or 3 (2-way ANOVA, $p > 0.8$). A maltodextrin:D-sorbitol ratio of 20:80 (on a dry basis, when cast as 10% w/v solids in solution) was selected as the best formulation because this ratio consistently enabled fabrication of MN patches with sharp microneedle tips.

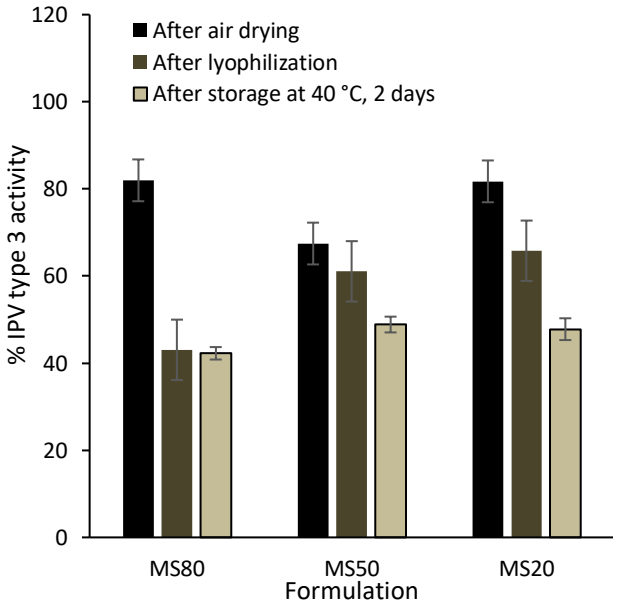

Figure 4-3: Effect of 1st cast excipient ratio (maltodextrin:D-sorbitol) on IPV type 3 activity after fabricating MN patches, air drying, lyophilization and storage with desiccant at 40 °C for 2 days. Trivalent IPV was formulated with stabilizing excipients at a total concentration of 10% w/v in the vaccine casting solution. The maltodextrin: D-sorbitol mass ratios were 80:20 (MS80), 50:50 (MS50) and 20:80 (MS20). The 2nd cast polymer matrix solution consisted of excipients at a total concentration of 45% w/v fish gelatin and D-sorbitol (at a mass ratio of 78:22) in 0.15 mM histidine buffer at pH 6.3. All IPV activity is expressed as a percentage of IPV activity in the vaccine casting solution. In each set of bars, the first bar shows IPV activity in MN patch after air drying at 5°C in a desiccator for 2 days; the second bar shows IPV activity after additional lyophilization; and the last bar shows

IPV activity after storage at 40 °C for 1 week with desiccant. There was no significant difference between the different ratios of maltodextrin-to-D-sorbitol (2-way ANOVA, p > 0.8). Data represent mean ± SEM of n= 3 replicates. Companion data on IPV types 1 and 2 are show in Figure A-3 in Appendix A.

4.3.3.2 Optimization of 2nd cast formulation

MN patch preparation process involves the addition of a second cast solution which not only forms the MN patch backing but also provides additional mechanical strength to the MNs. To determine the effect of ratio of 2nd cast excipients, MN patches were prepared with a 1st cast consisting of trivalent IPV formulated with maltodextrin and D-sorbitol (20:80) and a second cast solution consisting of varying ratios of fish gelatin to D-sorbitol in 0.15 mM histidine buffer (IPV type 3 in Figure 4-4; IPV types 1 and type 2 in Figure A-4 in Appendix A).

No significance differences in IPV type 1 and type 2 activities were observed between GS78 and GS55 formulations (ANOVA, $p > 0.05$), but GS78 was better in stabilizing IPV type 3 (ANOVA, $p < 0.05$). However, MN patches prepared with GS55 formulation were not mechanically robust enough to penetrate the skin. GS88 had adverse effects on all three IPV serotypes (ANOVA, $p< 0.05$), especially after extended storage at 40 °C.

Hence, a fish gelatin:D-sorbitol ratio of 77:22 (on a dry basis, when cast as 45% w/v solids in solution) was selected as the final 2nd cast formulation because it resulted in the best stabilization of all three IPVs types and produced MN patches with strong microneedle tips.

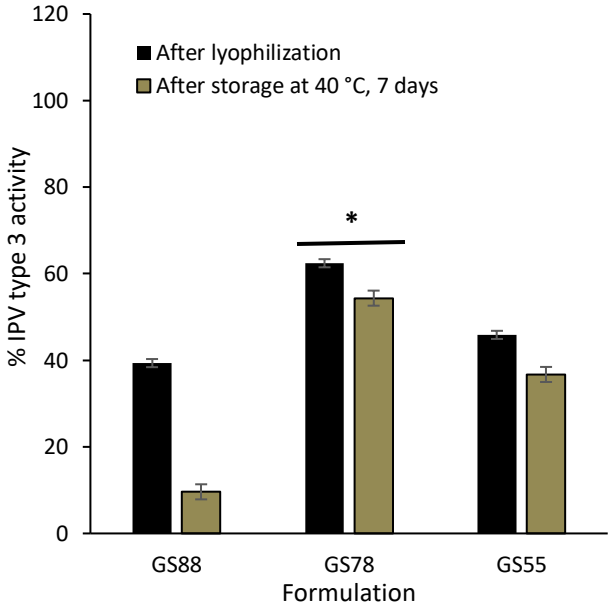

Figure 4-4: Effect of 2nd cast excipient ratio (fish gelatin-to-D-sorbitol) on IPV type 3 activity after fabricating MN patches, air drying, lyophilization and storing with desiccant at 40 °C for 7 days. Trivalent IPV was formulated with stabilizing excipients at a total concentration of 10% w/v in the vaccine casting solution. The maltodextrin: D-sorbitol mass ratios were Trivalent IPV was formulated with stabilizing excipients at a total concentration of 10% w/v in the vaccine casting solution. The maltodextrin: D-sorbitol ratio was 20:80 in 0.35 mM histidine buffer. The 2nd casting solution containined 45% w/v with varying mass ratios of fish gelatin-to-D-sorbitol in 0.15 mM histidine buffer. The mass ratios used were GS88 (fish gelatin:D-sorbitol = 88:11), GS78 (fish gelatin:D-sorbitol = 78:22) and GS55 (fish gelatin:D-sorbitol = 55:45). All IPV activity is expressed as a percentage of IPV activity in the vaccine casting solution. In each set of bars, the first bar shows IPV activity in MN patch after air drying followed by lyophilization and the second bar shows the IPV activity after storage at 40 °C for 1 week with desiccant. Asterisk (*) depicts a significant difference between IPV activity compared to other two ratios (ANOVA, $p < 0.05$). Data represent mean ± SEM of n= 3 replicates. Companion data on IPV types 1 and 2 are show in Figure A-4 in Appendix A.

4.3.4 Effect of drying conditions

Solid MN patches are formed by drying the cast formulations in the MN mold. As the vaccine is removed from an aqueous environment during drying, it undergoes changes that

can decrease its specific antigenicity, where the antigen's physicochemical environment affects antigen stability during the drying and subsequent storage processes[51]. Formulation with polyols such as D-sorbitol and polysaccharides such as maltodextrin, as well as drying at controlled temperature and/or by lyophilization, which influence the final water content of the MN patch, can maintain antigen activity during drying[144].To study the effect of drying temperature and lyophilization, the residual moisture content of MN patches were measured by TGA and the IPV activity was measured by ELISA after air drying, after subsequent lyophilization, after storage at 40 ˚C (without lyophilization), and after storage at 40˚C (with lyophilization).

The kinetics of water removal from MN patches depended on drying temperature and in some cases, lyophilization, but in all cases the final residual water content after patch storage at 40 ℃ for one week with desiccant was ~2.5%, suggesting an equilibrium state of water partitioning between the patch, surrounding air and desiccant at that temperature, MN patch formulation and desiccant type (Figure 4-5).

Concerning kinetics, residual moisture content of MN patches depended on temperature during initial air drying with desiccant for 2 days, where drying at 40 ℃, 25 ℃ and 5 ℃ resulted in significantly different residual moisture contents of 3.6%, 6.0% and 10.9%, respectively (one-way ANOVA, $p < 0.0004$) (Figure 4-5A). Lyophilization after air drying reduced residual moisture content after air drying at 5 ℃ (Student's t-test, $p < 0.015$), but had no significant effect on residual moisture content after air drying at 25 ℃ or 40 ℃ (Student's t-test, $p > 0.7$).

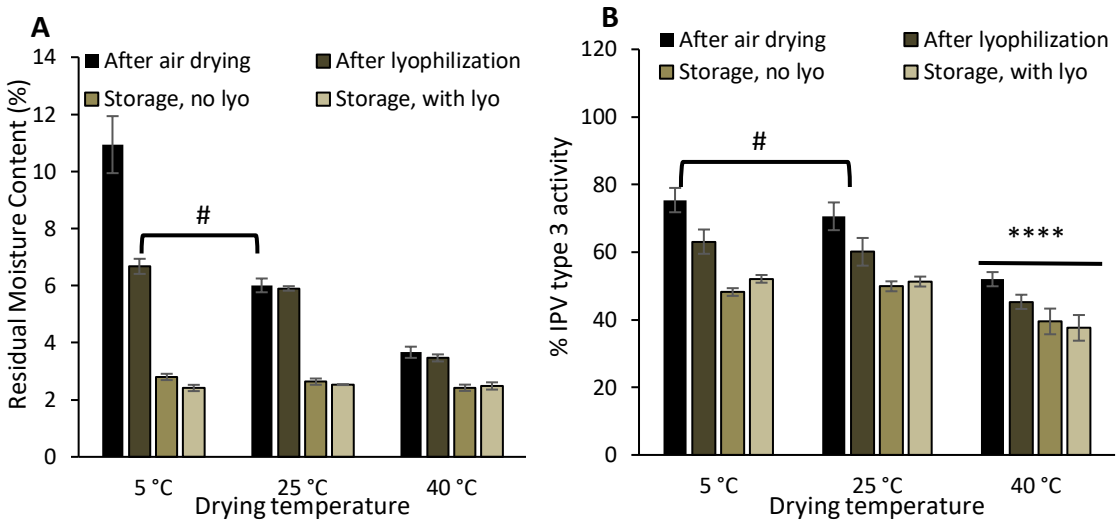

Figure 4-5: A) Effect of air drying, subsequent lyophilization and storage conditions on residual moisture content of MN patches. MN patches were fabricated and air dried at 5 °C, 25 °C or 40 °C with desiccant for 2 days. Half of the patches were stored at 40 °C for 1 week with desiccant. The other half of the patches were subjected to lyophilization followed by storage at 40 °C for 1 week with desiccant. In each set of bars, the first bar shows residual moisture content of MN patch after initial drying, the second bar shows the residual moisture content after subsequent lyophilization, the third bar shows residual moisture content for MN patches stored at 40 °C for 1 week with desiccant (no lyophilization) and the last bar shows residual moisture content for MN patches stored at 40 °C for 1 week with desiccant after lyophilization. Hash (#) depicts no statistical difference between the two samples (1-way ANOVA, $p > 0.05$). B) Effect of air drying, subsequent lyophilization and storage conditions on IPV type 3 activity. All IPV activity is expressed as a percentage of IPV activity in the liquid casting solution. In each set of bars, the first bar shows IPV type 3 activity in MN patches after air drying, the second bar shows the activity after lyophilization, the third bar shows activity for MN patches stored at 40 °C for 1 week with desiccant (no lyophilization) and the last bar shows the activity for MN patches stored at 40 °C for 1 week with desiccant after lyophilization. Hash (#) depicts no statistical difference between the two samples (1-way ANOVA, $p > 0.05$). Asterisk (*) indicates a significant difference in IPV activity (1-way ANOVA, $p < 0.05$). Data represent mean ± SEM of n= 3 replicates. Companion data on IPV types 1 and 2 are show in Figure A-5 in Appendix A.

Air drying at 5 °C or 25 °C resulted in similar IPV activities (1-way ANOVA, $p>0.05$), whereas drying at 40 °C resulted in lower IPV activity ,especially for IPV types 1 and 3

(1-way ANOVA, $p<0.05$) (Figure 4-5B and Figure A-5 in Appendix A). This is consistent with literature, which reports that heating IPV results in loss of D-antigenicity[145]. After storage at 40 °C for one week with desiccant (with or without prior lyophilization), IPV stability was similar when previously air dried at 5 °C or 25 °C, but was lower when previously dried at 40 °C. We therefore selected air drying at 25 °C (since it dries faster than at 5 °C) without lyophilization (since it adds time, cost and complexity with no apparent advantage in IPV stability) as the preferred MN patch drying method.

4.3.5 Polio MN patch characterization

Based on the optimization of 1st cast solution, 2nd cast solution and the drying conditions, we fabricated MN patches comprised of a 10 x 10 array of MNs measuring approximately 650 µm in height (Figure 4-6A). Upon pressing the MN patches to porcine cadaver skin, leaving them in place for 15 min and then removing them, microscopic imaging of the patch showed that the MNs had substantially dissolved, indicating successful skin penetration and dissolution (Figure 4-6B). Staining sites of skin penetration further demonstrated that the MNs had punctured the skin (Figure 4-6C). These findings show that a formulation optimized for IPV stability was also strong enough to penetrate skin and rapidly dissolve within the skin, thereby generating no sharps waste.

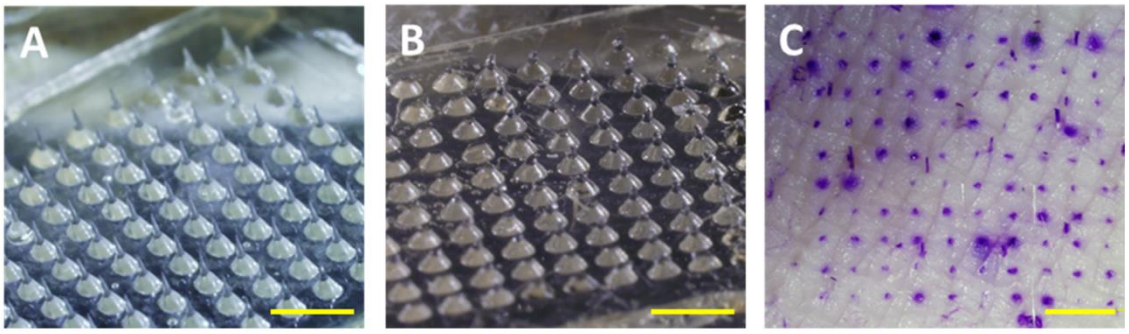

Figure 4-6: MN patch containing a 10 x 10 array of microneedles was manually inserted into shaved porcine cadaver skin and imaged (A) before insertion and (B) 15 min after

4.3.6 Long- term stability of polio MN patches

The next step was to determine stability of MN patches during long-term storage up to 1 year at up to 40 °C. Extended storage at elevated temperatures was studied because reduced need for a cold chain of storage is desirable, especially in polio-endemic countries which often have poor infrastructure. Consistent with literature[146],storage of commercial IPV at an elevated temperature of 40 °C led to complete loss of activity within days to weeks (Figure A-6 in Appendix A).

MN patches, however, were able to retain IPV activity much better than liquid vaccine. All three IPV serotypes maintained >70% activity after 2 months and >50% activity after 1 year storage at 5 °C or 25 °C with desiccant (Figure 4-7). It is notable that stability at 25 °C was as good as 5 °C. Storage at 40°C was not as good, but yielded >40%

activity after 2 months and >20% activity after 1 year for all three serotypes. We are not sure why IPV stability at the one-week time point was lower than the overall trend would suggest, and attribute this to experimental artifact.

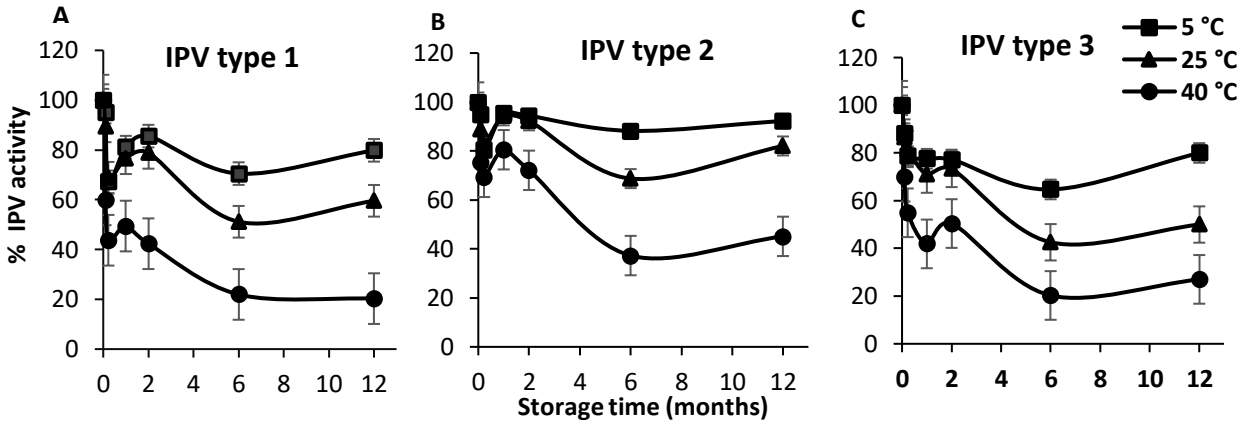

Figure 4-7: IPV activity in MN patches stored at 5, 25 or 40 ˚C with desiccant for up to 1 year. MN patches were analyzed using ELISA for (A) IPV type 1, (B) IPV type 2 and (C) IPV type 3 activity at various time points. IPV activity is expressed as a percentage of IPV activity of MN patches immediately after fabrication. Data represent mean ± SEM of n= 3 replicates.

4.3.7 Correlation of residual moisture content in patch to IPV stability

Our studies so far indicated that IPV instability was driven by elevated temperature (especially at 40 °C). However, IPV instability could also be caused by presence of water, which is a potent plasticizer because of its low glass transition temperature (T_g = -135 °C) [147], which can facilitate reactions controlled by molecular mobility, such as protein unfolding, aggregation and chemical degradation. We therefore prepared and stored MN patches at various temperatures and humidity levels to generate patches with a range of residual moisture content (Figure 4-8A and Figure A-7 in Appendix A).

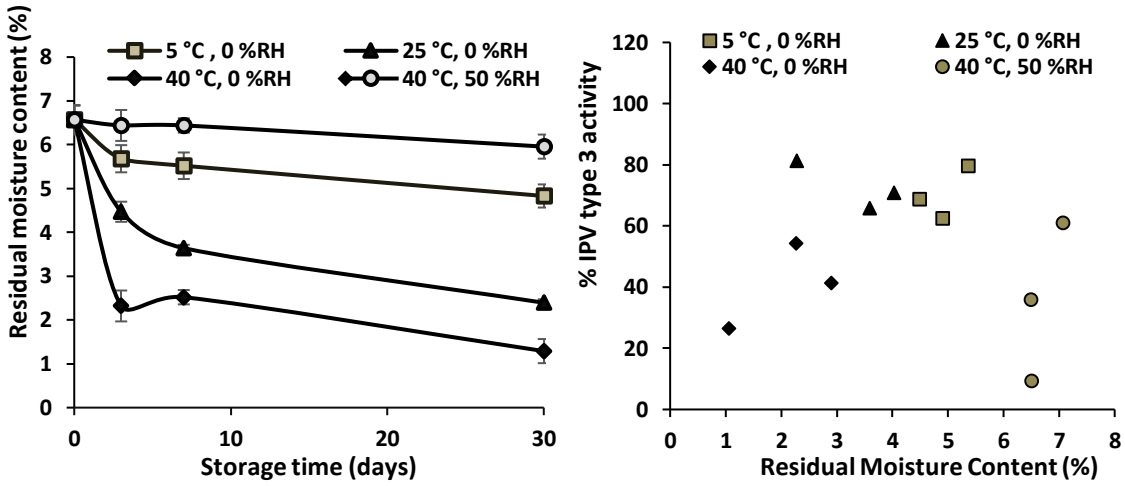

Figure 4-8: A) Effect of storage conditions on residual moisture content of polio MN patches stored at 5, 25 or 40 °C with desiccant or at 40 °C and 50% relative humidity (RH). B) Correlation of IPV type 3 stability in MN patches to residual moisture content of the patches stored at 5, 25 or 40 °C with desiccant or at 40 °C and 50% relative humidity (RH). Regression analysis showed an R^2 value of 0.009, indicating poor correlation. Data represent mean ± SEM of n= 3 replicates. Companion data on IPV types 1 and 2 are show in Figure A-7 in Appendix A.

Residual moisture content of MN patches immediately after fabrication was 6.6 ± 0.2%. Storage at different temperatures for different times produced patches with residual moisture contents as low as 1.3 ± 0.1%. Storage at 5°C, 25°C or 40 °C for 1 month with desiccant resulted in moisture loss of 2%, 4% or 5%, respectively. Storage at 40 °C and 50% RH resulted in minimal moisture loss of 0.5%.

At these different times and temperatures, IPV activity loss ranged between 91% and 7%. Correlation between IPV activity and residual moisture content (independent of temperature) was poor (Figure 4-8B and Figure A-7 in Appendix A), with R^2 values of <0.05. In contrast, there was a correlation (R^2 values of 0.38 – 0.67) between IPV activity and temperature (independent of residual water content) (Figure A-8 in Appendix A). This

shows that IPV destabilization processes are driven by elevated temperature with little influence from residual moisture content over the range of conditions studied.

4.3.8 Characterization of changes in MN matrix material properties during patch storage

Interaction between IPV and the excipients that make up the MNs could play a role in IPV activity loss. Because there can be mixing of 2nd cast excipients with 1st cast excipients during the MN fabrication process, we determined the composition of MNs (i.e., without the patch backing). Because gelatin was present only in the 2nd cast formulation and was the only protein in either formulation, we measured the amount of protein in MNs separated from patch backing and used that to calculate the amount of 2nd cast formulation that had mixed with the 1st cast formulation in the MNs. In this way, we determined the composition of MNs was 55% fish gelatin, 38% D-sorbitol and 7% maltodextrin, on a mass basis. To study changes in material properties in MNs during storage, we cast samples with this composition and stored them at 5 °C, 25 °C or 40 °C with desiccant and then characterized them as described below.

4.3.8.1 Determination of glass transition temperature of MNs by DSC

MNs stored below their T_g will be in an amorphous glass phase, which has high viscosity that can retard vaccine mobility and interactions and prevent crystallization, both of which can cause IPV instability[148]. Using DSC to determine T_g, we found that the MN matrix

initially had a T_g of 48 °C, which increased over time to as much as 59 °C (Figure 4-9). This finding is consistent with our prior observation that residual moisture content decreased with storage time (Figure 4-8A), since a decrease in moisture content is generally associated with an increase in T_g [52]. These data may also explain why stability at 5 °C and 25 °C are similar, since they are both well below the T_g, but stability was worse at 40 °C, which is closer to the T_g of the MNs.

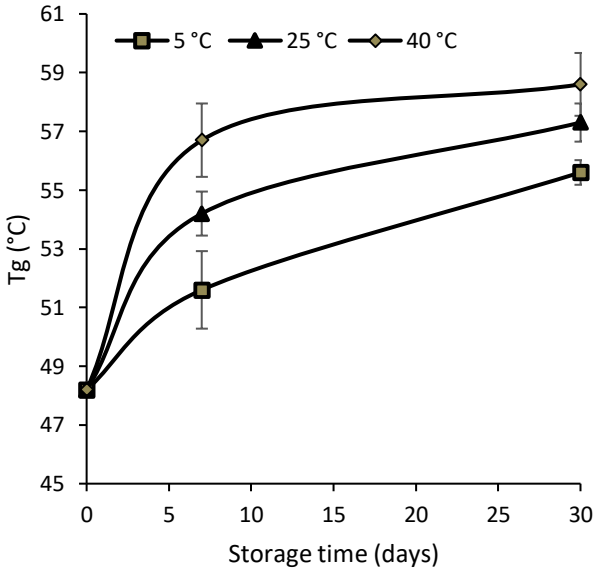

Figure 4-9: Effect of storage time and temperature on T_g of MN matrix material measured by DSC. T_g was measured at specific times for up to 30 days at 5 °C, 25 °C or 40 °C with desiccant. Data represent mean ± SEM of n= 3 replicates.

4.3.8.2 Determination of chemical composition changes of MNs by FTIR

We next used FTIR to study possible changes in molecular structure, chemical bonding and molecular environment in the MN matrix after 30 days at 5 °C, 25 °C or 40 °C (Figure 4-10). The spectra appear very similar, which means that chemical changes were not detected among the samples. In contrast, the long term stability study showed greater IPV instability at 40 °C when compared to 5 °C, and 25 °C. Hence, the lack of changes in molecular level interactions between IPV and excipients determined by FTIR could not be correlated to IPV instability.

We interpret the peaks situated at 3272-3370, 1627- 1632, 1532-1546 and 1235-1276 cm^{-1} to correspond to N-H stretching and free water, amide I, amide II and amide III, respectively[149]. We further interpret amide I to represent C=O stretching/hydrogen bonding coupled with COO; amide II to represent bending vibration of N–H groups and stretching vibrations of C-N groups; and amide-III to be related to the in-plane vibrations of C-N and N-H groups of bound amide or vibrations of CH_2 groups of proline side chains in gelatin[150]. The strong peak between 4000-3200 cm^{-1} and the peak at 1081 cm^{-1} are believed to be mainly from –OH stretching and C-O stretching vibrations from D-sorbitol and maltodextrin, respectively[151].

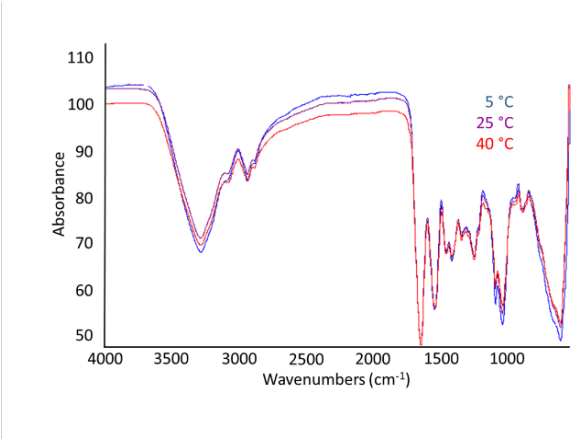

Figure 4-10: FTIR spectrum of MN matrix samples measured 30 days after storage at 5 °C, 25 °C or 40 °C with desiccant. Data represents averages of n= 3 replicates.

4.3.8.3 Determination of matrix structural changes in MN by XRD

XRD was performed to better understand structural changes in the MN matrix (Figure 4-11). The broad peak centered near 2θ = 20° observed in all samples indicates that the MN matrix is in an amorphous phase[152], which we interpret to be mainly composed of gelatin and maltodextrin based on the XRD patterns of the individual materials (Figure A-9 in Appendix A). The fresh and 1 week samples also show a sharp peak at approximately 2θ = 42-43°, which suggest an additional crystalline phase probably composed of D-sorbitol. The intensities and peak areas for fresh and 1 week samples were similar independent of the storage temperature. After 1 month, however, the crystalline peak heights for all the samples decreased by ~ 76% and the peak areas decreased by ~ 83%. This suggests that the MN matrix became more amorphous during storage, as residual water content decreases and T_g increases independent of the storage temperature. Since the long term stability study showed greater IPV instability at elevated temperature, we

conclude that the changes observed in the bulk matrix properties could not be correlated to the IPV instability.

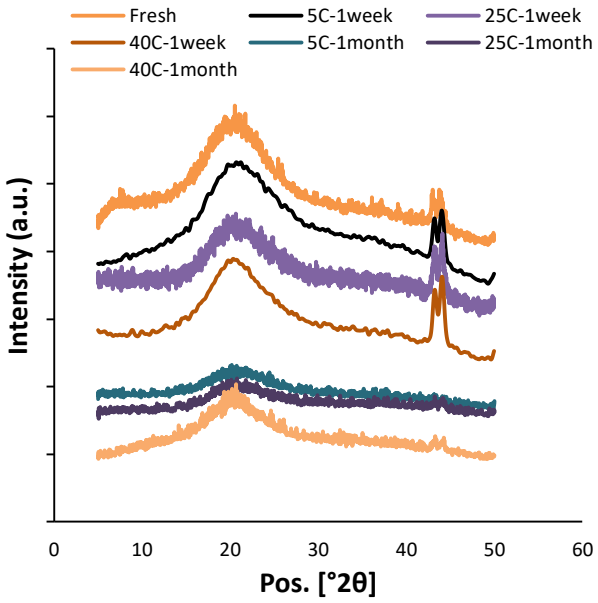

Figure 4-11: X-ray diffraction patterns corresponding to MN matrix samples stored at 5 °C, 25 °C or 40 °C for up to 30 days. Data represent averages of n= 3 replicates.

4.4 Discussion

The WHO has recommended replacing OPV with IPV worldwide to eliminate the risk of vaccine-derived polioviruses[131]. However, IPV as currently provided as a liquid administered by IM injection, has certain limitations such as the need for trained healthcare personnel, risk of transmission of blood-borne infectious diseases[24] from the sharps waste and the need for cold chain to avoid loss of IPV potency. MN patches can improve IPV delivery by enabling simple administration by minimally trained personnel and avoiding generation of biohazardous sharps waste[153]. In this study, we optimized MN

patch formulation to improve IPV stability during extended storage at elevated temperatures.

Initial formulation optimization studies showed that a combination of maltodextrin and sorbitol was optimal for minimizing IPV loss during drying. Buffer screening showed that histidine buffer at pH 6 was optimal for IPV stability. Guided by these findings, MN patch optimization studies identified a 1st cast composition of maltodextrin:D-sorbitol ratio of 20:80 (on a dry basis) and a 2nd cast composition of fish gelatin: D-sorbitol at ratio of 77:22 (on a dry basis, when cast as 45% w/v solids in solution) that provided the best stabilization of all three types of IPVs and produced MN patches with strong microneedle tips. Drying temperature optimization studies showed that air drying of the MN patches at 25 °C was effective, and subsequent lyophilization did not show any significant improvement in IPV stability.

The MN patch fabrication process is relatively simple and scalable to the potential demands for many millions of patches per year required by the polio eradication program. The IPV patches were tested in pig cadaver skin and found to insert into skin by thumb without the need for an applicator. This simple application process can enable administration by minimally trained personnel, thereby reducing costs by reducing the need for healthcare professionals. This simplified administration could facilitate more efficient mass IPV vaccination campaigns and routine IPV vaccination too. The inserted patches also showed near-complete MN dissolution in the skin within 15 min. This MN dissolution has the potential to eliminate the risks of biohazardous sharps. Finally, the MN patch was demonstrated significant thermostability even at 25 °C for up to 1 year (> 50% activity) or at 40 °C for up to 2 months (> 40% activity). This thermostability could aid reduce reliance

on cold chain storage, especially for short periods of time (days to weeks) during vaccination campaigns and transport to remote locations. This collection of capabilities represents a significant advanced that can overcome many of the hurdles posed by the transition from OPV to IPV.

Mechanistic studies were performed to understand the effect of MN matrix properties on IPV activity during storage. Residual moisture content of the patches decreased with increase in storage temperature but no correlation was seen between moisture content and IPV stability. MN patches showed an increase in T_g with increase in storage temperature, which was consistent with the moisture loss determined by TGA (i.e., where moisture loss correlates with increased T_g). This suggests that the MN matrix become more amorphous at elevated storage temperature and over time. XRD results also showed an increase in amorphousness of the matrix upon extended storage. Even though a more amorphous (i.e., glassy) matrix should retard diffusion-controlled reactions such as protein unfolding, and aggregation, IPV was less stable at elevated temperature and longer storage times (both of which promote diffusion-controlled, and most non-diffusion-controlled, reactions). Because none of these trends in macroscopic MN matrix changes correlated with changes in IPV activity, we hypothesize that molecular-scale interactions in IPV virus particles and between IPV and excipients could be the source of IPV instability.

4.5 Conclusions

This study presents the development of a dissolving MN patch for IPV vaccination. Formulation and process optimization studies were performed to identify an excipient combination and drying condition during MN patch fabrication that minimized IPV activity loss. The MN patch was simple to administer; generated no sharps waste; and maintained significantly improved thermostability during extended storage at elevated temperature compared to conventional liquid IPV. When stored with desiccant, IPV in MN patches maintained >70% activity after 2 months and >50% activity after 1 year at 5℃ or 25℃ , and maintained >40% activity after 2 months and >20% activity after 1 year at 40 ℃. Changes in MN matrix properties such as residual moisture content, T_g and crystallinity were measured, but did not correlate with changes in IPV activity. These findings suggest that a MN patch could enable increased thermostability and other advantages important to IPV vaccination and eradication programs.

4.6 Acknowledgements

We thank Dr. Jeong Woo Lee for his helpful discussions, Dr. Mohammad Mofidfar for performing the XRD testing , Dr. Meisha Shofner for providing us access to the TGA and DSC instruments in her lab and and Donna Bondy for administrative support. This work was supported by the Bill and Melinda Gates Foundation (Grant OPP1112700). XRD and FTIR studies were performed at the Georgia Tech Institute for Electronics and

Nanotechnology, a member of the National Nanotechnology Coordinated Infrastructure, which is supported by the National Science Foundation (Grant ECCS-1542174). Mark Prausnitz is an inventor of patents that have been or may be licensed to companies developing microneedle-based products, is a paid advisor to companies developing microneedle-based products and is a founder/shareholder of companies developing microneedle-based products, including Micron Biomedical. These potential conflicts of interest have been disclosed and are being managed by Georgia Tech and/or Emory University.

CHAPTER 5. RECRUITMENT AND COLLECTION OF DERMAL INTERSTITIAL FLUID USING A MICRONEEDLE PATCH

5.1 Introduction

There is rapidly increasing interest in personalized medicine and point-of-care diagnostics using novel biomarkers[154,155]. Blood is the primary source of body fluid containing these biomarkers. However, blood sampling by venipuncture is painful and requires trained medical professionals, while capillary blood sampling can be variable[156]. Alternate body fluids such as urine and saliva are more easily accessible but have their own limitations such as variability in urine biomarker concentrations due to circadian variations[67] and interference in saliva-based assays by food or drugs[69].

Interstitial fluid (ISF) is a relatively unexplored body fluid that is a rich source of biomarkers[7,77] that does not clot[79]. ISF comprises 15-25% of total body weight[74] and is formed by transcapillary exchange during blood flow. It fills extracellular space in tissues, which means that ISF biomarkers can provide systemic information due to its origins in blood and local information due to its contact with cells in tissues. Proteomic and metabolomics analysis of ISF from skin has shown that it has many biomarkers in common with companion serum and plasma samples, but also contains many other biomarkers that are unique or at much higher concentration compared to serum and plasma [6,7,121,157,158,159].

Some of the methods for ISF sampling include suction blister[82], which takes ~1 h to perform and leaves a lasting wound; reverse iontophoresis[98], which requires

calibration using blood samples and proprietary instrumentation; and microdialysis[94] and open-flow microperfusion[95], which require minor surgery and significant expertise. In large part because of the limitations of these methods, very few studies have examined ISF, and information on ISF properties and composition (other than glucose concentration) is extremely limited.

An alternate approach to collect ISF involves the use of microneedles (MNs), which are solid, tapered structures measuring hundreds of microns in length that painlessly penetrate into tissue, such as skin. MN patches were developed initially for delivery of vaccines and drugs, where they have been shown to be safe and simple to administer [29,160,161,162] . MNs have also been used to puncture the skin and collect a microliter quantities of ISF under suction[110,121], by passive diffusion through MN bore or built-in sensors[109,111,112], using MNs coated with capture antibodies to collect specific antigens[114,115] and with MNs made of swellable hydrogel that absorb ISF from the skin[118-120]. While ISF collection using MNs can be simple, minimally invasive and well-tolerated, most approaches are time consuming, requiring 15 - 30 min. The goal of this study is to develop a simple and easy-to-use MN patch that can collect ≥1 μl of ISF within 1 min.

5.2 Materials and methods

5.2.1 Microneedle patch fabrication

MN patches were cut from stainless steel sheets (Trinity Brand Industries, SS 304, 100 μm thick; McMaster-Carr, Atlanta, GA) using an infrared laser (Resonetics Maestro, Nashua, NH), as described previously[132]. The desired dimensions were drafted using AutoCAD

software (Autodesk, Cupertino, CA). MN patches were cut using the infrared laser at 1000 Hz, 20 J/cm^2 energy density and 40% attenuation of laser energy. A total of three passes were required to completely cut through the stainless steel sheet. A cutting speed of 2 mm/s and air purge at a constant pressure of 140 kPa were used. The MN patches were electropolished using an electropolishing solution (E972, ESMA, South Holland, IL) in an electropolisher (E399, ESMA) for 5 min at 2 A and room temperature. The electropolished array (each MN having final dimensions of 750 µm in length, 100 µm x 70 µm in cross section and tapering to a tip of <1 µm radius of curvature) was rinsed with isopropyl alcohol, cleaned with DI water and air dried.

MN patches were also prepared by lithographically defined chemical etching by Tech Etch (Plymouth, MA). Patches comprised either 5 MNs (750 µm long) or 9 MNs (650 µm) each measuring 50 µm x 150 µm in cross section and tapering to a tip of <1 µm radius of curvature.

5.2.2 MN surface pretreatment

5.2.2.1 Hydrophilic plasma treatment

To create a hydrophilic surface, MN arrays were air plasma treated by placing them in a plasma chamber (PDC-32G, Harrick Plasma, Ithaca, NY) for 5 min at the maximum radio frequency level under vacuum. MN patches were used for experiments within 15 min after treatment.

5.2.2.2 Hydrophobic Parylene coating

To create a hydrophobic surface, MN patches were coated with a conformal vapor deposition of 1 µm thick (using 1.6 g of dimer) Parylene C coating using a SCS Labcoater PDS 2010 (Specialty Coating Systems, Indianapolis, IN).

5.2.3 Paper reservoir

A strip of paper was adhered to the backing of each MN patch to create a reservoir to collect ISF that flowed out of the skin during MN insertion. For initial screening of paper for this application, samples of banana fiber paper, cotton fiber paper, and blotter paper were generously provided by the Renewable Bioproducts Institute (Georgia Institute of Technology, Atlanta, GA). Copy paper (Staples, Framingham, MA) and Whatman grade 1 filter paper (Sigma Aldrich, St. Louis, MO) were used as received.

The filter paper was ultimately selected as the material to use to form the reservoir. Filter paper strips were cut into rectangular strips of desired dimensions (1 mm x 7 mm or 2 mm x 7 mm) using a CO_2 laser (New Hermes Gravograph Model LS500XL, Gravotech, Duluth, GA). The patterns were made using a vector cut at 24 W power and a speed of 8 mm/s. To prevent excessive temperature rise that could cause burning during laser cutting, the filter paper was attached to an adhesive backing (3M, Maplewood, MN) first and soaked in DI water until completely wet to increase heat capacity.

The final MN patch was prepared by adhering the filter paper to the MN patch backing without covering the MNs.

5.2.4 Modified Cobb and Klemm methods for determining water absorptiveness of paper

The water absorptiveness of different types of paper was determined by modified Cobb (ISO 535:2014)[163] and Klemm (ISO 8787:1986)[164] methods. The modified Cobb method was performed by weighing each paper (precut to 10 cm x 1 cm strips) before soaking in 10 ml of deionized (DI) water for a specified amount of time. The paper was gently pressed to remove excess water and then reweighed. The Cobb value, which is the measure of water absorptiveness, is equal to the difference in the weight of the sample before and after soaking. Cobb values were normalized to the initial paper mass to account for thickness differences between the paper strips.

The modified Klemm method, which is a measure of capillary rise, was performed by vertically suspending a 10 cm x 1 cm rectangular strip of each paper sample so its lower edge just touched the surface of 10 ml of DI water in a beaker for a specified amount of time. The distance that water travelled up the strip was measured using a ruler. The obtained Klemm values were normalized to the initial weights of the samples to account for thickness differences between the papers.

5.2.5 Contact angle measurements

Static contact angle measurements were made placing 2 µL of DI water on plasma-treated, Parylene-coated and untreated MN surfaces by a goniometer (model 250, Rame'-hart

Instrument, Succasunna, NJ). Contact angle measurements are reported as the mean value of six measurements under the same conditions.

5.2.6 Quantification of ISF volume collected

The amount of ISF collected was quantified by determining sodium ion content in the MN patch paper backing using a sodium ion sensitive electrode (perfectION comb NA, Mettler Toledo, Columbus, OH). Paper backings were each incubated in 1 ml of DI water for 24 h at room temperature (21 – 25 ℃) to extract solutes from ISF that at least partially dried on the paper. The sodium ion content measured in the samples was divided by the physiological sodium ion concentration in rat ISF of 143 mEq/L [165] to determine ISF volume collected. This method relies on the expectation that sodium ion concentration is constant in the ISF of normal rats[166].

5.2.7 ISF collection from pig skin ex vivo

Pig ear skin was obtain freshly excised from feeder pigs (generously provided by Hollifield Farms, Conyers, GA) and then kept frozen at –80°C until use. Circular skin samples (2 cm diameter) were thawed and placed in vertical Franz diffusion cells (PermeGear, Bethlehem, PA). The donor chamber (on the top of the diffusion cell) was sealed using Parafilm (Bemis, Neenah, WI). The receptor chamber (on the bottom of the diffusion cell) was filled with 5 ml of 1 mg/ml fluorescein sodium salt (Sigma Aldrich) in DI water. The Franz cells

were placed overnight in a heating blocking (PermeGear) set to 37 °C to equilibrate the skin with the fluorescein solution.

The skin samples were removed from the Franz cells and then stretched and secured on a board using push pins. The MN patches were inserted with a force of 20 – 40 N for a specified number of times. Fluorescence imaging of the skin was performed using an Olympus SZX2 stereo microscope with a CCD camera (Leica DC 300, Leica Microsystems, Bannockburn, IL).

Paper backings were each incubated in 1 ml of DI water for 24 h. The fluorescein concentration in the reconstituted ISF samples was measured against a standard calibration curve of fluorescein in a 96 well plate (Costar Black Polypropylene, Corning, Corning, NY) using a Synergy H4 hybrid reader (BioTek, Winooski, VT) at an emission wavelength of 525 nm and absorption wavelength of 590 nm. The amount of ISF collected was calculated as the measured fluorescence content from the ISF divided by the known fluorescein concentration in skin, i.e., 1 mg/ml.

5.2.8 ISF collection from rat skin in-vivo

5.2.8.1 In-vivo study design

Fifteen Wistar rats (10-20 weeks old, female, Charles River Laboratories, Wilmington, MA) were anesthetized by isoflurane (AErrane, Baxter Healthcare, Deerfield, IL) inhalation in a prone position, during which all procedures were performed. A section of hair on the lateral side of the rat was removed using electric shears followed by brief

application of depilatory cream (Nair, Princeton, NJ), and then cleaned with gauze and DI water. The hair removal was performed at least 1 day prior to ISF collection to avoid possible ISF contamination by the depilatory cream. The rats were randomly divided into 3 groups, as shown in Figure 5-1. After each experiment, the rat was euthanized by carbon dioxide gas asphyxiation. These experiments have been approved by the Georgia Institute of Technology Institutional Animal Care and Use Committee.

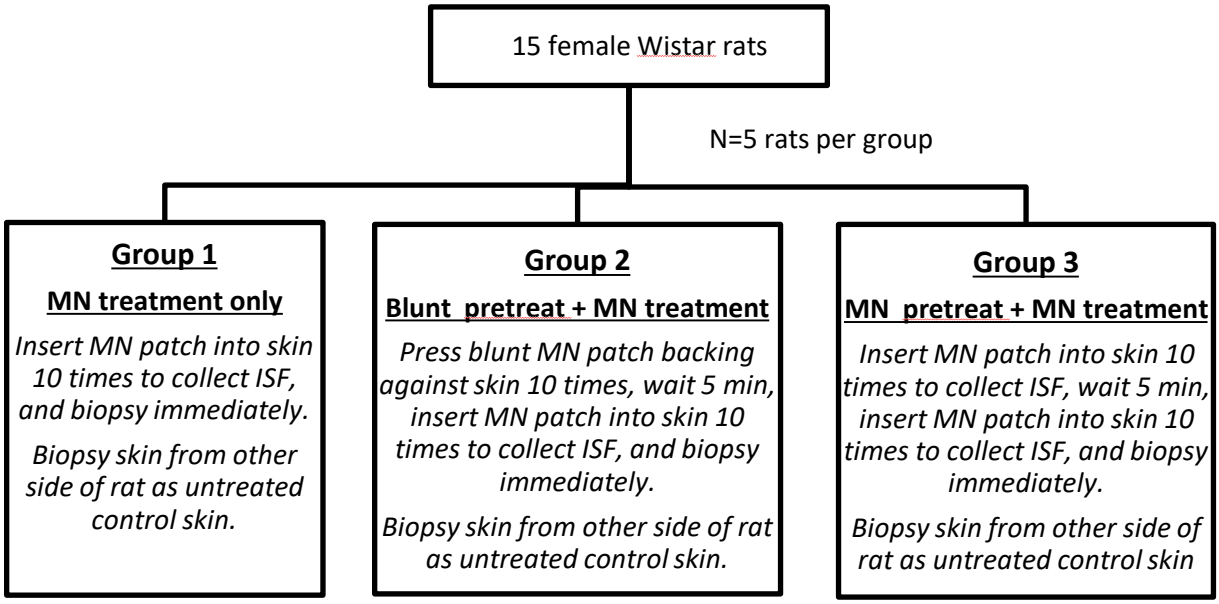

Figure 5-1: Experimental plan for study to determine the effect of skin pre-treatment on the amount of ISF collected from rat skin in vivo. Group 1 only received MN treatment to collect ISF, in which a MN patch containing 9 MNs with a 2 mm x 7 mm piece of filter paper glued on the patch backing was applied 10 times to the skin on the lateral side of the rat using a force of 20 – 40 N. Group 2 skin was pretreated with a MN patch backing with MNs cut off to provide a blunt pretreatment, followed by MN treatment to collect ISF after a 5 min delay. Group 3 followed the same protocol as Group 2, except sharp-tipped MNs were used during the pretreatment. Each treatment was performed on 3 sites per rat.

5.2.8.2 Determination of total water content of skin

To measure ISF content in the skin, pieces of rat skin were pre-weighed (60- 140 mg per piece) immediately after biopsy and lyophilized (Freezone 6 liter freeze dryer, Labconco, Kansas City, MO), as described previously[167].The mass loss after lyophilization was taken to equal the ISF content in the skin, assuming complete water removal by lyophilization. The percent increase in hydration due to skin pretreatment was determined as the difference between the water content of treated and control skin samples normalized to the water content of the control skin.

5.2.8.3 Imaging and histology

Skin biopsies were embedded in Optimum Cutting Temperature (OCT) media (Tissue-Tek, Torrance, CA) in a cryostat mold. Samples were fixed by freezing on dry ice. Frozen samples were sliced into approximately 6 μm thick sections using a cryostat (Cryo-star HM 560MV, Microm, Waldorf, Germany) and placed on glass slides. Hematoxylin and eosin (H&E) staining was performed on the skin sections using an automated staining machine (Leica Autostainer XL, Nussloch, Germany). A few drops of cytoseal 60 (low viscosity, Richard-Allan Scientific, Kalamazoo, MI) were applied onto the stained skin sections. The samples were then covered with glass cover slips and dried in a fume hood overnight. Imaging was performed using a Zeiss AxioObserver Z1 fluorescence microscope (Carl-Zeiss microscopy). Histopathological analysis of the images was performed.

5.2.9 Statistical analysis

Statistics were calculated using either MiniTab software version 18 (MiniTab, State College, PA). or Excel (Microsoft, Redmond, WA). All listed averages represent the arithmetic mean of the samples. Comparison between three or more samples was performed by one-way ANOVA or 2-way ANOVA. Comparisons between individual samples were done using an unpaired t-test. Probability (p) values of <0.05 were considered to be significant.

5.3 Results

5.3.1 Microneedle patch design

The MN patch was designed as a two-component system comprising a strip of paper (which serves as an ISF reservoir) on the backing of a stainless steel MN array (which creates micropores in the skin through which ISF can flow to the skin surface) (Figure 5-2A,B). To collect ISF, the MN patch was repeatedly applied to the skin surface, thereby inducing flow of ISF out of the skin and into the paper reservoirs (Figure 5-2C).

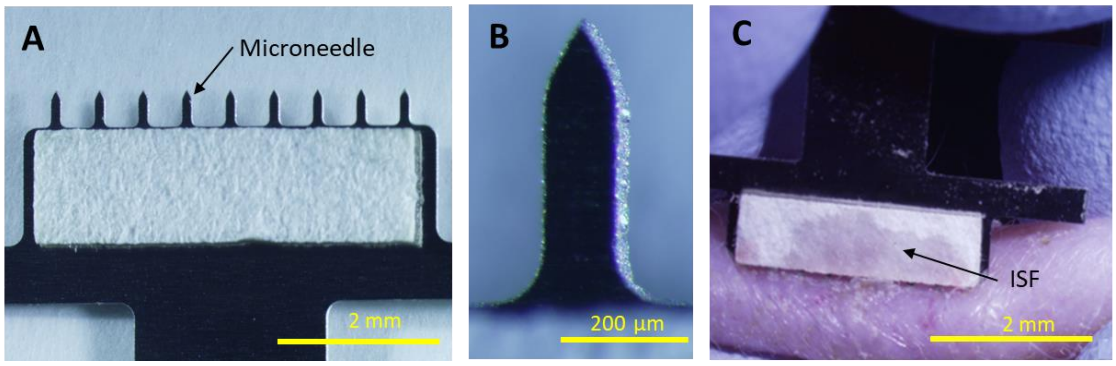

Figure 5-2: Representative images of MN patch for ISF collection. A) A patch comprising a row of nine microneedles (arrow) with a strip of white filter paper adhered to the patch backing. B) Magnified image of a single microneedle. C) Image of ISF collection after 5 insertions of a MN patch in the skin of a hairless rat in vivo. The MNs are on the lower edge of the patch and cannot be seen because they are inserted into the skin. Clear ISF is collected in the paper reservoir as observed by wetness of the paper (arrow).

The amount and speed of ISF collection could depend on the absorptiveness of the paper reservoir. We tested five different types of papers as candidate reservoir materials and measured their absorptiveness by modified Cobb and Klemm methods (Figure 5-3). Both methods indicated that the banana fiber paper was the most absorbent of all the tested papers, followed by filter paper. We chose filter paper for further optimization because of its ease of availability, low cost and widespread use by many researchers for development of paper-based sensor devices[168,169].

To calibrate the volume of ISF that filled reservoirs of filter paper, we inserted MN patches into the skin of anesthetized hairless rats until the reservoirs were completely wetted with ISF, as determined by visual examination. Rectangular strips of filter paper cut into 1 mm x 7 mm or 2 mm x 7mm strips collected 1.1 ± 0.3 µl and 2.0 ± 0.2 µl of ISF, respectively (mean ± standard error of the mean, n = 6 replicates).

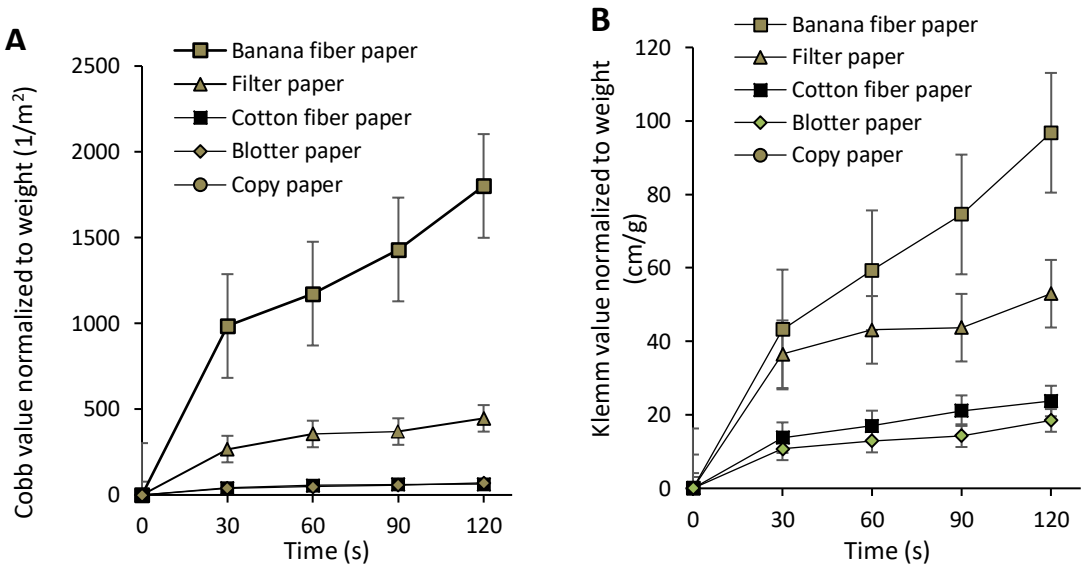

Figure 5-3: Water absorptiveness of different types of paper determined by modified Cobb method and modified Klemm method. (A) For the Cobb method, 10 cm^2 paper strips were weighed before and after soaking in DI water for 30, 60, 90 and 120 s. The Cobb value is the amount of water absorbed by the paper normalized to the initial paper mass to account for thickness differences between the paper strips. (B) For the Klemm method, 10 cm^2 paper strips were suspended vertically with their lower end immersed in 10 ml of DI water for 30, 60, 90 and 120 s. The Klemm value is the capillary rise of water determined by measuring the vertical distance travelled by water. The Klemm value was normalized to the initial paper mass to account for thickness differences between the paper strips. Data represents mean ± SEM (standard error of the mean) of n= 3 replicates.

5.3.2 Effect of multiple skin insertions, number of MNs per patch and MN thickness on ISF collected

We optimized ISF collection by studying the effect of MN parameters on amount of ISF collected from pig ear skin ex vivo, which was artificially hydrated with fluorescein to facilitate quantification of ISF collected). We found that the amount of ISF collected increased by increasing the number of skin insertions by MNs from 1 to 20 insertion, increasing MN thickness from 50 µm to 100 µm and increasing number of MNs from 5 to

9 MNs per patch (three-way ANOVA, $p < 0.03$) (Figure 5-4). Increasing number of skin insertions and number of MNs per patch both should increase the number of microscopic channels for ISF to flow out of skin. Puncturing skin with thicker microneedles should result in larger micropores, thereby allowing easier access to ISF.

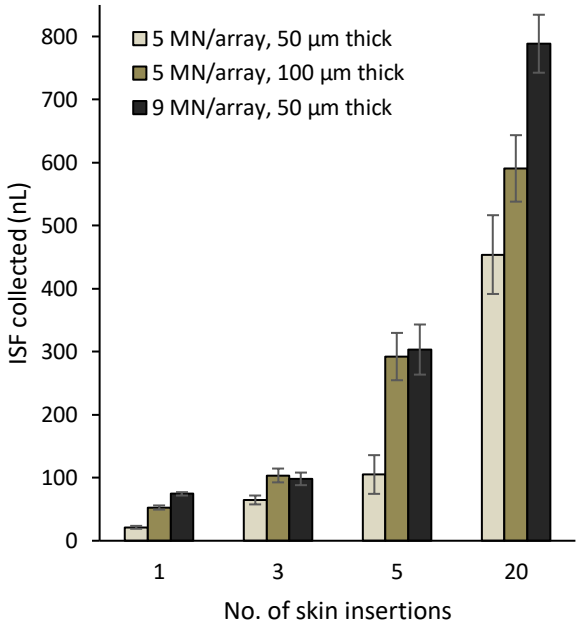

Figure 5-4: Effect of microneedle (MN) patch design on the amount of ISF collected. Patches were prepared with MN measuring either 50 µm or 100 µm in thickness and comprising either 5 or 9 MNs per patch. ISF was collected by applying a MN patch 1, 3, 5 or 20 times to stretched pig ear skin ex-vivo artificially hydrated with fluorescein row. Data represents mean ± SEM (standard error of the mean) of n= 3 replicates.

5.3.3 Effect of MN surface properties on ISF collected

Improving the wettability of the stainless steel MN surface could expedite ISF collection time by facilitating ISF flow on the MN surface to the paper reservoir. To test this hypothesis, we treated the MN patch with air plasma or coated the MN patch with Parylene C to render the MN surface more hydrophilic or hydrophobic, respectively, as shown through contact angle measurements (2-way ANOVA, $p < 0.001$) (Figure 5-5). While it required 15 skin insertions to collect 2 µl of ISF from hairless rat skin in vivo when using MN patches with no surface modification, increasing hydrophilicity of the MN surface decreased the required number of skin insertions to 10, whereas increasing hydrophobicity increase the number of skin insertions to 18 (Figure 5-5). This indicates that ISF collection involves fluid flow on the MN surface and that surface tension of the MN surface thereby plays an important role in ISF flow from the skin to the paper reservoir.

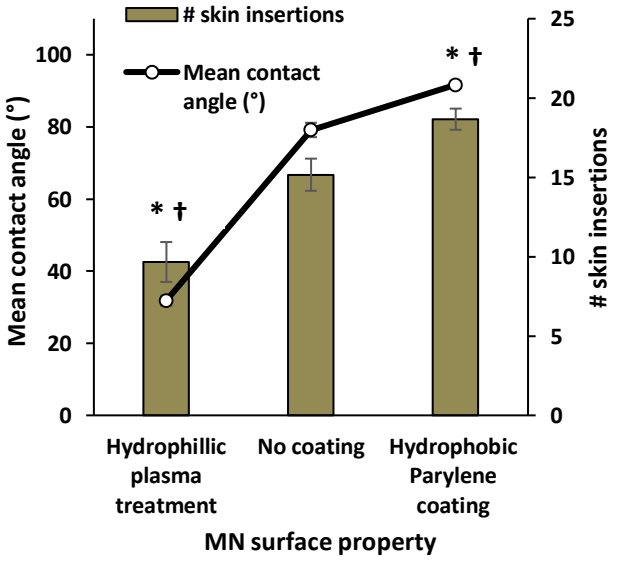

Figure 5-5: Effect of microneedle (MN) surface properties on ISF collection from skin. MN patches made of stainless steel (type 304) were (i) treated with air plasma for 5 min to increase hydrophilicity (ii) untreated or (iii) coated with 1 µm thick Parylene C to impart hydrophobicity. The y axis shows sessile drop contact angle of water of the MN surfaces and the secondary y-axis shows the number of insertions required to collect 2 µl of ISF from hairless rats in vivo. Asterisk (*) and cross (†) identify values significantly different from the corresponding value with no coating/treatment for mean contact angle and # skin insertions, respectively (2-way ANOVA $p < 0.01$). Data represent mean ± SEM (standard error of the mean) of n= 6 replicates.

5.3.4 Effect of skin pre-treatment on ISF collected

We have generally observed that very little ISF comes out of the skin during the first few MN insertions, and the more comes out as the number of insertions increases. This led us to hypothesize that the act of collecting ISF (e.g., piercing the skin with MNs) affects the rate at which ISF comes out of the skin, possibly by increasing skin hydration, which is known to increase hydraulic conductivity of tissues by increasing the spacing by tissue fibers (e.g., glycosaminoglycans making up extracellular matrix, collagen fibers in dermis)[170]. This hypothesis is supported by our visual observation of local edema in skin after ISF collection by MN patch (data not shown).

To test this hypothesis, ISF was collected from a first group of rats using 10 skin punctures with MN patches following our standard protocol (Group 1, see Figure 5-1). In a second group of rats, the skin was pre-treated with a blunt MN patch backing to simulate the mechanical interaction between MN patches and skin without the MN puncture into skin. No ISF was collected during this blunt pre-treatment (Figure 5-6A). After 5 min, ISF was collected using our standard protocol of 10 MN patch insertions into skin (Group 2). There was no significant effect of this blunt MN patch pretreatment on the amount of ISF

collected 5 min later (Figure 5-6A). In a third group of rats, the skin was pre-treated using the standard protocol of 10 MN patch insertions, which was followed 5 min later with another 10 MN patch insertions using our standard protocol to collect ISF (Group 3). The amount of ISF collected during the pre-treatment was not significantly different from the amount of ISF collected in Group 1 (Figure 5-6A). However, the amount of ISF collected when the identical treatment was performed 5 min later collected 4.3 times more ISF (Figure 5-6A). This results suggests that the act of collecting ISF by MN patch skin puncture affects the skin so that continued ISF collection is easier.

The percent increase in skin water content was measured immediately after treatments in the three test groups. In Group 1, skin hydration increase by 5%, presumably due to the effects of MN patch skin puncture (Figure 5-6B). When the blunt pre-treatment was performed in Group 2, skin hydration significantly increased to 12% after subsequent MN patch skin puncture (Figure 5-6B), even though ISF collection data did not indicate an effect of blunt pre-treatment Figure 5-6A). However, rats in Group 3 that received a sharp-tipped MN patch pre-treatment, exhibited a 21% increase in skin hydration after the subsequent MN patch skin puncture (Figure 5-6B), which was associated with a large increase in ISF collection (Figure 5-6A) and supports the hypothesis that MN patch skin puncture increases skin hydration which can be associated with increased rates of ISF collection.

Visual observation of the skin immediately after 10 MN patch skin punctures did not show evidence of erythema or edema. Very mild erythema appeared 2 - 3 min after the skin punctures, which was localized to a small rectangle (~3mm by ~1 cm) at the sites of MN puncture. The erythema resolved within one day (data not shown). Edema was also

seen within 2 – 3 min, which spread over a larger area of ~1 cm^2 surrounding the MN puncture site. The edema resolved within few hours. Examination of skin sections taken from the sites of MN patch skin puncture did not show evidence of inflammatory cells at the time of collection (i.e., immediately after MN patch skin puncture) (Figure 5-7).

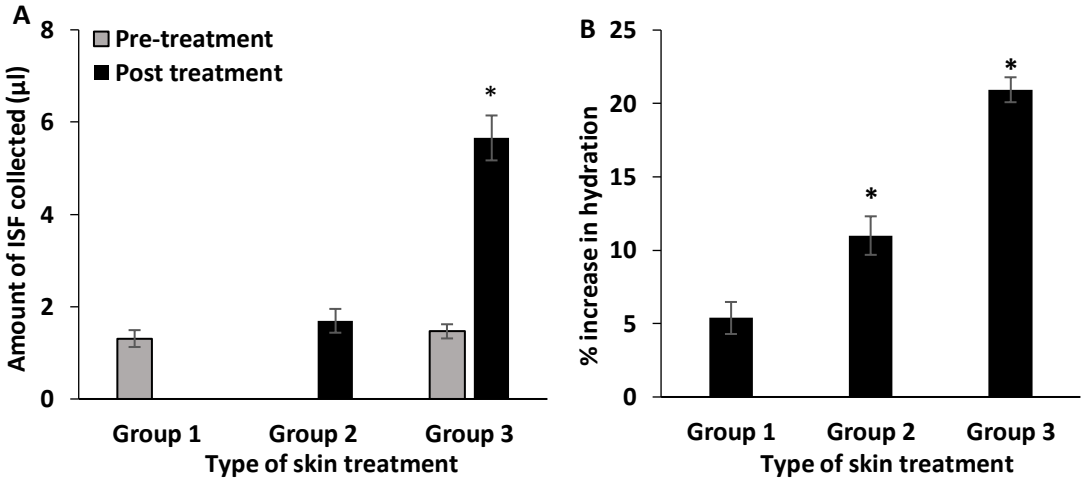

Figure 5-6: Effect of skin pre-treatment on amount of ISF collected and skin hydration. ISF was collected from the skin of shaved Wistar rats in vivo using 10 skin insertions with MN patches (Group 1), using a pre-treatment of 10 skin applications with a blunt MN patch backing (i.e., not expected to puncture skin) followed 5 min later by 10 skin insertions with MN patches (Group 2) or using a pre-treatment of 10 skin applications with a conventional, sharp-tipped MN patch backing (i.e., expected to puncture skin) followed 5 min later by 10 skin insertions with MN patches (Group 3), as described in Figure 1. A) Effect of skin pre-treatment of amount of ISF collected from shaved Wistar rat skin in vivo. B) Effect of skin pre-treatment on skin hydration in hairless rats in vivo. Immediately after the experiment in Part A, the weight of skin samples biopsied from the skin treatment area was measured before and after lyophilization (expected to fully dehydrate the skin) to determine hydration level. The percent increase in hydration due to skin pretreatment was determined by hydration levels of treated samples normalized to untreated control samples. Data represent mean ± SEM (standard error of the mean) of n= 15. Asterisk (*) depicts a significant increase in amount of ISF collected or percent increase in skin hydration compared to Group 1 (2 way ANOVA, $p < 0.01$).

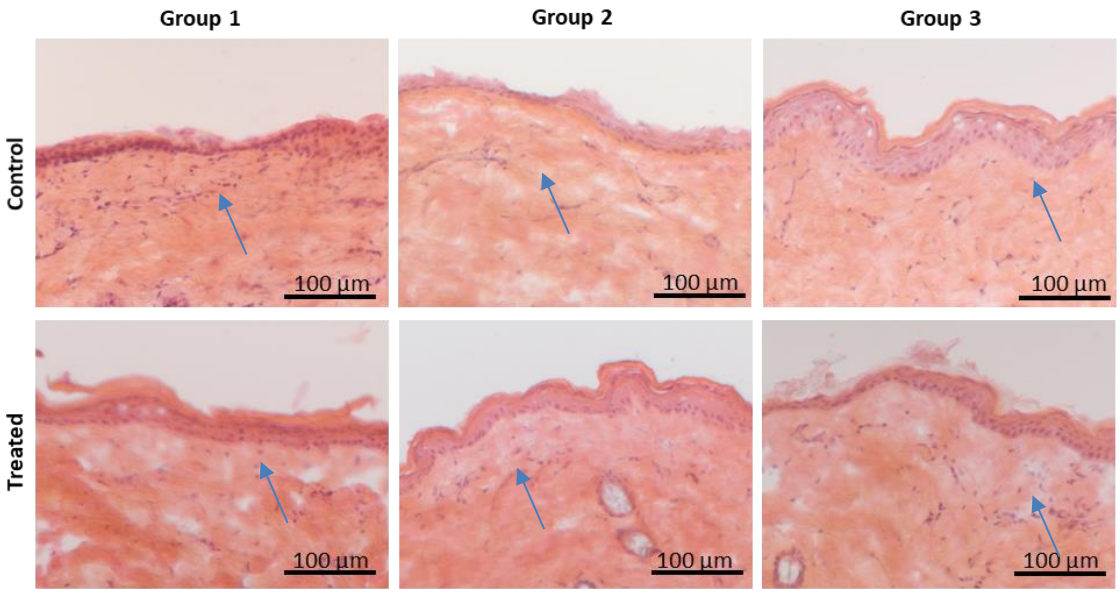

Figure 5-7: Representative images of H & E-stained sections of skin from shaved Wistar rats after ISF collection shown in Figure 6.The study plan for Groups 1, 2 and 3 is shown in Figure 1. Sections from skin treated with MN patches (Treated) is compared to skin from the same animals at untreated sites (Control). All skin samples showed mild signs of immune response, as evidenced by infiltration of immune cells (arrows), possibly due to hair removal due to shaving and application of depilatory cream. However, no meaningful differences in immune cell infiltration was observed between controls and treated samples or between the three test groups.

5.4 Discussion

5.4.1 Design of MN patch for simplified collection of ISF

ISF is a rich source of biomarkers but has been relatively unexplored due to lack of good sampling methods. Current methods like suction blister, microdialysis and open flow microperfusion cause significant skin trauma, are time consuming and require expert personnel and equipment to perform [92-95,159,171] . This study introduces a novel MN-based method to collect ISF that causes minimal skin trauma, takes just a few minutes to

perform and can be done using an inexpensive MN patch without the need for expert training to perform.

The MN patch causes minimal trauma because the MNs are of sub-millimeter dimensions. We demonstrated that >2 µl of ISF can be collected by inserting MNs up to 15 times within 20 s. Even more can be collected after additional insertions (e.g., we have collected up to 8 µL by administering 30 MN insertions within 2 min (data not shown)). We also demonstrated that microliter volumes of ISF can be collected with fewer insertions after skin pre-treatment followed by a 5 min delay. Microliter volumes should be sufficient for many assays, like glucose [172], cholesterol[173] and many drugs for therapeutic drug monitoring especially in neonates[174]. The MN patch should be cost effective when compared to other available ISF collection techniques because the cost of materials (stainless steel sheet, filter paper and adhesive) is nominal (estimated to cost less than a dollar) and the manufacturing and sterilization processes are straightforward. The MN patch is easy to use and does not require trained medical professionals for administration.

In contrast, conventional ISF collection methods such as reverse osmosis involve usage of proprietary equipment and methods such as micro dialysis or micro perfusion require minor surgery and significant expertise which can increase the overall cost of the collection procedure.

5.4.2 Factors affecting ISF collection

MN patch developed in this study consists of a simple two-component system: a stainless steel MN patch for puncturing the skin to form micro channels for ISF flow out of the skin

and a thin strip of paper to create a reservoir for the ISF. We tested five different types of paper for their water absorptiveness and chose Whatman grade 1 filter paper, which is commonly used in research applications for paper-based sensors due to its wicking ability[175]. The hydrophilic cellulose fibers in this paper allow ISF to penetrate the matrix without the need for active pumping or other driving forces[176]. This paper is also commonly functionalized for detection of specific analytes[169].

We tested the effect of multiple skin insertions, number of MNs per patch, MN thickness and wettability of the MN surface. All of these factors increased in ISF collection, enabling collection of >2 µL of ISF within 1 min. The multiple MN insertions facilitate ISF collection by increasing the number of pathways out of the skin and by their "pumping" action, which avoids the need to apply positive pressure or suction. A recent study showed that the rate-limiting step for ISF collection is often transport through the skin to the site of MN puncture, such that forces that generate convective flow in the skin can significantly facilitate ISF collection[121].

5.4.3 Effects of MN patch puncture on skin

An interesting finding was that MN patch pre-treatment of the skin followed by a 5 min wait time dramatically increased ISF collection. The effect was accompanied by an increase in tissue hydration of more than 20%. Because 1 cm^2 of skin contains on the order of 100 µL of ISF [121], it seems unlikely that the amount of ISF in the skin limited collection and just a ~20% increase in hydration increased ISF collection many fold. Instead, it is well established that hydraulic conductivity of the interstitial spaces of tissues

is low due to resistance provided by extracellular matrix (glycosaminoglycans) and collagen fibers. Even a relatively small increase in tissue hydration can increase spacing between fibers and thereby increase hydraulic conductivity. This is because volumetric flow rate through a porous medium increases with pore radius raised to the 4^{th} power, according to the Hagen–Poiseuille equation[177]. Additional studies are needed to more fully understand the relationship between skin hydration and ISF collection.

The cause of increased tissue hydration may be associated with an inflammatory response caused by minor tissue injury from repeated MN insertion into skin. In addition to edema, we observed a mild, highly localized erythema at the MN insertion site. Although inflammatory cells were not seen in skin histological sections collected immediately after MN patch treatment, it may have been too early to see inflammatory cells and examination of skin at later times would address this question. The mechanism of increased tissue hydration requires additional study.

5.4.4 Limitations of this study

There are limitations to this study in terms of the scope of the study and the ISF collection method itself. For example, this study used pig skin ex vivo and rat skin in vivo, which may not be fully predictive of results in human skin. This study also did not formally address the issue of safety other than acute effects at the time of ISF collection. However, we have used the same rats for many studies, especially during protocol development, and found that repeated collection of ISF using MN patches was well tolerated (data not shown). This study did not address the possibility of pain caused by ISF collection. While

similar MN patches applied to the skin of human subjects were reported as painless[132], multiple MN punctures of skin has not been studied. In terms of the ISF collection method itself, it is simple to perform but nonetheless requires ~1 min of active interaction with the patient. Also, the ISF partially or completely dries in the paper reservoir, which complicates determination of absolute biomarker concentrations, although this type of approach is used in dried blood spot tests in current clinical practice[178].

5.5 Conclusions

This study presents the development of a minimally invasive, rapid, simple-to-use and cost-effective MN patch to harvest >2 µl of ISF within 1 min. The technique represents a significant improvement over current ISF collection methods that cause significant skin trauma, are time consuming and require expert personnel and equipment to perform. The optimized MN patch was prepared by adhering a thin strip of filter paper serving as a reservoir to a stainless steel MN array prepared by lithographically defined chemical etching. Factors such as water absorptiveness of the paper, number of skin insertions, number of MNs per patch, thickness of the MNs and wettability of the MN surface all increased the amount of ISF collected in pig skin ex vivo. ISF collection was similar in rat skin in vivo skin, where skin pre-treatment with microneedles 5 min prior to ISF collection resulted in a marked increase in ISF collection, which was associated with increased skin hydration. This technique can simplify access to biomarkers in ISF for research and future medical diagnostic and monitoring applications.

5.6 Acknowledgements

We thank Richard Shafer for his help with laser cutting the filter paper and MN patches, and Donna Bondy for administrative support. The contact angle measurements were performed at the Georgia Tech Institute for Electronics and Nanotechnology, a member of the National Nanotechnology Coordinated Infrastructure, which is supported by the National Science Foundation (grant ECCS-1542174). This work was supported in part by that National Institutes of Health (grants U2CES026560 and R21EB025499). Mark Prausnitz is an inventor of patents that have been or may be licensed to companies developing microneedle-based products, is a paid advisor to companies developing microneedle-based products and is a founder/shareholder of companies developing microneedle-based products, including Micron Biomedical. These potential conflicts of interest have been disclosed and are being managed by Georgia Tech and/or Emory University.

CHAPTER 6. MONITORING DRUG PHARMACOKINETICS AND IMMUNOLOGIC BIOMARKERS IN DERMAL INTERSTITIAL FLUID USING A MICRONEEDLE PATCH

6.1 Introduction

Rapid disease detection and treatment depend on identification and reliable measurement of biomarkers [179]. Blood is the most common clinical sample for diagnostic assays [180]. However, limitations of blood sampling include the need for expert training to collect blood by venipuncture, especially in neonates, infants and patients with fragile veins; difficulty of continuous monitoring due to blood clotting; and apprehension by patients associated with blood draws [181]. Blood also requires downstream processing for most diagnostic assays to remove red blood cells [154].

Other body fluids such as saliva and urine are more easily accessible [182] but have limited biomarkers of variable concentrations [183]. Interstitial fluid (ISF) is a body fluid that fills the space between cells in tissues and constitutes 75% of extracellular fluid and 15-25% of body weight [158]. Recent studies have shown that ISF contains systemic biomarkers, but also contains other biomarkers that are unique or at much higher concentration compared to serum or plasma [6,7,121,157,158,159]. ISF is a clear fluid without red blood cells and does not clot, thus enabling simplified preparation for biochemical analysis.

ISF has been used for continuous glucose monitoring [184], analysis of tumor microenvironment [185] and bioavailability of topical drugs [186]. ISF has been sampled

by techniques such as reverse iontophoresis [98], which requires frequent calibration and is limited to small molecules; suction blister [171], which requires specialized equipment and causes lasting skin damage; and microdialysis [92], which requires minor surgery and expert personnel; microporation of upper non-viable layer of skin using a focused NIR laser followed by ISF collection under vacuum[187] which collects up to 10 μl of ISF in 1 hour .

More recently, microneedle (MN) technology has been developed for ISF sampling. MNs are micron-scale, sharp-tipped projections that can puncture micropores into the skin to access dermal ISF in a minimally invasive manner [29]. MN patches were developed initially for delivery of vaccines and drugs, where they have been shown to be painless, well-tolerated, easy-to-use and effective for delivering therapeutic molecules into skin [162,188]. MNs have also been used for detection of glucose and other biomarkers in dermal ISF [6,160].

Approaches to ISF collection using MNs include extracting ISF from skin through micropores for extracorporeal analysis [121], which typically takes 15 min or longer; swelling hydrogel-forming MNs with ISF in skin [118,120], which generally collects nanoliter quantities of ISF, which is insufficient for many biomarker assays; selectively binding biomarkers to MN surfaces modified for in-situ capture of biomarkers [8,115], which must be custom designed for each biomarker; and incorporation of sensors into MNs for in situ analysis of ISF [106,108,109], which is technically challenging and requires a different sensor for each biomarker.

To overcome the various limitations of prior MN technology, we developed a MN patch that collects microliters of ISF within one minute that can be assayed for any biomarker of interest. We used this MN patch to sample ISF, determine ISF concentrations of a model drug (vancomycin) and a model immunomarker (anti-polio antibodies), and compare them to serum concentrations. We chose vancomycin, an antibiotic commonly used to treat gram-positive methicillin-resistant *Staphylococcus aureus* infections (MRSA), because it's very narrow therapeutic index requires therapeutic drug monitoring to ensure efficacy and minimize toxicity during patient care [122,189]. We chose to monitor anti-polio antibodies because they can be measured using well-established immunoassays by our collaborators at the WHO Global Specialized Reference laboratory located at the Centers for Disease Control and Prevention (CDC).

6.2 Materials and methods

6.2.1 Materials

Monovalent, bulk inactivated polio vaccine (IPV) (Mahoney strain of type 1, Middle East Forces (MEF) strain of type 2 and Saukett strain of type 3) was kindly provided by Bilthoven Biologicals (Bilthoven, Netherlands). The antigen concentrations were 1675, 963 and 950 D-antigen units (DU)/ml for IPV types 1, 2 and 3, respectively, determined by antigen-capture sandwich enzyme-linked immunosorbent (ELISA), as previously described [42].

Vancomycin hydrochloride from *Streptomyces Orientalis* was purchased from Sigma Aldrich (St. Louis, MO). HPLC-MS grade acetonitrile, methanol and water were

purchased from MedSupply Partners (Atlanta, GA) and formic acid (98%, ACS grade) was obtained from EMD Millipore Chemicals (Darmstadt, Germany).

6.2.2 Microneedle patch fabrication

MN patch dimensions were drafted using AutoCAD software (Autodesk, Cupertino, CA) to prepare patches by lithographically defined chemical etching (Tech Etch, Plymouth, MA). Patches were comprised of 9 MNs (650 µm long) each measuring 50 µm x 150 µm in cross section at the base and tapering to a tip of <1 µm radius of curvature.

Whatman grade 1 filter paper (Sigma Aldrich, St. Louis, MO) was cut into rectangular strips of desired dimensions (2 mm x 7 mm) using a CO_2 laser (New Hermes Gravograph Model LS500XL, Gravotech, Duluth, GA). The patterns were made using a vector cut at 24 W power and a speed of 8 mm/s. To prevent burning due to excessive temperature rise during laser cutting, the heat capacity of the filter paper was increased by attaching it to an adhesive backing (3M, Maplewood, MN), followed by soaking in DI water until completely wet.

The final MN patch was prepared by adhering the paper strips to both sides of the base substrate of each MN patch to create a reservoir to collect ISF that flowed out of the skin during MN insertion.

6.2.3 ISF collection procedure

The MN patch was applied to rat skin up to 12 times while pinching the skin with a force of 20-40 N. The amount of ISF collected was estimated to be 4 µl once the 2 mm x 7 mm filter paper on both sides of the MN patch were saturated with ISF. This estimate was performed by determining sodium ion content in the MN patch paper backing using a sodium ion sensitive electrode (perfectION comb NA, Mettler Toledo, Columbus, OH). The sodium ion content measured in the samples was divided by the physiological sodium ion concentration in rat ISF of 143 mEq/L[165][165] to determine ISF volume collected. This method relies on the expectation that sodium ion concentration is constant in the ISF of normal rats [166].

6.2.4 Vancomycin pharmacokinetic study

Procedures were performed on six Wistar rats (10-20 weeks old, female, Charles River Laboratories, Wilmington, MA) anesthetized by inhalation of isoflurane (AErrane, Baxter Healthcare, Deerfield, IL) in 100% oxygen during drug administration and sample collection. To administer vancomycin and collect blood, a silicone rubber tube was placed in the right jugular vein and kept locked with sodium heparin solution in physiological saline (100 U/ml). Care was taken to avoid administration of air bubbles, and blood samples were replaced with an approximately equal volume of heparinized saline to maintain blood volume. A 0.75 mg/ml solution of vancomycin hydrochloride in 0.9% NaCl injection solution (Hospira, Lake Forest, IL) was prepared and each rat was administered 1 mg/kg dose via the jugular vein tube. Blood samples were obtained from the jugular tube before and 10, 20, 30, 45, 60 and 90 min after vancomycin administration. Companion ISF

samples were also collected at the same time points. At the end of the study, the rats were euthanized by carbon dioxide gas asphyxiation. These experiments were approved by the Georgia Institute of Technology Institutional Animal Care and Use Committee.

6.2.5 Extraction of vancomycin from ISF/serum samples

The extraction of vancomycin from ISF and serum samples was performed according to a previously reported method [189]. Serum samples were diluted by mixing 4 µl of serum in 100 µl of deionized water. ISF was extracted from MN patches by centrifuging 1 MN patch in 100 µl of deionized water at 6000 x *g* for 10 min. All samples were stored at 4 °C until testing. Then, 100 µL of formic acid/methanol (1:1, v/v) was added to each ISF or serum sample. The mixture was vortexed for 30 s and then centrifuged for 15 min at 12,000 x *g*. The supernatant was removed, diluted with 300 µL of high-performance liquid chromatography – mass spectrometry (HPLC-MS) grade water, and then transferred to an HPLC vial for HPLC-MS/MS analysis.

6.2.6 HPLC-MS/MS analysis

Calibrators were prepared by adding aliquots of vancomycin stock solution to a drug-free serum matrix to create the following concentrations: 1.0, 2.0, 6.0, 13, 32 and 75 µg/mL. The calibration curve was plotted using Mass Hunter QQQ Quantitative Analysis software (Agilent, Santa Clara, CA). The data were weighted 1/x and concentrations of vancomycin were calculated by the software.

Chromatography was performed by injecting 50 µl of extracted calibrator or sample onto an Agilent 1200 series HPLC fitted with an Agilent ZORBAX Eclipse C18 column (2.1 x 150 mm, 3.5 µm particle size). The column temperature was maintained at 35°C and the flow rate was maintained at 0.4 mL/min. Mobile phase A consisted of 0.25% formic acid in water and mobile phase B consisted of 0.25% formic acid in acetonitrile. Vancomycin was separated using a gradient method as follows: 5.0% mobile phase B from 0.00-3.00 min, increased to 30% mobile phase B from 3.01-10.00 min, increased to 90% mobile phase B from 10.01-12.00 min, decreased to 5.0% mobile phase B from 12.01-14.00 min, then maintained at 5.0% mobile phase B from 14.01-16.00 min.

An Agilent 6410 triple quadrupole mass spectrometer was used to analyze samples in positive ion mode. The mass spectrometer parameters were as follows: capillary voltage of 3500 V, electron multiplier voltage at 300 V, gas temperature of 350 °C, nebulizer pressure of 240 kPa and gas flow rate of 10 L/min. Vancomycin was monitored using multiple reaction monitoring of the transition m/z 725.6→144.2. Chromatographic peaks were then manually integrated and analyzed using MassHunter software (Agilent, Santa Clara, CA).

6.2.7 Polio immunization

Six Wistar rats (10-20 weeks old, female, Charles River Laboratories) were anesthetized by isoflurane (AErrane, Baxter Healthcare) inhalation during all procedures. IPV stock solutions were combined and diluted using medium 199 to a concentration of 44, 8 and 36 DUs of IPV types 1, 2 and 3, respectively in 100 µl, as determined by ELISA. We

administered two 100 µl intramuscular injections per rat (one in each hind limb) for a total dose of 88, 16 and 72 DU of IPV types 1, 2 and 3, respectively.

Sera and ISF samples for polio-specific IgG testing were collected before and 1, 3 and 4 weeks after immunization. Twelve weeks after the initial vaccination, all animals were given a second dose of trivalent IPV in the same manner as the first dose. Sera and ISF samples for neutralizing antibody titer assay were collected before and 1, and 2 weeks after the second dose.

Blood samples (≤ 500 µl) were collected in microtainer collection tubes with clot activator (BD Diagnostics, Franklin Lakes, NJ) by tail bleeding after making a small incision in the tail using a surgical blade. ISF samples were collected from the lateral side of the rat after hair removal using electric shears followed by application of depilatory cream (Nair, Princeton, NJ). Hair removal was performed at least 1 day prior to ISF collection to avoid possible ISF contamination by the depilatory cream. At the end of the study, the rats were euthanized by carbon dioxide gas asphyxiation. These experiments have been approved by the Georgia Institute of Technology Institutional Animal Care and Use Committee.

Serum was separated by centrifuging the blood samples at 6000 x *g* for 1.5 min in an Eppendorf Centrifuge 5415R (Eppendorf AG, Hamburg, Germany). For the anti-polio IgG testing, 6 µl of serum was diluted with 120 µl of dilution buffer (provided with the ELISA kit) and the MN patch containing 4 µl of ISF was placed in an Eppendorf tube containing 80 µl of dilution buffer and centrifuged at 6000 x *g* for 1.5 min.

For polio-specific neutralizing antibody titers, a 1:16 dilution of serum samples was performed by mixing 16 µl of serum with 240 µl of Dulbecco'smodified Eagle Medium

(DMEM, Gibco, Grand Island, NY) and 2% fetal bovine serum (FBS, Gibco) and a 1:16 dilution of ISF samples was performed by extracting ISF from the MN patches by centrifuging in DMEM (2 MN patches per 120 µl) at 6000 x *g* for 1.5 min. The undiluted serum samples and the diluted ISF/serum samples were stored in Eppendorf tubes at -20 °C until used.

6.2.7.1 Anti-polio IgG measurements and polio-specific neutralizing antibody titers

A commercially available ELISA IgG assay (Anti-Polio viruses 1-3 IgG ELISA kit, Alpha Diagnostics Intl, San Antonio, TX) was used for the detection and quantitative determination of IgG antibodies to polio virus in serum and ISF specimens. Prior to testing, the sera and ISF samples were thawed and diluted to 1:100 by adding 480 µl and 320 µl, respectively, of low Nsb diluent (provided with the ELISA kit).

Neutralizing antibody titers to poliomyelitis were measured from collected sera and ISF samples at the WHO Global Specialized Reference laboratory at CDC (Atlanta, GA) using methods previously described [190]. Briefly, 80-100 $CCID_{50}$ of Sabin strains 1, 2, and 3 poliovirus and two-fold serial dilutions of serum and ISF (starting at 1:4) were combined and incubated for 3 h at 35 °C prior to addition of HEp-2(C) cells. The plates were stained with crystal violet and cell viability was measured by optical density after 5 days of incubation at 35 °C and 5% CO_2. Each sample was run in triplicate. The neutralization titers were estimated by the Spearman-Karber method [191] and reported as the reciprocal of the calculated endpoint. The limit of detection for this assay is a 2.5 $\log_2$ titer, and the precision of detection is ± 0.5 $\log_2$ titer.

6.2.8 Statistical analysis

Statistics were calculated using either Prism software version 7.0 (Graphpad, La Jolla, CA) or Excel (Microsoft, Redmond, WA). Arithmetic mean and median values of the samples are reported. Comparison between three or more samples was performed by one-way ANOVA or two-way ANOVA. Correlation between data was determined by Pearson's correlation coefficient test. Probability (p) values of <0.05 were considered to be significant.

6.3 Results

6.3.1 ISF collection by microneedle patch

The MN patch comprised of a two-component system: 2 strips of filter paper (to create a reservoir for ISF) on both sides of the backing of a stainless steel MN array (which punctures the skin to create micropores for ISF to flow out of the skin) (Figure 6-1A). The ISF collection was performed by repeatedly inserting the MN patch to the skin surface with a force of 20-40 N, thereby inducing flow of ISF out of the skin and into the paper reservoirs (Figure 6-1B). The MN patch after ISF collection is shown as Figure 6-1C.

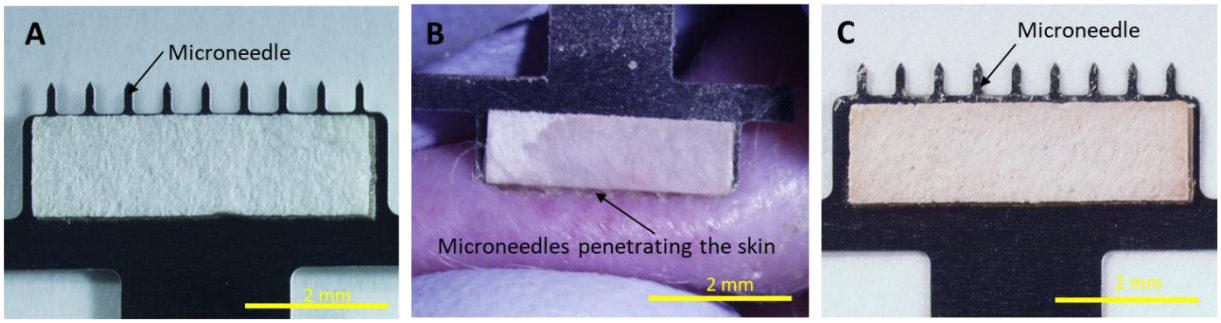

Figure 6-1: Collection of ISF using a microneedle (MN) patch. A) Representative photographic image of a MN patch showing a row of nine MNs measuring 650 µm in length extending from a patch backing with rectangular strips of filter paper adhered to both sides. B) Representative photographic image of ISF collection from hairless rat skin in vivo. Upon application of the MN patch to the skin, clear interstitial fluid (ISF) flowed out of the skin through micropores created by the MNs and was collected in the paper reservoirs. The paper reservoir shown in this image is mostly wetted by ISF, with only the upper left corner still dry, as indicated by different visual appearance. C) Representative photographic image of a MN patch after ISF collection by repeated application to skin. The amount of ISF collected on each strip of paper was ~2 µl, for a total of ~4 µl per MN patch.

6.3.2 Vancomycin pharmacokinetics

To assess the utility of ISF collection by MN patch, we studied the pharmacokinetics of vancomycin in ISF compared to serum of rats. For both ISF and serum, vancomycin concentration was rapidly increased by the first measurement made 10 min after bolus injection of vancomycin as shown in Figure 6-2A and B.

After reaching a peak, the vancomycin concentration decayed, which followed the expected pharmacokinetic curve for this drug [192]. Plotting paired individual ISF and serum drug levels yielded a roughly linear correlation with a slope of 0.75 ± 0.06 (R^2 = 0.40), indicating a generally higher vancomycin concentration in ISF compared to serum.

A one-way ANOVA analysis of the pharmacokinetic profiles of each rat showed no statistically significant difference between ISF and serum concentrations ($p \geq 0.15$) Pharmacokinetic analysis showed that the average peak vancomycin concentration (C_{max}) and area under the curve (AUC) were not significantly different in ISF and serum (Student's t-test, $p > 0.8$). A ~17 min delay in time to peak vancomycin concentration (T_{max}) in ISF compared to serum was statistically significant (Student's t-test, $p < 0.05$). This is consistent with prior literature, which reported correlation of vancomycin levels in ISF and blood and a delayed time for equilibration of vancomycin levels between ISF and blood [123,189].

In this study, each rat had ISF collected seven times over the course of 90 min (i.e., a total of 42 ISF collections among the six rats in the study). Each ISF collection was done at a different skin site. These ISF collection procedures involving insertion of MNs into the skin up to 12 times each were well tolerated, with only very mild erythema and edema seen at the site of ISF collection. There were no other notable effects of the ISF collection procedure on the animals.

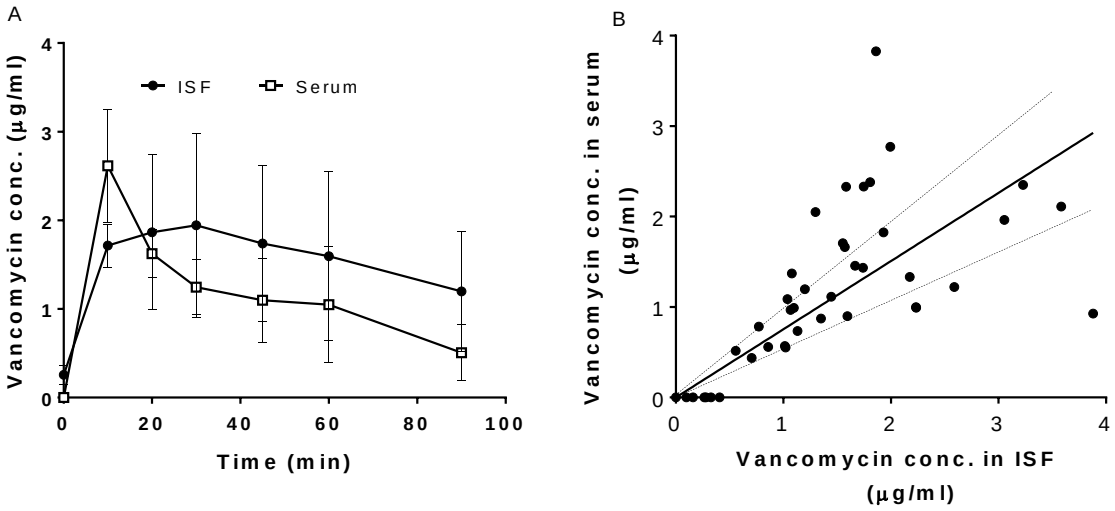

Figure 6-2: Pharmacokinetics of vancomycin in rat ISF and serum. A) Pharmacokinetic profile of vancomycin concentration in ISF and serum samples collected from rats administered a 1 mg/kg bolus intravenous injection of vancomycin. Data points show mean ± standard deviation (SD) (n = 6 rats). B) Correlation between vancomycin concentration in paired serum and ISF samples (r= 0.61, p<0.005, Pearson's correlation coefficient test). Dashed lines represent ± 30 % of the slope of the linear regression line (shown as solid black line), which are included as a visual guide. Data are the same as shown in (A)

Table 6-1: Comparison of AUC, C_{max} and T_{max} values of vancomycin pharmacokinetics between ISF and serum

Pharmacokinetic parameter[1]	**ISF**	**Serum**	**Ratio (ISF:serum)**
AUC (µg.min/ml)	138 ± 43	106 ± 25	1.3 ± 0.2
C_{max} (µg/ml)	2.5 ± 1	2.6 ± 0.6	0.9 ± 0.2
T_{max} (min)	26.6 ± 16*	10 ± 0	2.7 ± 1.6

[1]Data are presented as mean ± SD (n= 6 rats). AUC, area under the concentration-time curve. C_{max}, maximum concentration. T_{max}, time required to reach maximum concentration. Asterix (*) denotes parameters with statistically significant difference ($p < 0.05$) between ISF and the companion serum value.

6.3.3 Immune responses to inactivated polio vaccination

6.3.3.1 Anti-polio IgG responses

We also assessed the utility of ISF collection by MN patch in detection of anti-polio IgG responses in rats immunized with trivalent inactivated polio vaccine. Anti-polio IgG titers were negligible before and one week after vaccination. Three and four weeks after vaccination, IgG titer in both ISF and serum increased dramatically, but titers in ISF were ~23% lower than in serum (Student's t-test, $p < 0.03$). Plotting paired individual ISF and serum IgG titers yielded a linear correlation with a slope of 1.27 ± 0.09 ($R^2 = 0.81$), indicating a generally lower IgG titer in ISF compared to serum.

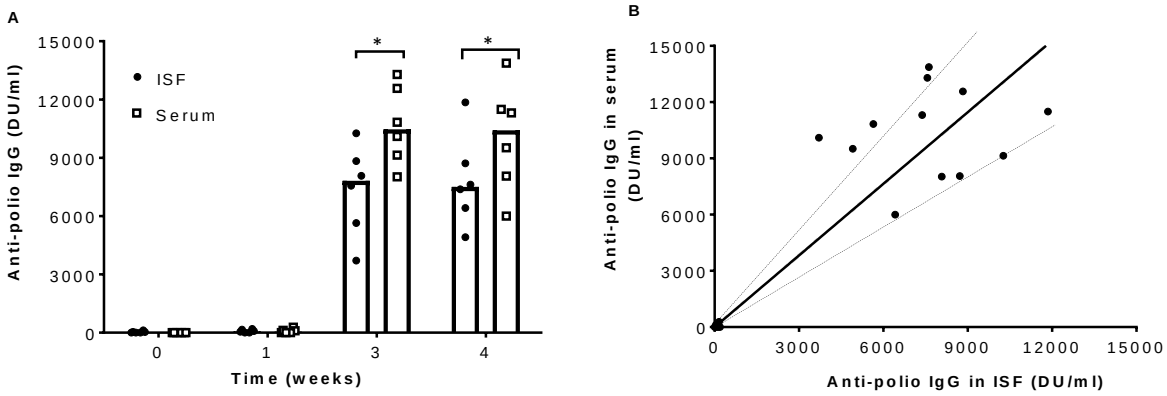

Figure 6-3: Anti-polio IgG responses to inactivated polio vaccination in rats. a) Anti-polio IgG titers determined by ELISA in ISF and serum samples collected before and 1, 3 and 4 weeks after vaccination with trivalent IPV by intramuscular injection. Each data point represents a single animal while the bars represents the median values of each group (n = 6 rats). Asterisk (*) represents a significant difference (Student's t-test, $p < 0.03$). b) Correlation between anti-polio IgG titers in paired serum and ISF samples ($r = 0.90$, $p<0.005$, Pearson's correlation coefficient test). Dotted lines represent ± 30% of the slope of the linear regression line (shown as solid black line), which are included as a visual guide. Data are the same as shown in (a)

6.3.3.2 Polio-specific neutralizing antibody responses

After observing the anti-polio IgG response in ISF, we performed a follow-up study to detect polio-specific neutralizing antibody responses by collecting ISF and companion blood samples after vaccinating the rats with a booster dose of trivalent inactivated polio vaccine. Before vaccination, neutralizing antibody titers in ISF and serum samples for all three serotypes were below the limit of detection (Figure 4a). One and two weeks after vaccination, neutralizing antibody titers increased in both ISF and serum, but titers in ISF were ~30% lower than in serum (Student's t-test, $p<0.01$). This rapid increase of titer within one week is expected because responses to booster vaccination are typically seen on this time scale [27]. Paired individual ISF and serum titers were linearly correlated with

a slope of 1.36 ± 0.07 (R^2 = 0.79), 1.41 ± 0.06 (R^2 = 0.78) and 1.36 ± 0.06 (R^2 = 0.82) for IPV types 1, 2 and 3, respectively, indicating a generally lower neutralizing antibody titer in ISF compared to serum.

These were the same rats that were used in the study of polio-specific IgG, meaning that each rat had ISF collected seven times over the course of 14 weeks. The procedures were well tolerated, with only very mild, transient erythema and edema seen at the site of ISF collection.

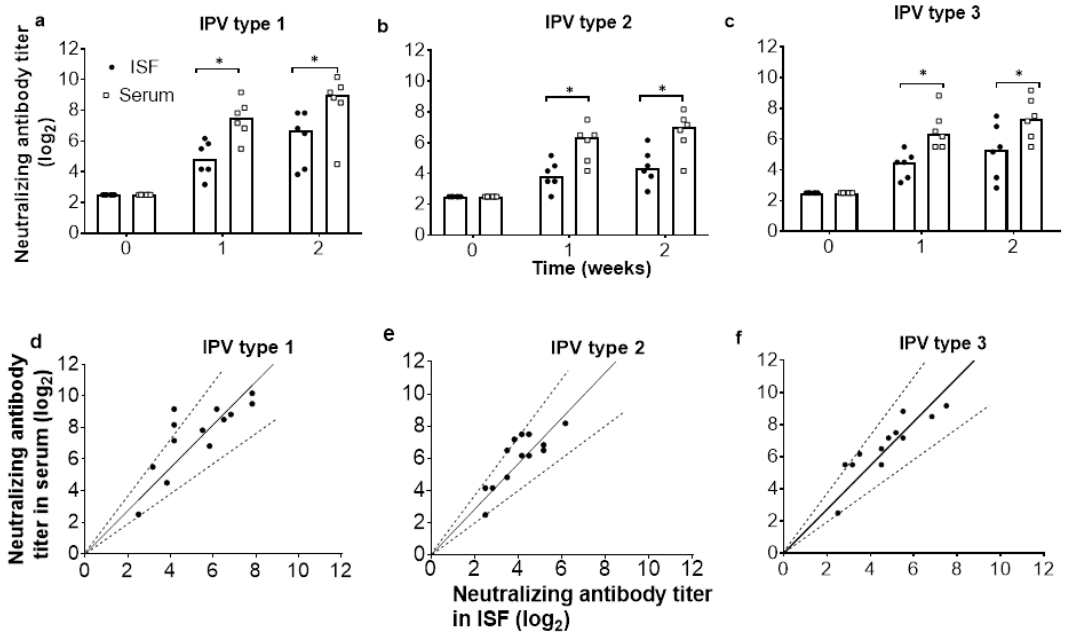

Figure 6-4: Neutralizing antibody responses to inactivated polio vaccination. Neutralizing antibody titers to a) IPV type 1, b) IPV type 2 and c) IPV type 3 in ISF and serum samples collected before and 1 and 2 weeks after administration of a booster dose of trivalent IPV by intramuscular injection in rats (the first dose was administered 12 weeks earlier). The limit of detection for the assay was 2.5 log_2. Each data point represents a single animal while the bars represents the median values of each group (n = 6 rats). Asterisk (*) represents a significant difference (Student's t-test, p < 0.01). Correlation between neutralizing antibody titers in paired serum and ISF samples for d) IPV type 1, (r= 0.89, p<0.005, Pearson's correlation coefficient test), e) IPV type 2 (r= 0.87, p<0.005) and f) IPV type 3 (r= 0.91, p<0.005). Dotted lines

represent ± 30% of the slope of the linear regression line (shown as solid black line), which are included as a visual guide. Data are the same as shown in (a)

6.4 Discussion

6.4.1 MN patch for simplified ISF sampling

ISF is a relatively unexplored body fluid in major part due to lack of simple, reliable techniques to sample this fluid. In this study, we used a simple MN patch-based method to collect microliters of ISF in a minimally invasive manner within one minute. The MN patch consists of a steel MN array with strips of filter paper adhered on both sides of the patch backing. The MN patch should be inexpensive and the manufacturing process should be straightforward. ISF collection can be performed without expert training and the amount of ISF sampled can be controlled by changing the number of insertions into skin and the size/type of paper used for the ISF reservoir. We have performed repeated ISF collection on the same rats during these studies (i.e., ISF was collected a total of 84 times among 12 rats) and found that the procedure was well tolerated with a mild, localized erythema at the MN insertion site which resolved within one day (data not shown).

6.4.2 Drug monitoring in ISF

While other body fluids such as saliva and urine have been investigated for therapeutic drug monitoring [182], ISF is a body fluid of increasing interest as a source of biomarkers providing dermal and systemic physiological information, as well as drug pharmacokinetics. Most research has been focused on detection of glucose in ISF, and

indwelling subcutaneous sensors are now commonly used to continuously measure glucose concentration in subcutaneous ISF as a surrogate for blood glucose levels in diabetic patients [100].

Other biomarkers have also been investigated in ISF, largely for research purposes. A comprehensive review of 87 individual pharmacokinetics comparisons of various classes of antibiotics demonstrated different ratios of drug concentration in ISF versus plasma, which was largely explained by different degrees of protein binding [123]. Other drugs such as scopolamine, theophylline, methotrexate, vancomycin, carbamazepine and phenobarbital have also been measured in ISF and had similar AUC in serum/plasma and ISF samples [124,126]. On the other hand, some drugs such as phenytoin were not detectable in ISF [126]. These studies involved ISF collection using microdialysis and ultrafiltration probes, which cause significant skin damage, are time consuming to perform, require expert personnel and specialized equipment, and are not suitable for routine clinical use.

We demonstrated the ability of a minimally invasive MN patch to quickly collect ISF and detect biomarkers of interest, which provides an alternative approach to therapeutic drug monitoring in ISF. We collected microliters of ISF within 1 min, which should be sufficient to run many assays to detect biomarkers of clinical significance [172,193]. This contrasts with other MN-based methods that typically sample nanoliters of ISF and/or require as long as an hour of collecting [118,121]. In this study, pharmacokinetics of vancomycin showed similar AUC and C_{max} values in ISF and serum samples in rats, although vancomycin concentrations overall were slightly higher on average compared to serum levels. A delay in T_{max} was observed in ISF, which is consistent with literature

[123,189]. More studies are needed to understand the factors that influence drug distribution between ISF and blood. For example, vancomycin was shown to distribute into ISF at levels similar to serum in healthy patients with limb infections [194], but had wide variability in vancomycin penetration into ISF in diabetic patients [195].

6.4.3 Immunodiagnostic markers in ISF

We also used ISF collected by MN patch to detect polio-specific IgG and neutralizing antibodies, which were at similar concentrations in ISF and plasma, although ISF levels were slightly lower. It has been shown that skin vaccination, especially by MN patch, can provide stronger, broader, longer-lasting and otherwise improved humoral and cellular immune responses compared to intramuscular injection [196]. Likewise, skin-associated B cells are believed to play an important role in skin immunity and inflammation [197] . Therefore, the ability to measure local antibody titers in tissue ISF could play an important role in understanding tissue-specific immune responses.

6.5 Conclusion

We studied ISF collected from the skin using a minimally invasive, simple-to-use, low-cost MN patch that can collect microliters of ISF within 1 min. Of interest to therapeutic drug monitoring, we performed a pharmacokinetic study of vancomycin in rats and found that AUC and C_{max} were similar in ISF, but T_{max} was delayed in ISF by ~17 min compared to serum. Another study examined immunologic biomarkers in ISF by administering

inactivated polio vaccine to rats and determined that polio-specific IgG and neutralizing antibody titers were similar in ISF and companion serum samples. We conclude that ISF collection using a novel MN patch can provide simple and rapid collection of microliters of ISF for future medical and research applications.

6.6 Acknowledgments

The authors would like to thank William Weldon of the CDC for conducting the serum and ISF neutralizing antibody assays and Donna Bondy for administrative support. Mark Prausnitz is an inventor of patents that have been or may be licensed to companies developing microneedle-based products, is a paid advisor to companies developing microneedle-based products and is a founder/shareholder of companies developing microneedle-based products, including Micron Biomedical. These potential conflicts of interest have been disclosed and are being managed by Georgia Tech and/or Emory University.

CHAPTER 7. CONCLUSIONS

7.1 Dissolving MN patch for polio vaccination

Poliomyelitis is a highly infectious disease which can only be prevented by immunization. The aim of this study was to develop a thermostable dissolving MN patch for polio vaccination. The formulation optimization studies involved screening of different excipients, buffers and pH conditions for the 1st and 2nd cast of the MN patch. The four best excipients found from primary screening were D-sorbitol, maltodextrin, sucrose and trehalose. Further optimization of the ratios of these excipients resulted in a final MN patch with a first cast of IPV mixed with D-sorbitol and maltodextrin, and a second cast containing fish gelatin and D-sorbitol in histidine buffer.

Process optimization studies based on the ELISA showed the air drying at 25°C with desiccant for 2 days resulted in minimal loss of IPV and subsequent lyophilization did not show any significant advantage. Drying at elevated temperatures resulted in reduction in IPV potency. Using TGA, we found that the residual moisture content (RMC) in the MN patches was initially 6.5 % which continued to drop down to 1.2 % depending on storage conditions. However, the moisture content did not correlate with the IPV activity, implying that further removal of bound and unbound water did not influence the thermal stability. In contrast, IPV activity and temperature were correlated. This shows that IPV destabilization processes are significantly driven by elevated temperature over the range of conditions studied.

The final optimized MN patch was deemed to be sufficiently mechanically robust based

on successful insertion in ex-vivo pig skin. Examination of used microneedle patch after 15 min showed complete dissolution of the microneedles.

The optimized MN patch maintained >70% activity of all three serotypes after 2 months and >50% activity after 1 year storage at 5°C or 25°C with desiccant. Storage at 40°C yielded >40% activity after 2 months and >20% activity after 1 year. In contrast, IPV completely lost its potency if dried without any excipients, and commercial liquid IPV showed <10% activity after 1 month of storage at 40 °C and is recommended to be stored at 2°C to 8°C.

Using DSC, we found that the MN matrix initially had a T_g of 48 °C, which increased over time to as much as 59 °C depending on storage condition. This increase in T_g is consistent with the observed decrease in RMC with storage time because water is a potential plasticizer, and loss of moisture from MN matrix during storage would result in increase in T_g. since water acts as a plasticizer. The observed thermal stability at 5 °C and 25 °C may be because they are well below the T_g, but stability was worse at 40 °C, which is closer to the T_g of the MNs. Fourier-transform infrared spectra of samples after storage for 30 days at 5 °C, 25 °C or 40 °C appeared very similar, which means that no significant chemical changes were detected among the samples. Structural changes in MN patches measured by X-ray diffraction showed a decrease in crystalline phase and an increase in amorphous phase with storage. This finding is consistent with the observed increase in T_g and decrease in RMC. Studies aimed at understanding this stabilization mechanism have shown that sorbitol is preferentially excluded from the surface of the native protein, i.e. in the presence of sorbitol, proteins are preferentially hydrated. This preferential hydration induces protein stabilization[198]. It is theorized that polyols such as sorbitol stabilize IPV

based on a preferential exclusion effect. Elevated temperatures may be affecting these microscopic interactions between sorbitol and IPV there by resulting in destabilization.

7.2 Paper based MN patch for ISF sampling and detection of biomarkers

Measurement of biomarkers in body fluids is a valuable tool for accurate disease diagnosis and monitoring. In addition to body fluids such as blood, urine, saliva, sweat, and tears, ISF is a rich source of biomarkers for diagnostic applications. Development of simple-to-use point-of-care (POC) devices is highly desirable due to the need for regular or continuous monitoring of analytes, and the need to non-invasively sample biomarkers has opened the potential for ISF as an alternate body fluid.

Current methods like suction blister, microdialysis, sensor implantation and open flow microperfusion cause significant skin trauma resulting in long healing times, require expert personnel and are time consuming. Other non-invasive methods such as reverse iontophoresis are limited by the inability to sample large molecules. MNs have been demonstrated as a minimally invasive technique for ISF collection. Previous studies for ISF collection using MNs have been limited by the sub-microliter volumes of ISF which are not sufficient for multiple analyte measurement and often require 15-20 min time for collection.

The second half of the thesis was focused on development of a minimally invasive, rapid, simple-to-use and cost-effective method to collect ISF from the skin involving a microneedle (MN) patch.

The patch consists of a simple two component system: A steel MN array to penetrate the skin and form micro-channels for ISF to flow out of the skin and a thin strip of filter paper to create a reservoir for ISF.

We identified different parameters which influenced the ISF collection and found an increase in the ISF collected by increasing the number of skin insertions, MN thickness and increasing number of MNs. Increasing number of skin insertions and number of MNs per patch both should increase the number of micropores for ISF to flow out of skin. Thicker microneedles should result in larger micropores, thereby allowing easier access to ISF. We also found that improving the wettability of steel MN surface resulted in faster ISF collection by facilitating ISF flow to the paper reservoir.

An interesting finding was that MN patch pre-treatment of the skin followed by a 5 min wait time dramatically increased ISF collection by 4 times. The effect involved an increase in skin hydration of more than 20% which can be associated with increased rates of ISF collection. In addition to edema, we observed a mild, highly localized erythema at the MN insertion site which resolved within a day.

We then, tested the utility of this optimized MN patch by demonstrating the suitability of using ISF for therapeutic drug monitoring (TDM). We performed rat in-vivo studies and showed similar vancomycin concentration-time profiles and pharmacokinetic parameters in the ISF and blood. We also, for the first time, detected polio specific neutralizing antibodies, and anti-polio IgG in ISF similar to blood in rats immunized with polio vaccine. These studies demonstrate the potential application of our MN patch in TDM and immunodiagnostic applications.

CHAPTER 8. FUTURE DIRECTIONS

8.1 MN patch with faster dissolution kinetics, shorter wear time with biocompatible excipients

Even though the optimized dissolving MN patch was thermostable, and mechanically robust, the dissolution time was ~ 15 minutes. This patch will be used in a pediatric population which is challenging, partially due to the age ranges within this population. Studies have shown a strong consensus regarding MN technology in children[199], however, it would be highly desirable to have a MN patch with faster dissolution in the order of 1-2 minutes for a shorter wear time. Another approach could be to design an MN patch with separable MNs for shorter administration time[40].

Fish gelatin is one of the components of the MN patch and there is a risk related with allergic reactions and sensitization. Future studies may focus on other more biocompatible biopolymer IPV stabilizers.

The studies performed showed that the dissolving MN patch maintained >70% activity after 2 months and >50% activity after 1 year at 5°C or 25°C, but maintained >40% activity after 2 months and >20% activity after 1 year at 40 °C. It would be desirable to have an MN patch which is more stable at elevated temperatures. A more complete screen of various excipients could be performed which may result in formulations with an even higher level of stabilizing activity especially at elevated temperature. Due to temperature fluctuations between night and day, the MN patches may not need to maintain activity at elevated temperatures for an extended period of time. Transient temperature stability may

be sufficient. While MN patches were tested for IPV activity after storage, they were not tested for mechanical robustness. Mechanical testing must be performed after extended storage to ensure that the microneedle patches remain sharp and retain the ability to easily insert into the skin.

The immunogenicity of this optimized MN patch was not tested in animal models which has to be addressed in the future.

8.2 Microneedle patch for ISF collection

The optimized MN patch was demonstrated to be capable of collecting >2 µl of ISF within a minute upon repeated skin insertions in rats. We also demonstrated that multiple microliters of ISF can be collected by MN skin pre-treatment followed by a 5 min delay. Nevertheless, the method involves repeated MN insertions and its effect on skin tolerability and the possible pain has not been studied in detail, especially in humans. This study was performed in pig skin ex vivo and rat skin in vivo only. Human feasibility studies should be performed in the future to test the effect of MN skin pre-treatment on skin hydration. Future studies should also formally address the issue of safety and the possibility of pain caused by ISF collection.

An important finding from this study was that the need to apply positive pressure and suction could be avoided by multiple MN insertions. The ISF collection was facilitated by the “pumping” action of multiple insertions which increases the number of pathways out of the skin. Since the rate-limiting step for ISF collection is often transport through the skin

to the site of MN puncture, such that forces that generate convective flow in the skin can significantly facilitate ISF collection[121]. Future studies could test the minimum number of insertions required to cause the ISF recruitment. More mechanistic studies should be performed to understand time scales for ISF recruitment, effect of other factors such as age, ethnicity and hydration levels.

Other studies may be focused on determining other less invasive methods for ISF recruitment without the need for multiple MN insertions.

8.3 Microneedles for detection of biomarkers in ISF

We demonstrated the utility of our MN patch in detection of vancomycin in ISF for TDM and detection of polio specific antibodies and anti-polio IgG. This MN technology could be used for detection of many other drugs and disease specific biomarkers. Some drugs may not partition well into ISF and future mechanistic studies should address intrinsic factors that influence the distribution in ISF.

The filter paper used in our optimized MN patch acted as a reservoir for ISF. This involved additional processing steps for extraction of the biomarkers from the paper. Future studies should address improvement of the MN patch to develop an in-built detection system by methods such as functionalization of the paper using gold nanoparticles (GNP) or usage of paper based microfluidic device. GNPs possess distinct physical and chemical attributes which make them excellent choice for biosensors. GNPs are inert, they possess high surface-volume ratio and high surface energy to stabilize biomolecules while retaining their bioactivity.

GNPs could be functionalized with aptamers, or other peptides for targeted detection of potential biomarker and immobilized on the paper. Factors such as functionalization efficiency, concentration of GNP solution, amount of aggregation, and immobilization time will have to be tested to determine GNP loading onto the paper. The amount of biomarker collected could be quantified by using GNPs as signal amplification tags as in Surface Enhanced Raman Spectroscopy (SERS) or for localized surface plasmon resonance (LSPR) spectroscopy.

The MN patch maybe attached to a paper-based microfluidic devices functionalized with reagents for colorimetric assays[200]. The color changes could be captured with a camera and the assay results could be quantified by comparing the intensities of the color developed in each assay with those of calibration curves.

CHAPTER 9. APPENDIX A. SUPPORTING INFORMATION FOR CHAPTER 4

A.1.1 Excipient screening for IPV stabilization shown in Table A-1.

Table A-1: Design of Experiments table showing excipient combinations tested for IPV stabilization[1]

	Sorbitol (%)	Sucrose (%)	Trehlose (%)	Maltodextrin (%)
D1	5	0	5	0
D2	0	5	5	5
D3	0	5	5	0
D4	5	5	0	5
D5	0	0	5	5
D6	0	0	0	0
D7	0	0	5	0
D8	5	0	0	5
D9	5	5	5	5
D10	5	0	5	5
D11	5	5	5	0
D12	0	5	0	5
D13	0	0	0	5
D14	5	5	0	0
D15	0	5	0	0
D16	5	0	0	0

[1]The left column shows the formulation number and the other columns show the composition of the formulation on a percent w/v basis in 150 mM histidine buffer at pH 6.5.

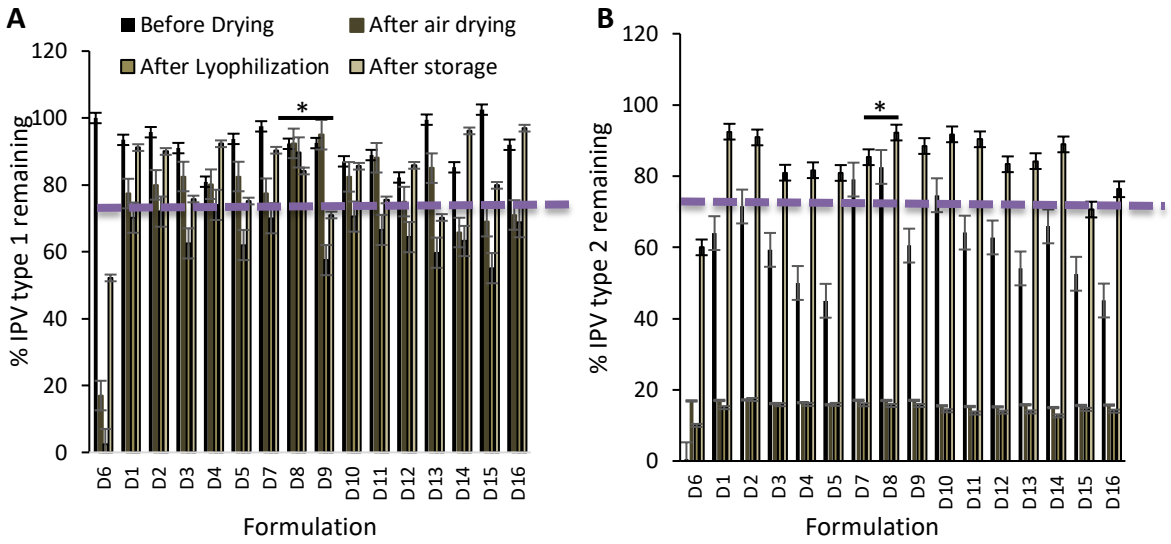

Figure A-1: Effect of stabilizing excipients on (A) IPV type 1 and (B) IPV type 2 activity before drying, after air drying, after subsequent lyophilization and after storage. Vaccine was formulated with combinations of different excipients (each present at a concentration of 5% w/v) in 150 mM histidine buffer at pH 6.5 (see Table S1 for key to excipient formulations). In each set of bars, the first bar shows activity of liquid IPV formulated with excipients before drying. The second bar shows IPV activity after air drying at 5°C with desiccant overnight after casting onto PDMS chips. The third bar shows IPV activity after lyophilization. The fourth bar shows IPV activity after storage at 25 °C with desiccant for 1 week. The unformulated vaccine control data is shown as D6 bars on the far left. All IPV activity (determined by ELISA) is shown as percentage of concentrated stock vaccine solution. Asterisk (*) indicates combination excipient formulation which maintained >80% activity drying and storage. Data represent mean ± SEM (standard error of the mean) of n= 3 replicates.

A.1.2 Buffer and pH Screening

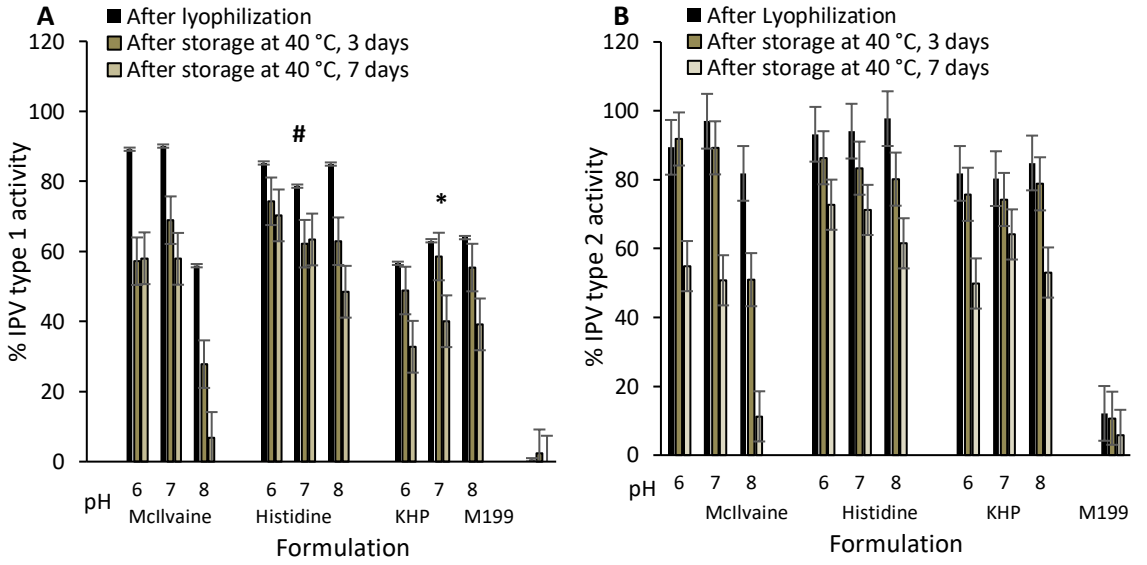

Figure A-2: Effect of formulation buffer and pH on (A) IPV type 1 and (B) IPV type 2 activity after air drying on PDMS chips, after subsequent lyophilization and after storage. IPV was formulated with 5% w/v maltodextrin and 5% w/v D-sorbitol in 0.1 M buffer with pH adjusted using 1 N HCl or 1 N NaOH. Storage was carried out at 40 °C for 3 or 7 days with desiccant. KHP: Potassium hydrogen pthalate, M199: Medium 199. In each set of bars, IPV activity (determined by ELISA) is shown in the first bar after air drying at 5°C overnight and lyophilization, in the second bar after storage in a desiccator at 40 °C for 3 days and in the last bar after storage at 40 °C in a desiccator for 1 week. Stability of unformulated IPV (i.e., without maltodextrin or D-sorbitol) in M199 media is shown in the bars on the far right. Hash (#) represents buffer which did not significantly affect IPV activity compared to activity in the vaccine casting solution (general linear model, $p > 0.80$). Asterisk (*) represents buffer which had the most adverse effect on IPV stability compared to activity in the vaccine casting solution (general linear model, $p < 0.03$). All IPV activity is shown as percentage of activity in the vaccine casting solution. Data represent mean ± SEM (standard error of the mean) of n= 3 replicates.

A.2 Optimization of IPV MN patches

A.2.1 Optimization of 1st cast formulation

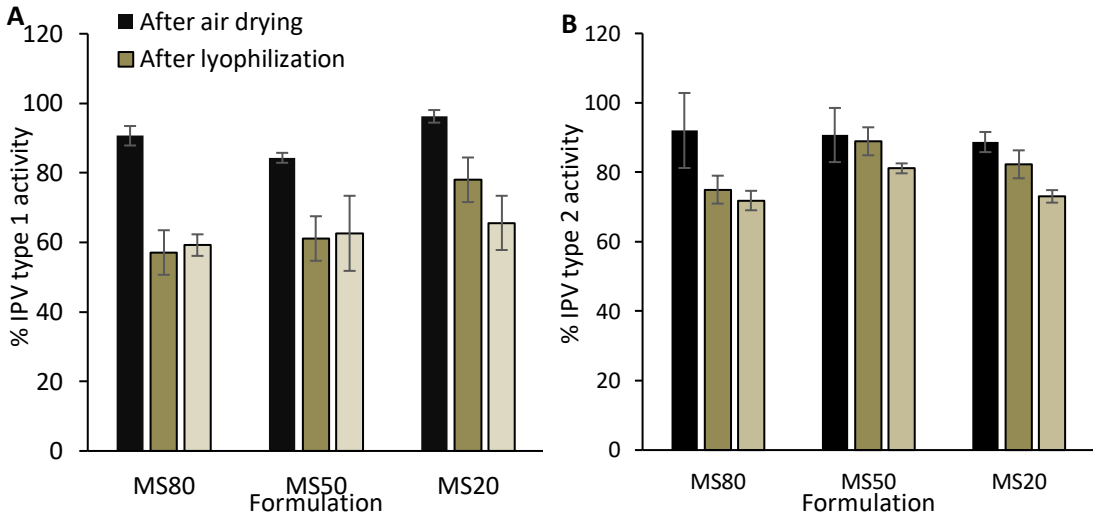

Figure A-3: Effect of 1st cast excipient ratio (maltodextrin to D-sorbitol) on (A) IPV type 1 and (B) IPV type 2 activity after fabricating MN patches, air drying, subsequent lyophilization and storage with desiccant at 40 °C for 2 days. Trivalent IPV was formulated with stabilizing excipients at a total concentration of 10 w/v% in the vaccine casting solution. The mass ratios used were MS80 (maltodextrin: D-sorbitol 80:20), MS50 (maltodextrin: D-sorbitol 50:50) and MS20 (maltodextrin: D-sorbitol 20:80). The 2nd cast polymer matrix solution consisted of 45 wt% fish gelatin to D-sorbitol (78:22) in 0.15 mM histidine buffer. All IPV activity (determined by ELISA) is shown as percentage of vaccine activity in the casting solution. In each set of bars, the first bar shows IPV activity in MN patch after air drying at 5°C in a desiccator for 2 days, the second bar shows IPV activity after additional lyophilization and the last bar shows the IPV activity after storage at 40 °C for 1 week with desiccant. There was no significant difference between the different ratios of maltodextrin to D-sorbitol (Student's t-test, $p > 0.05$). Data represent mean ± SEM (standard error of the mean) of n= 3 replicates.

A.2.2 Optimization of second cast

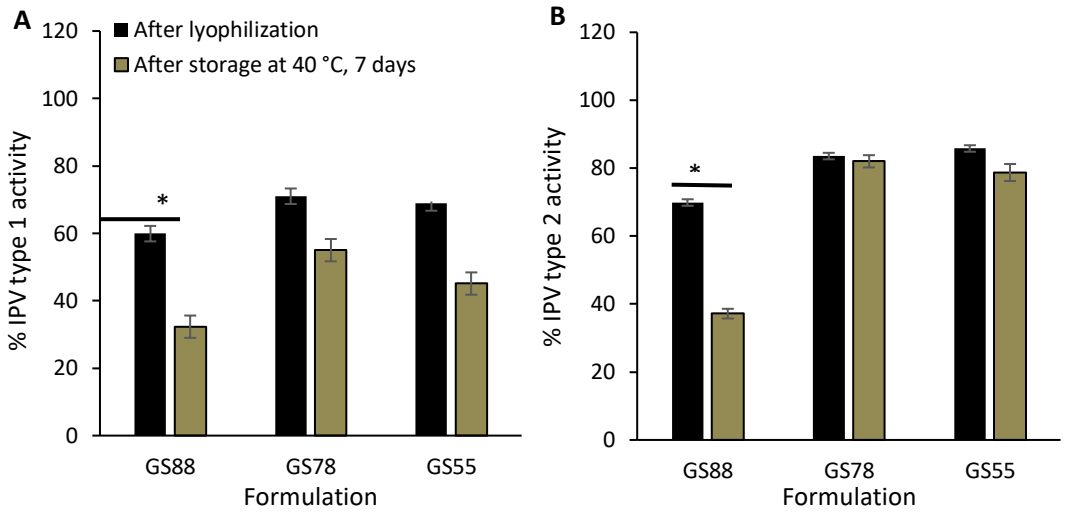

Figure A-4: Effect of 2nd cast excipient ratio (fish gelatin to D-sorbitol) on (A) IPV type 1 and (B) IPV type 2 activity after fabricating MN patches, air drying, further lyophilization and storing with desiccant at 40 °C for 7 days. Trivalent IPV was formulated with 10 w/v% casting solution of maltodextrin: D-sorbitol (20:80) and a 45 wt% 2nd cast solution consisting of varying mass ratios of fish gelatin to D-sorbitol. GS88 (fish gelatin: D-sorbitol 88:11), GS78 (fish gelatin: D-sorbitol 78:22) and GS55 (fish gelatin: D-sorbitol 55:45) in 0.15 mM histidine buffer. All IPV activity (determined by ELISA) is expressed as a percentage of IPV activity in the vaccine casting solution. In each set of bars, the first bar shows IPV activity in MN patch after air drying followed by lyophilization and the second bar shows the IPV activity after storage at 40 °C for 1 week with desiccant. Asterisk (*) indicates a significant difference between the IPV activity compared to other samples (Student's t test, $p < 0.05$). Data represent mean ± SEM (standard error of the mean) of n= 3 replicates.

A.3. Effect of drying conditions

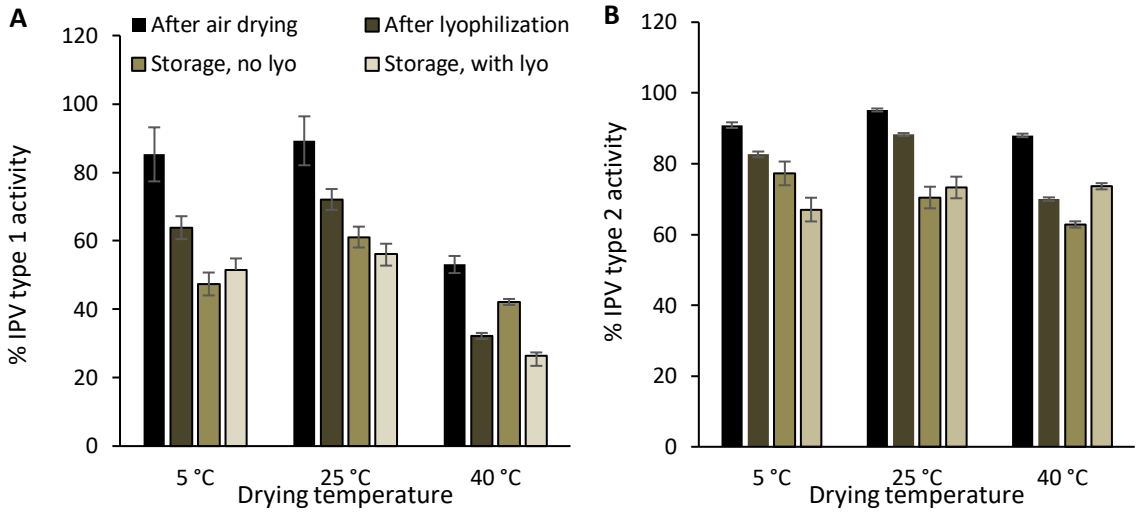

Figure A-5: Effect of air drying, subsequent lyophilization and storage conditions on (A) IPV type 1 and (B) IPV type 2 activity of MN patches air dried at 5 °C, 25 °C or 40°C with desiccant. Trivalent IPV was formulated with 10 w/v% casting solution of maltodextrin: D-sorbitol (20:80) and a 45 wt% 2nd cast solution consisting of fish gelatin to D-sorbitol (78:22). All IPV activity (determined by ELISA) is expressed as a percentage of IPV activity in the vaccine casting solution. In each set of bars, the first bar shows IPV type 2 activity in MN patch after air drying, the second bar shows the activity after subsequent lyophilization, the third bar shows activity for MN patches storage at 40 °C for 1 week with desiccant (no lyophilization) and the last bar shows the activity for MN patches storage at 40 °C for 1 week with desiccant after lyophilization. Data represent mean ± SEM (standard error of the mean) of n= 3 replicates.

A.4 Long term stability of polio MN patches

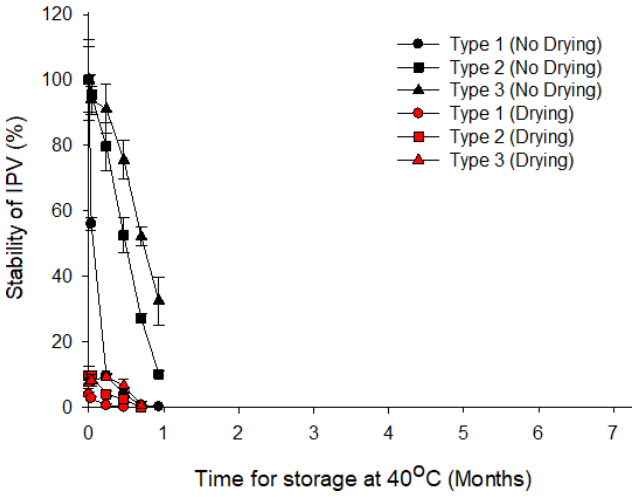

Figure A-6: Effect of storage temperature on IPV types 1, 2 and 3 activities of commercially available vaccine, IPOL® Sanofi Pasteur SA, Rockville, MD) stored with desiccant for up to 1 months at 40 ˚C. Data represent mean ± SEM (standard error of the mean) of n= 3 replicates.

A.5 Correlation of residual moisture content in patch to IPV stability

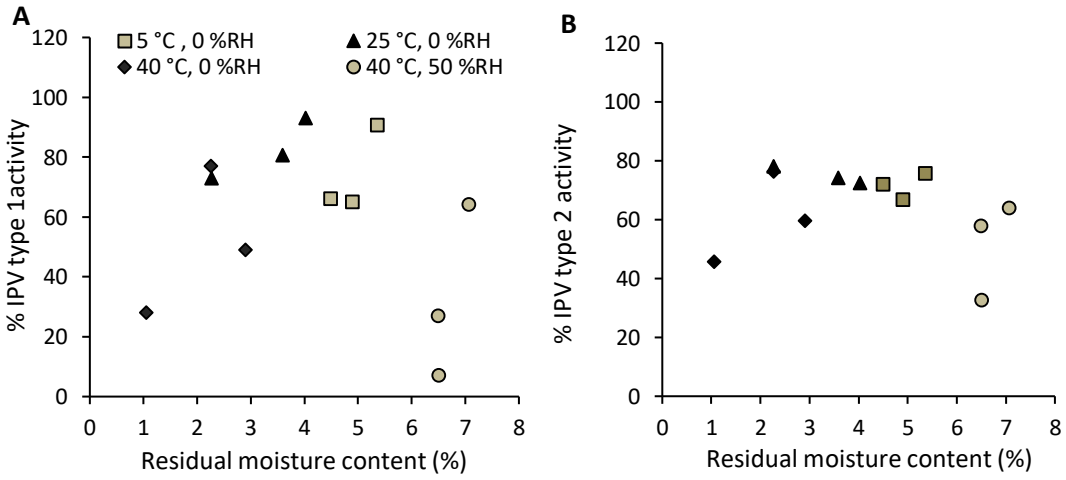

Figure A-7: Correlation of (A) IPV type 1 and (B) IPV type 2 activity in MN patches to RMC of the patches measured after storage at 5, 25 or 40 °C with desiccant or after storage at 40 °C and 50% relative humidity (RH). Regression analysis showed

an R^2 value of 0.032 and 0.049 for IPV type 1 and IPV type 2, respectively. Data represent mean ± SEM (standard error of the mean) of n= 3 replicates.

A.6 Correlation of IPV stability to storage temperature

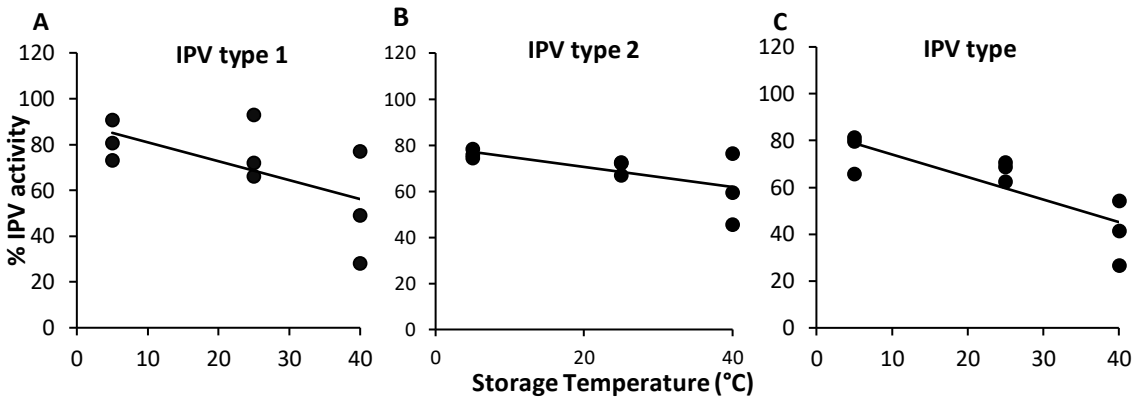

Figure A-8: Correlation of (A) IPV type 1 and (B) IPV type 2 (C) IPV type 3 activity in MN patches to storage temperature of 5, 25 or 40 °C with desiccant. Regression analysis showed an R^2 value of 0.38, 0.39 and 0.67 for IPV type 1, IPV type 2, and IPV type 3 respectively. Data represent mean ± SEM (standard error of the mean) of n= 3 replicates.

A.7 XRD patterns for raw materials used for MN matrix patch preparation

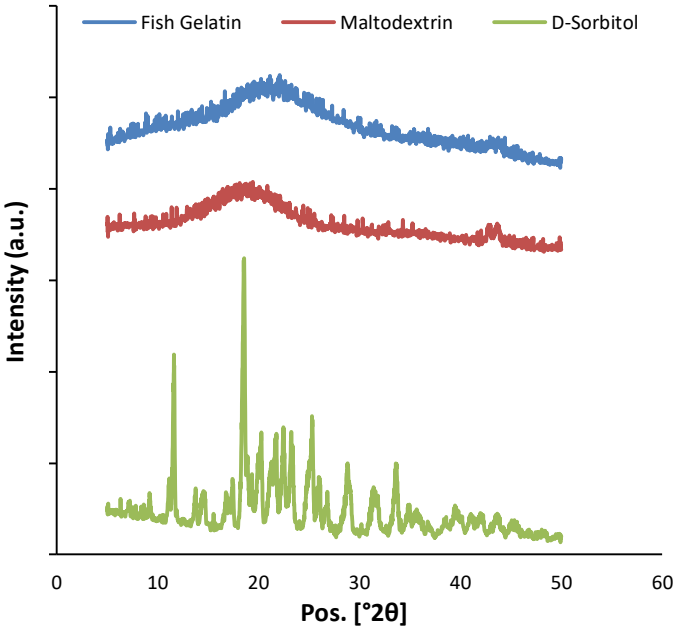

Figure A-9: Representative X-ray diffraction (XRD) patterns corresponding to fish gelatin, maltodextrin and D-sorbitol used in preparation of MN matrix samples.

REFERENCES

1] World Health Organization-Poliomyelitis (polio), http://www.who.int/topics/poliomyelitis/en/ (accessed on 6/13/18)

[2] Pandit, N., & Choudhary, S. Unsafe injection practices in Gujarat, India. *Singapore Med. J., 49*(11), 936. (2008)

[3] Sullivan, S. P., Koutsonanos, D. G., del Pilar Martin, M., Lee, J. W., Zarnitsyn, V., Choi, S.-O., Murthy, N., Compans, R. W., Skountzou, I., & Prausnitz, M. R. Dissolving polymer microneedle patches for influenza vaccination. *Nature Med., 16*(8), 915. (2010)

[4] Sullivan, S. P., Murthy, N., & Prausnitz, M. R. Minimally invasive protein delivery with rapidly dissolving polymer microneedles. *Adv. Mater., 20*(5), 933-938. (2008)

[5] Lee, J. W., Choi, S. O., Felner, E. I., & Prausnitz, M. R. Dissolving microneedle patch for transdermal delivery of human growth hormone. *Small, 7*(4), 531-539. (2011)

[6] Tran, B. Q., Miller, P. R., Taylor, R. M., Boyd, G., Mach, P. M., Rosenzweig, C. N., Baca, J. T., Polsky, R., & Glaros, T. Proteomic Characterization of Dermal Interstitial Fluid Extracted Using a Novel Microneedle-Assisted Technique. *J. Proteome Res., 17*(1), 479-485. (2017)

[7] Niedzwiecki, M. M., Samant, P., Walker, D. I., Tran, V., Jones, D. P., Prausnitz, M. R., & Miller, G. W. Human Suction Blister Fluid Composition Determined Using High-Resolution Metabolomics. *Anal. Chem., 90*(6), 3786-3792. (2018)

[8] Coffey, J. W., Meliga, S. C., Corrie, S. R., & Kendall, M. A. Dynamic application of microprojection arrays to skin induces circulating protein extravasation for enhanced biomarker capture and detection. *Biomater., 84*, 130-143. (2016)

[9] Bodian, D. Poliovirus in chimpanzee tissues after virus feeding. *Am. J. Hyg., 64*(2), 181-197. (1956)

[10] Nathanson, N., & Martin, J. R. The epidemiology of poliomyelitis: enigmas surrounding its appearance, epidemicity, and disappearance. *Am. J. Epidemiol., 110*(6), 672-692. (1979)

[11] Melnick, J., Agol, V., Bachrach, H., Brown, F., Cooper, P., Fiers, W., Gard, S., Gear, J., Ghendon, Y., & Kasza, L. Picornaviridae. *Intervirol., 4*(5), 303-316. (1974)

[12] De Jesus, N. H. Epidemics to eradication: the modern history of poliomyelitis. *Virol. J.*, *4*(1), 70. (2007)

[13] Rodríguez-Álvarez, M., Jiménez-Corona, M. E., Cervantes-Rosales, R., & de León-Rosales, S. P. Polio eradication: how long and how much to the end? *Arch. Med. Res.*, *44*(5), 401-404. (2013)

[14] World Health Organization-Poliomyelitis Key facts, http://www.who.int/en/news-room/fact-sheets/detail/poliomyelitis (accessed on 4/13/18).

[15] Eichner, M., & Dietz, K. Eradication of Poliomyelitis: When Can One Be Sure That Polio Virus Transmission Has Been Terminated? *Am. J. Epidemiol.*, *143*(8), 816-822. (1996)

[16] Schoub, B. D. Introduction of inactivated polio vaccine (IPV) into the routine immunization schedule of South Africa. *Vaccine*, *30*, C35-C37. (2012)

[17] World Health Organization, Combined immunization of infants with oral and inactivated poliovirus vaccines: results of a randomized trial in The Gambia, Oman, and Thailand. *J. Infect. Dis.*, *175*(Supplement_1), S215-S227. (1997)

[18] Sabin, A. B. Properties and behavior of orally administered attenuated poliovirus vaccine. *J. Am. Med. Assoc.*, *164*(11), 1216-1223. (1957)

[19] Kohler, K. A., Banerjee, K., Gary Hlady, W., Andrus, J. K., & Sutter, R. W. Vaccine-associated paralytic poliomyelitis in India during 1999: decreased risk despite massive use of oral polio vaccine. *Bull. W. H. O.*, *80*, 210-216. (2002)

[20] Ehrenfeld, E., Modlin, J., & Chumakov, K. Future of polio vaccines. *Expert Rev. Vaccines*, *8*(7), 899-905. (2009)

[21] Hamborsky, J., Kroger, A., Wolfe, S., Control, C. f. D., & Prevention. (2015). *Epidemiology and prevention of vaccine-preventable diseases*: US Department of Health & Human Services, Centers for Disease Control and Prevention.

[22] Barrett, S. Polio eradication: strengthening the weakest links. *Health Aff.*, *28*(4), 1079-1090. (2009)

[23] Duchêne, M. Production, testing and perspectives of IPV and IPV combination vaccines: GSK biologicals' view. *Biologicals*, *34*(2), 163-166. (2006)

[24] Simonsen, L., Kane, A., Lloyd, J., Zaffran, M., & Kane, M. Unsafe injections in the developing world and transmission of bloodborne pathogens: a review. *Bull. W. H. O.*, *77*(10), 789. (1999)

[25] Gyawali, S., Rathore, D. S., Shankar, P. R., & Kumar, K. V. Strategies and challenges for safe injection practice in developing countries. *J. Pharmacol. Pharmacother.*, *4*(1), 8. (2013)

[26] Giudice, E. L., & Campbell, J. D. Needle-free vaccine delivery. *Adv. Drug Delivery Rev., 58*(1), 68-89. (2006)

[27] Plotkin, S. A., Orenstein, W. A., & Offit, P. A. *Vaccines*: Saunders, (2004)

[28] Chen, D., & Kristensen, D. Opportunities and challenges of developing thermostable vaccines. *Expert Rev. Vaccines, 8*(5), 547-557. (2009)

[29] Prausnitz, M. R. Engineering microneedle patches for vaccination and drug delivery to skin. *Annu. Rev. Chem. Biomol. Eng., 8*, 177-200. (2017)

[30] Thakoersing, V. S., Gooris, G. S., Mulder, A., Rietveld, M., El Ghalbzouri, A., & Bouwstra, J. A. Unraveling barrier properties of three different in-house human skin equivalents. *Tissue Eng., Part C, 18*(1), 1-11. (2011)

[31] Schuler, G. *Epidermal Langerhans Cells*: CRC Press, (1990)

[32] Itano, A. A., McSorley, S. J., Reinhardt, R. L., Ehst, B. D., Ingulli, E., Rudensky, A. Y., & Jenkins, M. K. Distinct dendritic cell populations sequentially present antigen to CD4 T cells and stimulate different aspects of cell-mediated immunity. *Immunity, 19*(1), 47-57. (2003)

[33] Bashkatov, A., Genina, E., Kochubey, V., & Tuchin, V. Optical properties of human skin, subcutaneous and mucous tissues in the wavelength range from 400 to 2000 nm. *J. Phys. D: Appl. Phys., 38*(15), 2543. (2005)

[34] Henry, S., McAllister, D. V., Allen, M. G., & Prausnitz, M. R. Microfabricated microneedles: a novel approach to transdermal drug delivery. *J. Pharm. Sci., 87*(8), 922-925. (1998)

[35] Arya, J., Henry, S., Kalluri, H., McAllister, D. V., Pewin, W. P., & Prausnitz, M. R. Tolerability, usability and acceptability of dissolving microneedle patch administration in human subjects. *Biomater., 128*, 1-7. (2017)

[36] Zhu, Q., Zarnitsyn, V. G., Ye, L., Wen, Z., Gao, Y., Pan, L., Skountzou, I., Gill, H. S., Prausnitz, M. R., & Yang, C. Immunization by vaccine-coated microneedle arrays protects against lethal influenza virus challenge. *Proc. Natl. Acad. Sci., 106*(19), 7968-7973. (2009)

[37] Gill, H. S., Söderholm, J., Prausnitz, M. R., & Sällberg, M. Cutaneous vaccination using microneedles coated with hepatitis C DNA vaccine. *Gene Ther., 17*(6), 811. (2010)

[38] Mikszta, J. A., Dekker, J. P., Harvey, N. G., Dean, C. H., Brittingham, J. M., Huang, J., Sullivan, V. J., Dyas, B., Roy, C. J., & Ulrich, R. G. Microneedle-based intradermal delivery of the anthrax recombinant protective antigen vaccine. *Infect. Immun., 74*(12), 6806-6810. (2006)

[39] Lee, K., Lee, C. Y., & Jung, H. Dissolving microneedles for transdermal drug administration prepared by stepwise controlled drawing of maltose. *Biomater., 32*(11), 3134-3140. (2011)

[40] Chu, L. Y., & Prausnitz, M. R. Separable arrowhead microneedles. *J. Controlled Release, 149*(3), 242-249. (2011)

[41] Norman, J. J., Arya, J. M., McClain, M. A., Frew, P. M., Meltzer, M. I., & Prausnitz, M. R. Microneedle patches: usability and acceptability for self-vaccination against influenza. *Vaccine, 32*(16), 1856-1862. (2014)

[42] Edens, C., Dybdahl-Sissoko, N. C., Weldon, W. C., Oberste, M. S., & Prausnitz, M. R. Inactivated polio vaccination using a microneedle patch is immunogenic in the rhesus macaque. *Vaccine, 33*(37), 4683-4690. (2015)

[43] Rouphael, N. G., Paine, M., Mosley, R., Henry, S., McAllister, D. V., Kalluri, H., Pewin, W., Frew, P. M., Yu, T., & Thornburg, N. J. The safety, immunogenicity, and acceptability of inactivated influenza vaccine delivered by microneedle patch (TIV-MNP 2015): a randomised, partly blinded, placebo-controlled, phase 1 trial. *The Lancet, 390*(10095), 649-658. (2017)

[44] Poliovirus Vaccine Inactivated- IPOL®, https://www.fda.gov/downloads/biologicsbloodvaccines/vaccines/approvedproducts/ucm133479.pdf (accessed on 4/12/18)

[45] Wu, R., Georgescu, M.-M., Delpeyroux, F., Guillot, S., Balanant, J., Simpson, K., & Crainic, R. Thermostabilization of live virus vaccines by heavy water (D2O). *Vaccine, 13*(12), 1058-1063. (1995)

[46] Robinson, C. M., Jesudhasan, P. R., & Pfeiffer, J. K. Bacterial lipopolysaccharide binding enhances virion stability and promotes environmental fitness of an enteric virus. *Cell host & microbe, 15*(1), 36-46. (2014)

[47] Dorval, B. L., Chow, M., & Klibanov, A. M. Stabilization of poliovirus against heat inactivation. *Biochem. Biophys. Res. Commun., 159*(3), 1177-1183. (1989)

[48] Dorval, B. L., Chow, M., & Klibanov, A. M. Lysine and other diamines dramatically stabilize poliovirus against thermoinactivation. *Biotechnol. Bioeng., 35*(10), 1051-1054. (1990)

[49] Rombaut, B., Andries, K., & Boeye, A. Stabilisation of poliovirus with pirodavir. *Dev. Biol. Stand., 87*, 173-180. (1996)

[50] Crainic, R., Wu, R., Otelea, D., Georgescu, M., Delpeyroux, F., Guillot, S., Balanant, J., & Tardy-Panit, M. The replacement of water with deuterium oxide significantly improves the thermal stability of the oral poliovirus vaccine. *Dev. Biol. Stand., 87*, 161-166. (1996)

[51] Kim, Y.-C., Quan, F.-S., Compans, R. W., Kang, S.-M., & Prausnitz, M. R. Formulation and coating of microneedles with inactivated influenza virus to improve vaccine stability and immunogenicity. *J. Controlled Release, 142*(2), 187-195. (2010)

[52] Carpenter, J. F., Pikal, M. J., Chang, B. S., & Randolph, T. W. Rational design of stable lyophilized protein formulations: some practical advice. *Pharm. Res., 14*(8), 969-975. (1997)

[53] Luo, T., Yang, L., Wu, J., Zheng, Z., Li, G., Wang, X., & Kaplan, D. L. Stabilization of natural antioxidants by silk biomaterials. *ACS Appl. Mater. Interfaces, 8*(21), 13573-13582. (2016)

[54] Sutherland, T. D., Sriskantha, A., Church, J. S., Strive, T., Trueman, H. E., & Kameda, T. Stabilization of viruses by encapsulation in silk proteins. *ACS Appl. Mater. Interfaces, 6*(20), 18189-18196. (2014)

[55] Kraan, H., van Herpen, P., Kersten, G., & Amorij, J.-P. Development of thermostable lyophilized inactivated polio vaccine. *Pharm. Res., 31*(10), 2618-2629. (2014)

[56] Kraan, H., Ploemen, I., van de Wijdeven, G., Que, I., Löwik, C., Kersten, G., & Amorij, J.-P. Alternative delivery of a thermostable inactivated polio vaccine. *Vaccine, 33*(17), 2030-2037. (2015)

[57] Mayeux, R. Biomarkers: potential uses and limitations. *NeuroRx, 1*(2), 182-188. (2004)

[58] Burgess, D. C. H., Wasserman, J., & Dahl, C. A. Global health diagnostics. *Nature, 444*(1s), 1. (2006);

[59] Organization, W. H. (2017). *Guide to cancer early diagnosis*; Moon, H., Rote, S., & Haley, W. E. Factors that contribute to remaining in the community among older adults. *Aging & mental health*, 1-8. (2017)

[60] Mitchell, P. S., Parkin, R. K., Kroh, E. M., Fritz, B. R., Wyman, S. K., Pogosova-Agadjanyan, E. L., Peterson, A., Noteboom, J., O'Briant, K. C., & Allen, A. Circulating microRNAs as stable blood-based markers for cancer detection. *Proc. Natl. Acad. Sci., 105*(30), 10513-10518. (2008)

[61] Hendriks, R., Dijkstra, S., Trooskens, G., Van Criekinge, W., Cornel, E., Jannink, S., De Jong, H., Hessels, D., Smit, F., & Melchers, W. 383 Multicenter validation study of a urine-based molecular biomarker algorithm to predict high-grade prostate cancer. *Eur. Urol., Suppl., 15*(3), e383a. (2016)

[62] Malamud, D. Saliva as a diagnostic fluid. *Dent. Clin., 55*(1), 159-178. (2011)

[63] Baca, J. T., Finegold, D. N., & Asher, S. A. Tear glucose analysis for the noninvasive detection and monitoring of diabetes mellitus. *Ocul. Surf., 5*(4), 280-293. (2007)

[64] Gao, W., Emaminejad, S., Nyein, H. Y. Y., Challa, S., Chen, K., Peck, A., Fahad, H. M., Ota, H., Shiraki, H., & Kiriya, D. Fully integrated wearable sensor arrays for multiplexed in situ perspiration analysis. *Nature, 529*(7587), 509. (2016)

[65] Olansky, L., & Kennedy, L. Finger-stick glucose monitoring: issues of accuracy and specificity. *Diabetes Care, 33*(4), 948. (2010)

[66] Gnoth, C., & Johnson, S. Strips of hope: accuracy of home pregnancy tests and new developments. *Geburtshilfe Frauenheilkd., 74*(7), 661. (2014)

[67] Perrier, E., Demazieres, A., Girard, N., Pross, N., Osbild, D., Metzger, D., Guelinckx, I., & Klein, A. Circadian variation and responsiveness of hydration biomarkers to changes in daily water intake. *Eur. J. Appl. Physiol., 113*(8), 2143-2151. (2013)

[68] Giskeødegård, G. F., Davies, S. K., Revell, V. L., Keun, H., & Skene, D. J. Diurnal rhythms in the human urine metabolome during sleep and total sleep deprivation. *Sci. Rep., 5*, 14843. (2015)

[69] Pfaffe, T., Cooper-White, J., Beyerlein, P., Kostner, K., & Punyadeera, C. Diagnostic potential of saliva: current state and future applications. *Clin. Chem., 57*(5), 675-687. (2011)

[70] Restituto, P., Galofré, J., Gil, M., Mugueta, C., Santos, S., Monreal, J., & Varo, N. Advantage of salivary cortisol measurements in the diagnosis of glucocorticoid related disorders. *Clin. Biochem., 41*(9), 688-692. (2008)

[71] Parry, J. V., Perry, K. R., Mortimer, P. P., & Panday, S. Diagnosis of hepatitis A and B by testing saliva. *J. Med. Virol., 28*(4), 255-260. (1989)

[72] Bandodkar, A. J., Molinnus, D., Mirza, O., Guinovart, T., Windmiller, J. R., Valdés-Ramírez, G., Andrade, F. J., Schöning, M. J., & Wang, J. Epidermal tattoo potentiometric sodium sensors with wireless signal transduction for continuous non-invasive sweat monitoring. *Biosens. Bioelectron., 54*, 603-609. (2014)

[73] Lebrecht, A., Boehm, D., Schmidt, M., Koelbl, H., Schwirz, R., & Grus, F. Diagnosis of breast cancer by tear proteomic pattern. *Cancer Genomics-Proteomics, 6*(3), 177-182. (2009)

[74] Aukland, K., & Nicolaysen, G. Interstitial fluid volume: local regulatory mechanisms. *Physiol. Rev., 61*(3), 556-643. (1981)

[75] Bauer, J., & Brooks, C. Body-fluid composition in normal and hypertensive man. *Clin. Sci., 62*(1), 43-49. (1982)

[76] Scallan, J., Huxley, V., & Korthuis, R. Capillary Fluid Exchange: Regulation. *Func. Pathol.* (2010)

[77] Wiig, H., Reed, R. K., & Tenstad, O. Interstitial fluid pressure, composition of interstitium, and interstitial exclusion of albumin in hypothyroid rats. *Am. J. Physiol. Heart Circ. Physiol., 278*(5), H1627-H1639. (2000)

[78] Kool, J., Reubsaet, L., Wesseldijk, F., Maravilha, R. T., Pinkse, M. W., D'Santos, C. S., van Hilten, J. J., Zijlstra, F. J., & Heck, A. J. Suction blister fluid as potential body fluid for biomarker proteins. *Proteomics, 7*(20), 3638-3650. (2007)

[79] Kastellorizios, M., & Burgess, D. J. Continuous metabolic monitoring based on multi-analyte biomarkers to predict exhaustion. *Sci. Rep., 5*, 10603. (2015)

[80] Matuleviciene, V., Joseph, J. I., Andelin, M., Hirsch, I. B., Attvall, S., Pivodic, A., Dahlqvist, S., Klonoff, D., Haraldsson, B., & Lind, M. A clinical trial of the accuracy and treatment experience of the Dexcom G4 sensor (Dexcom G4 system) and Enlite sensor (guardian REAL-time system) tested simultaneously in ambulatory patients with type 1 diabetes. *Diabetes Technol. Ther., 16*(11), 759-767. (2014)

[81] Calhoun, P., Lum, J., Beck, R. W., & Kollman, C. Performance comparison of the medtronic sof-sensor and enlite glucose sensors in inpatient studies of individuals with type 1 diabetes. *Diabetes Technol. Ther., 15*(9), 758-761. (2013)

[82] Kiistala, U. Suction blister device for separation of viable epidermis from dermis. *J. Invest. Dermatol., 50*, 129-137. (1968)

[83] Krawczyk, W. S. A pattern of epidermal cell migration during wound healing. *J. Cell Biol., 49*(2), 247-263. (1971)

[84] Meinardi, M., Eendenburg, J., Oosting, J., Boxtel, C., Rie, M., & Bos, J. Cyclosporin A levels in suction-blister fluid of patients with psoriasis treated systemically. *Br. J. Dermatol., 122*(5), 671-676. (1990)

[85] Hatchome, N., Kato, T., & Tagami, H. Therapeutic success of epidermal grafting in generalized vitiligo is limited by the Koebner phenomenon. *J. Am. Acad. Dermatol., 22*(1), 87-91. (1990)

[86] Kayashima, S., Arai, T., Kikuchi, M., Nagata, N., Ito, N., Kuriyama, T., & Kimura, J. Suction effusion fluid from skin and constituent analysis: new candidate for interstitial fluid. *Am. J. Physiol. Heart Circ. Physiol., 263*(5), H1623-H1627. (1992)

[87] Aukland, K., & Fadnes, H. Protein concentration of interstitial fluid collected from rat skin by a wick method. *Acta Physiol., 88*(3), 350-358. (1973)

[88] Markhus, C. E., & Wiig, H. Isolation of interstitial fluid from skeletal muscle and subcutis in mice using a wick method. *Am. J. Physiol. Heart Circ. Physiol., 287*(5), H2085-H2090. (2004); Heir, S., & Wiig, H. Subcutaneous interstitial fluid colloid osmotic pressure in dehydrated rats. *Acta Physiol., 133*(3), 365-371. (1988); Negrini, D., Tenstad, O., & Wiig, H. Interstitial exclusion of albumin in rabbit lung measured with the continuous infusion method in combination with the wick technique. *Microcirc., 10*(2), 153-165. (2003)

[89] Wiig, H., & Noddeland, H. Interstitial fluid pressure in human skin measured by micropuncture and wick-in-needle. *Scand. J. Clin. Lab. Invest., 43*(3), 255-260. (1983)

[90] Leegsma-Vogt, G., Janle, E., Ash, S. R., Venema, K., & Korf, J. Utilization of in vivo ultrafiltration in biomedical research and clinical applications. *Life Sci., 73*(16), 2005-2018. (2003)

[91] Ungerstedt, U., & Pycock, C. Functional correlates of dopamine neurotransmission. *Bull. Schweiz. Akad. Med. Wiss., 30*(1-3), 44. (1974)

[92] Schmidt, S., Banks, R., Kumar, V., Rand, K. H., & Derendorf, H. Clinical microdialysis in skin and soft tissues: an update. *J. Clin. Pharmacol., 48*(3), 351-364. (2008)

[93] Lonnroth, P., Jansson, P., & Smith, U. A microdialysis method allowing characterization of intercellular water space in humans. *Am. J. Physiol. Endocrinol. Metab., 253*(2), E228-E231. (1987)

[94] Krogstad, A., Jansson, P. A., Gisslen, P., & Lönnroth, P. Microdialysis methodology for the measurement of dermal interstitial fluid in humans. *Br. J. Dermatol., 134*(6), 1005-1012. (1996)

[95] Pieber, T., Birngruber, T., Bodenlenz, M., Höfferer, C., Mautner, S., Tiffner, K., & Sinner, F. (2013) *Microdialysis in Drug Development* (pp. 283-302): Springer.

[96] Benjamin, F., Kempen, R., Mulder, A., & Ivy, A. Sodium-potassium ratio of human skin as obtained by reverse iontophoresis. *J. Appl. Physiol., 6*(7), 401-407. (1954)

[97] Potts, R. O., A Tamada, J., & J Tierney, M. Glucose monitoring by reverse iontophoresis. *Diabetes/Metab. Res. Rev., 18*(S1). (2002)

[98] Sieg, A., Guy, R. H., & Delgado-Charro, M. B. Noninvasive glucose monitoring by reverse iontophoresis in vivo: application of the internal standard concept. *Clin. Chem., 50*(8), 1383-1390. (2004)

[99] Mitragotri, S., Coleman, M., Kost, J., & Langer, R. Analysis of ultrasonically extracted interstitial fluid as a predictor of blood glucose levels. *J. Appl. Physiol., 89*(3), 961-966. (2000)

[100] El-Laboudi, A., Oliver, N. S., Cass, A., & Johnston, D. Use of microneedle array devices for continuous glucose monitoring: a review. *Diabetes Technol. Ther., 15*(1), 101-115. (2013)

[101] Kobayashi, K., & Suzuki, H. A sampling mechanism employing the phase transition of a gel and its application to a micro analysis system imitating a mosquito. *Sens. Actuators, B, 80*(1), 1-8. (2001)

[102] Suzuki, H., Tokuda, T., Miyagishi, T., Yoshida, H., & Honda, N. A disposable on-line microsystem for continuous sampling and monitoring of glucose. *Sens. Actuators, B, 97*(1), 90-97. (2004)

[103] Mukerjee, E., Issseroff, R., Collins, S., & Smith, R. *Microneedle array with integrated microchannels for transdermal sample extraction and in situ analysis.* Paper presented at the Transducers, Solid-State Sensors, Actuators and Microsystems, 12th International Conference on, (2003)

[104] Mukerjee, E., Collins, S., Isseroff, R., & Smith, R. Microneedle array for transdermal biological fluid extraction and in situ analysis. *Sens. Actuators, A, 114*(2-3), 267-275. (2004)

[105] Vesper, H. W., Wang, P. M., Archibold, E., Prausnitz, M. R., & Myers, G. L. Assessment of trueness of a glucose monitor using interstitial fluid and whole blood as specimen matrix. *Diabetes Technol. Ther., 8*(1), 76-80. (2006)

[106] Miller, P. R., Gittard, S. D., Edwards, T. L., Lopez, D. M., Xiao, X., Wheeler, D. R., Monteiro-Riviere, N. A., Brozik, S. M., Polsky, R., & Narayan, R. J. Integrated carbon fiber electrodes within hollow polymer microneedles for transdermal electrochemical sensing. *Biomicrofluidics, 5*(1), 013415. (2011)

[107] Windmiller, J. R., Zhou, N., Chuang, M.-C., Valdés-Ramírez, G., Santhosh, P., Miller, P. R., Narayan, R., & Wang, J. Microneedle array-based carbon paste amperometric sensors and biosensors. *Analyst, 136*(9), 1846-1851. (2011)

[108] Miller, P. R., Skoog, S. A., Edwards, T. L., Lopez, D. M., Wheeler, D. R., Arango, D. C., Xiao, X., Brozik, S. M., Wang, J., & Polsky, R. Multiplexed microneedle-based biosensor array for characterization of metabolic acidosis. *Talanta, 88*, 739-742. (2012)

[109] Miller, P. R., Xiao, X., Brener, I., Burckel, D. B., Narayan, R., & Polsky, R. Microneedle-Based Transdermal Sensor for On-Chip Potentiometric Determination of K+. *Adv. Healthcare Mater., 3*(6), 876-881. (2014)

[110] Wang, P. M., Cornwell, M., & Prausnitz, M. R. Minimally invasive extraction of dermal interstitial fluid for glucose monitoring using microneedles. *Diabetes Technol. Ther., 7*(1), 131-141. (2005)

[111] Zimmermann, S., Fienbork, D., Flounders, A. W., & Liepmann, D. In-device enzyme immobilization: wafer-level fabrication of an integrated glucose sensor. *Sen. Actuators B, 99*(1), 163-173. (2004)

[112] Jina, A., Tierney, M. J., Tamada, J. A., McGill, S., Desai, S., Chua, B., Chang, A., & Christiansen, M. Design, development, and evaluation of a novel microneedle array-based continuous glucose monitor. *J. Diabetes Sci. Technol., 8*(3), 483-487. (2014)

[113] Yu, J., Zhang, Y., Ye, Y., DiSanto, R., Sun, W., Ranson, D., Ligler, F. S., Buse, J. B., & Gu, Z. Microneedle-array patches loaded with hypoxia-sensitive vesicles provide fast glucose-responsive insulin delivery. *Proc. Natl. Acad. Sci., 112*(27), 8260-8265. (2015)

[114] Corrie, S. R., Fernando, G. J., Crichton, M. L., Brunck, M. E., Anderson, C. D., & Kendall, M. A. Surface-modified microprojection arrays for intradermal biomarker capture, with low non-specific protein binding. *Lab Chip, 10*(20), 2655-2658. (2010)

[115] Muller, D. A., Corrie, S. R., Coffey, J., Young, P. R., & Kendall, M. A. Surface modified microprojection arrays for the selective extraction of the dengue virus NS1 protein as a marker for disease. *Anal. Chem., 84*(7), 3262-3268. (2012)

[116] Sato, T., Okada, S., Hagino, K., Asakura, Y., Kikkawa, Y., Kojima, J., Watanabe, T., Maekawa, Y., Isobe, K., & Koike, R. Measurement of glucose area under the curve using minimally invasive interstitial fluid extraction technology: evaluation of glucose monitoring concepts without blood sampling. *Diabetes Technol. Ther., 13*(12), 1194-1200. (2011)

[117] Donnelly, R. F., McCrudden, M. T., Alkilani, A. Z., Larrañeta, E., McAlister, E., Courtenay, A. J., Kearney, M.-C., Singh, T. R. R., McCarthy, H. O., & Kett, V. L. Hydrogel-forming microneedles prepared from "super swelling" polymers combined with lyophilised wafers for transdermal drug delivery. *PloS one, 9*(10), e111547. (2014)

[118] Caffarel-Salvador, E., Brady, A. J., Eltayib, E., Meng, T., Alonso-Vicente, A., Gonzalez-Vazquez, P., Torrisi, B. M., Vicente-Perez, E. M., Mooney, K., & Jones, D. S. Hydrogel-forming microneedle arrays allow detection of drugs and glucose in vivo: potential for use in diagnosis and therapeutic drug monitoring. *PloS one, 10*(12), e0145644. (2015)

[119] Romanyuk, A. V., Zvezdin, V. N., Samant, P., Grenader, M. I., Zemlyanova, M., & Prausnitz, M. R. Collection of analytes from microneedle patches. *Anal. Chem., 86*(21), 10520-10523. (2014)

[120] Chang, H., Zheng, M., Yu, X., Than, A., Seeni, R. Z., Kang, R., Tian, J., Khanh, D. P., Liu, L., & Chen, P. A Swellable Microneedle Patch to Rapidly Extract Skin Interstitial Fluid for Timely Metabolic Analysis. *Adv. Mater., 29*(37). (2017)

[121] Samant, P. P., & Prausnitz, M. R. Mechanisms of sampling interstitial fluid from skin using a microneedle patch. *Proc. Natl. Acad. Sci., 115*, 4583. (2018)

[122] Rybak, M., Lomaestro, B., Rotschafer, J. C., Moellering, R., Craig, W., Billeter, M., Dalovisio, J. R., & Levine, D. P. Therapeutic monitoring of vancomycin in adult patients: a consensus review of the American Society of Health-System Pharmacists, the Infectious Diseases Society of America, and the Society of Infectious Diseases Pharmacists. *Am. J. Health-Syst. Pharm., 66*(1), 82-98. (2009)

[123] Kiang, T. K., Häfeli, U. O., & Ensom, M. H. A comprehensive review on the pharmacokinetics of antibiotics in interstitial fluid spaces in humans: implications on dosing and clinical pharmacokinetic monitoring. *Clin. Pharmacokinet., 53*(8), 695-730. (2014)

[124] Stetina, P., Madai, B., Kulemann, V., Kirch, W., & Joukhadar, C. Pharmacokinetics of scopolamine in serum and subcutaneous adipose tissue in healthy volunteers. *Int. J. Clin. Pharmacol. Ther., 43*(3), 134-139. (2005)

[125] Kiang, T. K., Schmitt, V., Ensom, M. H., Chua, B., & Häfeli, U. O. Therapeutic drug monitoring in interstitial fluid: a feasibility study using a comprehensive panel of drugs. *J. Pharm. Sci., 101*(12), 4642-4652. (2012)

[126] Lindberger, M., Tomson, T., & Ståhle, L. Microdialysis sampling of carbamazepine, phenytoin and phenobarbital in subcutaneous extracellular fluid and subdural cerebrospinal fluid in humans: an in vitro and in vivo study of adsorption to the sampling device. *Basic Clin. Pharmacol. Toxicol., 91*(4), 158-165. (2002)

[127] Dove, A. W., & Racaniello, V. R. The polio eradication effort: should vaccine eradication be next? *Science, 277*(5327), 779-780, (1997)

[128] Kew, O. M., Sutter, R. W., de Gourville, E. M., Dowdle, W. R., & Pallansch, M. A. Vaccine-derived polioviruses and the endgame strategy for global polio eradication. *Annu. Rev. Microbiol., 59*, 587-635. (2005)

[129] Cáceres, V. M., & Sutter, R. W. Sabin monovalent oral polio vaccines: review of past experiences and their potential use after polio eradication. *Clin. Infect. Dis., 33*(4), 531-541. (2001)

[130] Heinsbroek, E., & Ruitenberg, E. J. The global introduction of inactivated polio vaccine can circumvent the oral polio vaccine paradox. *Vaccine, 28*(22), 3778-3783. (2010)

[131] Davis, R., & Biellik, R. Inactivated Polio Vaccine: Its proposed role in the final stages of polio eradication. *Pan Afr. Med. J., 14*(1). (2013)

[132] Gill, H. S., Denson, D. D., Burris, B. A., & Prausnitz, M. R. Effect of microneedle design on pain in human subjects. *Clin. J. Pain, 24*(7), 585. (2008)

[133] Kaushik, S., Hord, A. H., Denson, D. D., McAllister, D. V., Smitra, S., Allen, M. G., & Prausnitz, M. R. Lack of pain associated with microfabricated microneedles. *Anesth. Analg., 92*(2), 502-504. (2001)

[134] van der Maaden, K., Jiskoot, W., & Bouwstra, J. Microneedle technologies for (trans) dermal drug and vaccine delivery. *J. Controlled Release, 161*(2), 645-655. (2012)

[135] Muller, D. A., Pearson, F. E., Fernando, G. J., Agyei-Yeboah, C., Owens, N. S., Corrie, S. R., Crichton, M. L., Wei, J. C., Weldon, W. C., & Oberste, M. S. Inactivated poliovirus type 2 vaccine delivered to rat skin via high density microprojection array elicits potent neutralising antibody responses. *Sci. Rep., 6*, 22094. (2016)

[136] Mistilis, M. J., Joyce, J. C., Esser, E. S., Skountzou, I., Compans, R. W., Bommarius, A. S., & Prausnitz, M. R. Long-term stability of influenza vaccine in a dissolving microneedle patch. *Drug Delivery Transl. Res., 7*(2), 195-205. (2017); Pearson, F. E., McNeilly, C. L., Crichton, M. L., Primiero, C. A., Yukiko, S. R., Fernando, G. J., Chen, X., Gilbert, S. C., Hill, A. V., & Kendall, M. A. Dry-coated live viral vector vaccines delivered by nanopatch microprojections retain long-term thermostability and induce transgene-specific T cell responses in mice. *PloS one, 8*(7), e67888. (2013)

[137] Grassly, N. C. The final stages of the global eradication of poliomyelitis. *Philos. Trans. R. Soc., B, 368*(1623), 20120140. (2013)

[138] Park, J.-H., Allen, M. G., & Prausnitz, M. R. Biodegradable polymer microneedles: fabrication, mechanics and transdermal drug delivery. *J. Controlled Release, 104*(1), 51-66. (2005)

[139] Lee, J. W., Park, J.-H., & Prausnitz, M. R. Dissolving microneedles for transdermal drug delivery. *Biomater., 29*(13), 2113-2124. (2008)

[140] Rockland, L. B. Saturated salt solutions for static control of relative humidity between 5° and 40° C. *Anal. Chem., 32*(10), 1375-1376. (1960)

[141] Back, J. F., Oakenfull, D., & Smith, M. B. Increased thermal stability of proteins in the presence of sugars and polyols. *Biochem., 18*(23), 5191-5196. (1979)

[142] Schlehuber, L. D., McFadyen, I. J., Shu, Y., Carignan, J., Duprex, W. P., Forsyth, W. R., Ho, J. H., Kitsos, C. M., Lee, G. Y., & Levinson, D. A. Towards ambient temperature-stable vaccines: the identification of thermally stabilizing liquid formulations for measles virus using an innovative high-throughput infectivity assay. *Vaccine, 29*(31), 5031-5039. (2011)

[143] Moynihan, M., & Petersen, I. The durability of inactivated poliovirus vaccine: studies on the stability of potency in vivo and in vitro. *J. Biol. Stand., 10*(3), 261-268. (1982)

[144] Brandau, D. T., Jones, L. S., Wiethoff, C. M., Rexroad, J., & Middaugh, C. R. Thermal stability of vaccines. *J. Pharm. Sci., 92*(2), 218-231. (2003); Amorij, J., Huckriede, A., Wilschut, J., Frijlink, H., & Hinrichs, W. Development of stable influenza vaccine powder formulations: challenges and possibilities. *Pharm. Res., 25*(6), 1256-1273. (2008)

[145] Beale, A., & Mason, P. The measurement of the D-antigen in poliovirus preparations. *Epidemiol. Infect., 60*(1), 113-121. (1962)

[146] Milstien, J. B., Galazka, A. M., Kartoglu, U. m., Zaffran, M., & Organization, W. H. Temperature sensitivity of vaccines. (2006)

[147] Capaccioli, S., & Ngai, K. Resolving the controversy on the glass transition temperature of water? *J. Chem. Phys., 135*(10), 104504. (2011)

[148] Kumru, O. S., Joshi, S. B., Smith, D. E., Middaugh, C. R., Prusik, T., & Volkin, D. B. Vaccine instability in the cold chain: mechanisms, analysis and formulation strategies. *Biologicals, 42*(5), 237-259. (2014)

[149] Hanani, Z. N., Roos, Y., & Kerry, J. P. Use of beef, pork and fish gelatin sources in the manufacture of films and assessment of their composition and mechanical properties. *Food Hydrocolloids, 29*(1), 144-151. (2012)

[150] da Almeida, P. F., da Silva Lannes, S. C., Calarge, F. A., da Brito Farias, T. M., & Santana, J. C. C. FTIR characterization of gelatin from chicken feet. *J. Chem. Chem. Eng., 6*(11), 1029. (2012)

[151] Sibik, J., Korter, T. M., & Zeitler, J. A. (2015). *Combined infrared and terahertz analysis of amorphous sorbitol.* Paper presented at the Infrared, Millimeter, and Terahertz waves (IRMMW-THz), 2015 40th International Conference on; Cilurzo, F., Cupone, I. E., Minghetti, P., Selmin, F., & Montanari, L. Fast dissolving films made of maltodextrins. *Eur. J. Pharm. Biopharm., 70*(3), 895-900. (2008)

[152] Cullity, B. *Elements of X-Ray Diffraction 2nd edition.* (Vol. 197): Addision-Wesley Pub. Co Inc., CA, USA, (1978)

[153] Estívariz, C. F., Pallansch, M. A., Anand, A., Wassilak, S. G., Sutter, R. W., Wenger, J. D., & Orenstein, W. A. Poliovirus vaccination options for achieving eradication and securing the endgame. *Curr. Opin. Virol., 3*(3), 309-315. (2013)

[154] Yager, P., Domingo, G. J., & Gerdes, J. Point-of-care diagnostics for global health. *Annu. Rev. Biomed. Eng., 10*, 107-144. (2008)

[155] Gubala, V., Harris, L. F., Ricco, A. J., Tan, M. X., & Williams, D. E. Point of care diagnostics: status and future. *Anal. Chem., 84*(2), 487-515. (2011)

[156] Bond, M. M., & Richards-Kortum, R. R. Drop-to-drop variation in the cellular components of fingerprick blood: implications for point-of-care diagnostic development. *Am. J. Clin. Pathol., 144*(6), 885-894. (2015)

[157] Sloop, C. H., Dory, L., & Roheim, P. S. Interstitial fluid lipoproteins. *J. Lipid Res., 28*(3), 225-237. (1987); Müller, A. C., Breitwieser, F. P., Fischer, H., Schuster, C., Brandt, O., Colinge, J., Superti-Furga, G., Stingl, G., Elbe-Bürger, A., & Bennett, K. L. A comparative proteomic study of human skin suction blister fluid from healthy individuals using immunodepletion and iTRAQ labeling. *J. Proteome Res., 11*(7), 3715-3727. (2012)

[158] Fogh-Andersen, N., Altura, B. M., Altura, B. T., & Siggaard-Andersen, O. Composition of interstitial fluid. *Clin. Chem., 41*(10), 1522-1525. (1995)

[159] Hadrévi, J., Ghafouri, B., Sjörs, A., Antti, H., Larsson, B., Crenshaw, A., Gerdle, B., & Hellström, F. Comparative metabolomics of muscle interstitium fluid in human trapezius myalgia: an in vivo microdialysis study. *Eur. J. Appl. Physiol., 113*(12), 2977-2989. (2013)

[160] Donnelly, R. F., Mooney, K., Caffarel-Salvador, E., Torrisi, B. M., Eltayib, E., & McElnay, J. C. Microneedle-mediated minimally invasive patient monitoring. *Ther. Drug Monit., 36*(1), 10-17. (2014)

[161] Marshall, S., Sahm, L. J., & Moore, A. C. The success of microneedle-mediated vaccine delivery into skin. *Hum. Vaccines Immunother., 12*(11), 2975-2983. (2016); Nguyen, T. T., & Park, J. H. Human studies with microneedles for evaluation of their efficacy and safety. *Expert Opin. Drug Delivery, 15*(3), 235-245. (2018)

[162] Ye, Y., Yu, J., Wen, D., Kahkoska, A. R., & Gu, Z. Polymeric microneedles for transdermal protein delivery. *Adv. Drug Delivery Rev., 127,* 106-118. (2018)

[163] ISO 535:2014(en) Paper and board — Determination of water absorptiveness — Cobb method, https://www.iso.org/obp/ui/#iso:std:iso:535:ed-3:v1:en (accessed on 4/12/18)

[164] ISO 8787:1986(en) Paper and board — Determination of capillary rise — Klemm method, https://www.iso.org/obp/ui/#iso:std:iso:8787:ed-1:v1:en (accessed on 4/12/18)

[165] Laboratories, C. R. https://www.criver.com/sites/default/files/resources/BaselineHematologyandClinicalChemistryValuesforCharlesRiverWistarRats%5BCrlWIBR%5DasaFunctionofSexandAgeSpring1998.pdf. (accessed on 4/12/18)

[166] Nachbaur, J., Clarke, M., Provost, J., & Dancla, J. Variations of sodium, potassium, and chloride plasma levels in the rat with age and sex. *Lab. Anim. Sci., 27*(6), 972-975. (1977)

[167] Franzen, L., Vidlářová, L., Kostka, K. H., Schaefer, U. F., & Windbergs, M. Freeze-drying as a preserving preparation technique for in vitro testing of human skin. *Exp. Dermatol., 22*(1), 54-56. (2013)

[168] Martinez, A. W., Phillips, S. T., Nie, Z., Cheng, C.-M., Carrilho, E., Wiley, B. J., & Whitesides, G. M. Programmable diagnostic devices made from paper and tape. *Lab Chip, 10*(19), 2499-2504. (2010); Carvalhal, R. F., Simão Kfouri, M., de Oliveira Piazetta, M. H., Gobbi, A. L., & Kubota, L. T. Electrochemical detection in a paper-based separation device. *Anal. Chem., 82*(3), 1162-1165. (2010)

[169] Bracher, P. J., Gupta, M., & Whitesides, G. M. Patterned paper as a template for the delivery of reactants in the fabrication of planar materials. *Soft Matter, 6*(18), 4303-4309. (2010)

[170] Levick, J. Flow through interstitium and other fibrous matrices. *Exp. Physiol., 72*(4), 409-437. (1987)

[171] Kiistala, U., & Mustakallio, K. Dermo-epidermal separation with suction: electron microscopic and histochemical study of initial events of blistering on human skin. *J. Invest. Dermatol., 48*(5), 466-477. (1967)

[172] Garg, S. K., Potts, R. O., Ackerman, N. R., Fermi, S. J., Tamada, J. A., & Chase, H. P. Correlation of fingerstick blood glucose measurements with GlucoWatch biographer glucose results in young subjects with type 1 diabetes. *Diabetes Care, 22*(10), 1708-1714. (1999)

[173] Parini, P., Johansson, L., Bröijersén, A., Angelin, B., & Rudling, M. Lipoprotein profiles in plasma and interstitial fluid analyzed with an automated gel-filtration system. *Eur. J. Clin. Invest., 36*(2), 98-104. (2006); Parikh, P., Mochari, H., & Mosca, L. Clinical utility of a fingerstick technology to identify individuals with abnormal blood lipids and high-sensitivity C-reactive protein levels. *Am. J. Health Promot., 23*(4), 279-282. (2009)

[174] Koren, G. Therapeutic drug monitoring principles in the neonate. *Clin. Chem., 43*(1), 222-227. (1997)

[175] Fenton, E. M., Mascarenas, M. R., López, G. P., & Sibbett, S. S. Multiplex lateral-flow test strips fabricated by two-dimensional shaping. *ACS Appl. Mater. Interfaces, 1*(1), 124-129. (2008); Li, X., Tian, J., Garnier, G., & Shen, W. Fabrication of paper-based microfluidic sensors by printing. *Colloids Surf., B, 76*(2), 564-570. (2010)

[176] Martinez, A. W., Phillips, S. T., Whitesides, G. M., & Carrilho, E. (2009). Diagnostics for the developing world: microfluidic paper-based analytical devices: ACS Publications.

[177] Poiseuille, J. L. (1844). *Recherches expérimentales sur le mouvement des liquides dans les tubes de très-petits diamètres*: Imprimerie Royale.

[178] Edelbroek, P. M., van der Heijden, J., & Stolk, L. M. Dried blood spot methods in therapeutic drug monitoring: methods, assays, and pitfalls. *Ther. Drug Monit., 31*(3), 327-336. (2009)

[179] Downing, G. J. (2010). Biomarkers: Facing the Challenges at the Crossroads of Research and Health Care *Pharm. Sci. Encyclopedia* (pp. 1-16): John Wiley & Sons, Inc; Mabey, D., Peeling, R. W., Ustianowski, A., & Perkins, M. D. Tropical infectious diseases: diagnostics for the developing world. *Nat. Rev. Microbiol., 2*(3), 231. (2004)

[180] Anderson, N. L., & Anderson, N. G. The human plasma proteome history, character, and diagnostic prospects. *Mol. Cell. Proteomics, 1*(11), 845-867. (2002)

[181] Deacon, B., & Abramowitz, J. Fear of needles and vasovagal reactions among phlebotomy patients. *J. Anxiety Disord., 20*(7), 946-960. (2006)

[182] Pichini, S., Altieri, I., Zuccaro, P., & Pacifici, R. Drug monitoring in nonconventional biological fluids and matrices. *Clin. Pharmacokinet., 30*(3), 211-228. (1996)

[183] Fischbach, F. T., & Dunning, M. B. *A manual of laboratory and diagnostic tests*: Lippincott Williams & Wilkins, (2009)

[184] Renard, E. Implantable continuous glucose sensors. *Curr. Diabetes Rev., 4*(3), 169-174. (2008)

[185] Wiig, H., Tenstad, O., Iversen, P. O., Kalluri, R., & Bjerkvig, R. Interstitial fluid: the overlooked component of the tumor microenvironment? *Fibrog. Tissue Repair, 3*(1), 12. (2010)

[186] Herkenne, C., Alberti, I., Naik, A., Kalia, Y. N., Mathy, F.-X., Préat, V., & Guy, R. H. In vivo methods for the assessment of topical drug bioavailability. *Pharm. Res., 25*(1), 87. (2008)

[187] Venugopal, M., Feuvrel, K. E., Mongin, D., Bambot, S., Faupel, M., Panangadan, A., Talukder, A., & Pidva, R. Clinical evaluation of a novel interstitial fluid sensor system for remote continuous alcohol monitoring. *IEEE Sens. J., 8*(1), 71-80. (2008)

[188] Vrdoljak, A., Allen, E. A., Ferrara, F., Temperton, N. J., Crean, A. M., & Moore, A. C. Induction of broad immunity by thermostabilised vaccines incorporated in

dissolvable microneedles using novel fabrication methods. *J. Controlled Release, 225*, 192-204. (2016)

[189] Ito, Y., Inagaki, Y., Kobuchi, S., Takada, K., & Sakaeda, T. Therapeutic drug monitoring of vancomycin in dermal interstitial fluid using dissolving microneedles. *Int. J. Med. Sci., 13*(4), 271. (2016)

[190] Greenwood, B., Hall, A., Rowe, M., Whittle, H., George, M., Al-Ghassani, A., Elbualy, M., Malankar, P., Suleiman, A., & Clements, G. Combined immunization of infants with oral and inactivated poliovirus vaccines: Results of a randomized trial in the Gambia, Oman, and Thailand. *Bull. W. H. O., 74*, 253-268. (1996)

[191] Finney, D. J. *Statistical method in biological assay*: Charles Griffin: London, (1952)

[192] Rybak, M. J. The pharmacokinetic and pharmacodynamic properties of vancomycin. *Clin. Infect. Dis., 42*(Supplement_1), S35-S39. (2006)

[193] Loewenstein, D., Stake, C., & Cichon, M. Assessment of using fingerstick blood sample with i-STAT point-of-care device for cardiac troponin I assay. *Am. J. Emerg. Med., 31*(8), 1236-1239. (2013)

[194] Housman, S. T., Bhalodi, A. A., Shepard, A., Nugent, J., & Nicolau, D. P. Vancomycin tissue pharmacokinetics in patients with lower-limb infections via in vivo microdialysis. *J. Am. Podiatric Med. Assoc., 105*(5), 381-388. (2015)

[195] Hamada, Y., Kuti, J. L., & Nicolau, D. P. Vancomycin serum concentrations do not adequately predict tissue exposure in diabetic patients with mild to moderate limb infections. *J. Antimicrob. Chemother., 70*(7), 2064-2067. (2015)

[196] Suh, H., Shin, J., & Kim, Y.-C. Microneedle patches for vaccine delivery. *Clin. Exp. Vaccine Res., 3*(1), 42-49. (2014)

[197] Geherin, S. A., Fintushel, S. R., Lee, M. H., Wilson, R. P., Patel, R. T., Alt, C., Young, A. J., Hay, J. B., & Debes, G. F. The skin, a novel niche for recirculating B cells. *J. Immunol.*, 1102639. (2012)

[198] Gekko, K., & Morikawa, T. Preferential hydration of bovine serum albumin in polyhydric alcohol-water mixtures. *J. Biochem., 90*(1), 39-50. (1981)

[199] Caffarel-Salvador, E., Tuan-Mahmood, T.-M., McElnay, J. C., McCarthy, H. O., Mooney, K., Woolfson, A. D., & Donnelly, R. F. Potential of hydrogel-forming and dissolving microneedles for use in paediatric populations. *Int. J. Pharm., 489*(1-2), 158-169. (2015)

[200] Martinez, A. W., Phillips, S. T., Carrilho, E., Thomas III, S. W., Sindi, H., & Whitesides, G. M. Simple telemedicine for developing regions: camera phones

and paper-based microfluidic devices for real-time, off-site diagnosis. *Analytical Chemistry, 80*(10), 3699-3707. (2008)